Caractérisation et analyse des risques incendie dans les toitures végétalisées

Thèse

Nataliia Gerzhova

Doctorat en sciences du bois
Philosophiæ doctor (Ph. D.)

Québec, Canada

Caractérisation et analyse des risques incendie dans les toitures végétalisées

Thèse

Nataliia Gerzhova

Sous la direction de :

Pierre Blanchet, directeur de recherche

Christian Dagenais, codirecteur de recherche

Sylvain Ménard, codirecteur de recherche

Résumé

En l'absence d'études scientifiques sur le comportement au feu des toitures végétalisées, des inquiétudes se posent quant à leur sécurité et à l'adéquation des mesures de protection existantes contre la propagation du feu. La province de Québec a publié le guide technique sur l'installation de ces toitures où la section sur la sécurité incendie est élaborée de manière très détaillée, en recueillant les règles de différentes sources, ce qui dans certains cas pose des limites pour la conception. Cette recherche visait à étudier les risques d'incendie que ces toits présentent et à analyser leurs performances dans des conditions extrêmes pour une meilleure compréhension des possibilités du feu et de l'importance des mesures de sécurité incendie.

La conductivité thermique effective de substrat de croissance en fonction de la température pour les toitures végétalisées a été déterminée pour une utilisation dans des simulations numériques d'analyse de transfert de chaleur. Une série d'essais en laboratoire a été effectuée afin d'ajuster un modèle existant de calcul de la conductivité thermique des sols minéraux pour l'application sur des substrats de toitures végétalisées. Les résultats montrent une petite différence dans les valeurs mesurées et calculées, spécifiquement 1.07 et 0.9 W/(m·K), ce qui confirme la validité du modèle pour les substrats de toitures végétalisées. Le modèle a permis le calcul de la conductivité thermique en considérant séparément les matériaux organiques et inorganiques, ce qui facilite la détermination de cette propriété à différentes températures compte tenu de la décomposition de la matière organique entre 250 et 700 °C. L'analyse de décomposition thermique a également été effectuée pour obtenir des proportions de composants minéraux et organiques. Les résultats satisfaisants du test de validation et des simulations numériques montrent l'applicabilité de la conductivité thermique effective déterminée en fonction de la température pour les problèmes de transfert de chaleur.

L'analyse de la propagation de la chaleur à travers le toit végétalisé a été réalisée afin d'évaluer le risque d'endommagement de la structure du toit par la chaleur lorsqu'une surface d'un toit végétalisé est exposée à des températures élevées. Plusieurs simulations numériques ont été effectuées pour déterminer les conditions dans lesquelles la défaillance du toit se produit. Un toit végétalisé extensif avec le substrat de croissance sec contenant 5% de matière organique a été pris pour la modélisation. Il a été constaté que le substrat de moins de 10 cm

d'épaisseur à l'état sec peut protéger efficacement le platelage de toit, retardant la propagation de la chaleur. Un retard d'au moins 30 min est obtenu avec la couche de substrat de 3 cm d'épaisseur. L'effet de la porosité du substrat (entre 0.5 et 0.7) sur le temps de défaillance était faible et observable uniquement sous une charge thermique de 200 kW/m².

Les caractéristiques d'inflammabilité des toitures végétalisées, telles que la vitesse de dégagement de chaleur, la densité de la charge combustible et le temps d'allumage ont été déterminés. Des mesures en laboratoire à l'aide d'un calorimètre à cône ont été effectuées sur les substrats de croissance de toit vert à l'état sec et humide. Les résultats ont montré que même à l'état sec, le substrat libère beaucoup moins d'énergie qu'une couverture de toiture typique en bitume modifié. Généralement, la performance des toits végétalisés en feu est meilleure qu'un toit typique en bitume.

Le risque d'incendie des toits végétalisés pour les bâtiments adjacents a été analysé en termes d'exposition à la chaleur rayonnante produite par un incendie sur un toit vert. Les résultats des calculs montrent que la présence d'humidité dans les plantes réduit considérablement la distance sécuritaire entre le toit et la façade d'un bâtiment voisin et est le principal facteur de réduction des risques d'incendie. Il a également été montré qu'en raison du fait que le vent a un fort effet sur la propagation du feu, il est important de le considérer lors de la conception d'un toit vert.

Abstract

In the lack of scientific studies on fire performance of green roofs concerns arise about their safety and the adequacy of existing protection measures against the spread of fire. Province of Quebec issued the technical guide on installation of such roofs where fire safety section is drawn up in considerable detail, collecting the rules from different sources, which in some cases poses limitations for design. This research aimed at investigating the fire risks that such roofs present and analyzing their performance in extreme conditions for better understanding of fire possibilities and the importance of fire safety measures.

The effective thermal conductivity as a function of temperature of green roof growing media was determined for using in numerical simulations of heat transfer analysis. A series of laboratory measurements were conducted in order to adjust an existing model of calculation of thermal conductivity of mineral soils for the application to green roof substrates. The results show small difference in measured and calculated values, specifically 1.07 and 0.9 W/(m·K), that confirms the suitability of model for green roof substrates. The model allowed the calculation of thermal conductivity considering organic and inorganic materials separately, which facilitates the determination of this property at different temperatures considering the decomposition organic matter between 250 and 700 °C. The thermal decomposition analysis was also performed to obtain proportions of mineral and organic components. Satisfactory results of validation test and numerical simulations show applicability of predicted effective thermal conductivity as a function of temperature for heat transfer problems.

The analysis of heat propagation through the green roof assembly was conducted in order to assess the risk of roof structure being damaged by heat when a surface of a green roof is exposed to elevated temperatures. Multiple numerical simulations were performed to determine conditions at which the roof failure occurs. Extensive green roof with dry growing media containing 5% of organic matter was taken for the modeling. It was found that the substrate of less than 10 cm thickness in dry state can effectively protect the roof deck, retarding the heat propagation. At least 30 min of retardation is achieved with the substrate layer of 3 cm thickness. The effect of porosity of the substrate (between 0.5 and 0.7) on time to failure was found to be small and noticeable only under heating load of 200 kW/m².

Flammability characteristics of green roofs, such as heat release rate, fire load density and time to ignition was determined. Laboratory measurements using a cone calorimeter were conducted over the green roof growing media in dry and moist state. The results showed that even in dry condition the substrate releases much less energy compared to a typical roof covering made of modified bitumen. Generally, the performance of green roofs in fire is better than a typical bitumen roof.

Fire risk of green roofs to adjacent buildings was analyzed in terms of exposure to the radiation heat produced by a fire on a green roof. The results of calculation show that the presence of moisture in plants greatly reduces safe distance to façade and is the main factor in reducing fire hazard. It was also shown due to the fact that the wind has a strong effect on fire spread it is important to consider it when designing a green roof.

Table des matières

Liste des figures

Liste des tableaux

Liste des abréviations

CRCA :	Canadian Roofing Contractors' Association
MO, OM :	Matière organique, Organic Matter
RBQ :	Régie du bâtiment du Québec
TV :	Toiture végétalisée

Liste des symboles

α	angle d'inclinaison de la flamme
β	paramètre empirique
C_p	capacité calorique spécifique, J/(kg·K)
C_{Pn_T}	capacité calorique spécifique normalisée à une certaine température T
C_{P_T}	capacité calorique spécifique à une certaine température T, J/(kg·K)
d	distance, m
$d_{12.5}$	distance de séparation à un flux de chaleur rayonnante de 12.5 kW/m², m
d_{10}	diamètre des particules (diamètre effectif des particules qui correspond à 10% du passant), mm
E	facteur d'échange
E_f	pouvoir émissif du feu, W/m²
ε	émissivité
ε_p	émissivité des particules
ξ	rapport de flux de propagation
F	facteur de forme
ϕ_W	coefficient de vent
ϕ_S	facteur de pente
H	pouvoir calorifique, kJ/kg
h	hauteur de la cible, m
h_i	coefficient de transfert thermique par convection, W/(m²·K)
θ	pente du terrain
I	intensité du feu, kW/m
I_r	intensité de la réaction, kJ/(min·m²)
κ_{2P}	paramètre de structure
L	longueur de flamme, m
σ	constante de Stefan-Boltzmann, W/(m²·K⁴)
λ	conductivité thermique, W/(m·K)
λ_c	conductivité thermique, contribution de la conduction pure, W/(m·K)
λ_e	conductivité thermique efficace, W/(m·K)
λ_f	conductivité thermique des fluides, W/(m·K)
λ_n	conductivité thermique normalisée
λ_{rad}	conductivité thermique, contribution du rayonnement interarticulaire, W/(m·K)
λ_s	conductivité thermique des solides, W/(m·K)
λ_w	conductivité thermique de l'eau, W/(m·K)
m_{OMn}	quantité normalisée de la MO
n	porosité

Q_{ig}	chaleur de pré-allumage, kJ/kg
q''_{conv}	flux de chaleur convectif, kW/m²
$q''_{net,r}$	flux de chaleur rayonnante net, kW/m²
q''_{rad}	flux de chaleur rayonnante, kW/m²
RoS	vitesse de propagation, km/h
ρ_{dry}	masse volumique d'un échantillon sec, g/cm³
ρ_s	masse volumique de particules solides, g/cm³
ρ_{total}	masse volumique apparente, g/cm³
T	température, °C, K
T_0	température initiale, °C
t	temps, s
τ	transmissivité atmosphérique
V	vitesse du vent, km/h
VH	hauteur de végétation, m
W	charge combustible, t/ha
W_f	largeur de flamme, m
x_i	fraction volumique

Remerciements

La réalisation de cette thèse était le plus beau défi de ma vie. Au cours des trois dernières années passées à l'Université Laval, j'ai pu compter sur le soutien de plusieurs personnes qui ont fait la différence dans mon cheminement.

Je remercie, tout d'abord, mon directeur de recherche, le professeur Pierre Blanchet pour m'avoir donné l'opportunité de venir au Québec et de réaliser ce projet. Je le remercie également pour sa confiance, son encouragement, ses conseils précieux ainsi que son soutien financier. Je tiens également à exprimer toute ma reconnaissance à mes codirecteurs, Dr. Christian Dagenais, chercheur chez FPInnovations et professeur invité au Département des sciences du bois et de la forêt, ainsi que le professeur Sylvain Ménard, professeur au Département des sciences appliquées à l'Université du Québec à Chicoutimi. Merci pour vos conseils, votre apport d'idées, votre soutien et votre grande disponibilité. Cela m'a toujours aidée à avancer dans mes recherches. J'adresse aussi mes sincères remerciements à M. Jean Côté, le professeur au Département de génie civil et de génie des eaux, pour sa grande contribution, sans laquelle ce projet de doctorat n'aurait pas été possible à réaliser.

Mes remerciements particuliers vont aux partenaires du projet, les membres du Groupe de travail sur les toitures végétalisées (GTTV) du Conseil du bâtiment durable du Canada. Merci à Marjolaine Auger (Hydrotech) pour m'avoir fourni les matériaux et pour avoir été disponible pour répondre à mes questions. Merci également à Marie-Anne Boivin et Roxanne Miller (Soprema) pour avoir partagé leurs connaissances avec moi.

Je souhaite remercier aussi le personnel du CIRCERB, Pierre Gagné, Jenny McKenzie, Myriam Drouin et Torsten Lihra, pour leur aide, leur soutien durant mon projet, ainsi que leur contribution indéniable à créer une ambiance de travail agréable grâce aux activités organisées. Merci à Mme. Guylaine Bélanger et Caroline Trahan pour leur aide administrative précieuse.

J'aimerais remercier Olivier Lachance, le professionnel de recherche dans le Département de génie civil et de génie des eaux, et Francine Côté (FPInnovations) pour leur assistance au cours de mes travaux expérimentaux.

Je remercie mes amis qui m'ont constamment soutenu tout au long de mon projet, merci à Marzieh, Trang et Sagar. J'ai grandement apprécié l'encouragement que vous m'avez apporté.

Finalement, je remercie ma famille qui est un grand support dans ma vie. Merci à ma sœur Alina et mon beau-frère Cheslav qui croient toujours en moi et sont toujours prêts à aider. Vous êtes pour moi un exemple à suivre pour atteindre les objectifs de vie. Merci à ma mère Valentina pour son amour inconditionnel, sa gentillesse et une attitude positive.

Avant-propos

Ce projet de doctorat a été réalisé dans le cadre de la Chaire industrielle de recherche du CSRNG sur la construction écoresponsable en bois (CIRCERB), sous la direction de M. Pierre Blanchet, professeur au Département des sciences du bois et de la forêt de l'Université Laval, sous la codirection de Dr. Christian Dagenais, ingénieur, chercheur leader chez FPInnovations et professeur invité au Département des sciences du bois et de la forêt de l'Université Laval, sous la codirection de M. Sylvain Ménard, professeur au Département des sciences appliquées à l'Université du Québec à Chicoutimi, et en collaboration avec le professeur Jean Côté au Département de génie civil et de génie des eaux de l'Université Laval. Cette étude a été réalisée dans le cadre du programme de doctorat en sciences du bois et est présentée sous forme d'une thèse par insertion d'articles. La thèse est composée de six chapitres et comprend quatre articles écrits en langue anglaise.

Chapitre 1 : Présente la revue de la littérature et les objectifs de la recherche.

Chapitre 2 : Rétrospective méthodologique.

Chapitre 3 : « *A Conceptual Framework for Modelling the Thermal Conductivity of Dry Green Roof Substrates* », publié dans *BioResources* Vol. 14 (2019), Issue 4, Pages 8573-8599. Auteurs : Gerzhova, N., Côté, J., Blanchet, P., Dagenais, C. et Ménard, S.

Chapitre 4 : « *Heat Transfer Behavior of Green Roof Systems under Fire Condition: A Numerical Study* », publié dans *Buildings* Vol. 9 (2019), Issue 9. Auteurs : Gerzhova, N., Blanchet, P., Dagenais, C., Côté, J. et Ménard, S.

Chapitre 5 : « Flammability Characteristics of Green Roofs », publié dans *Buildings* Vol. 10 (2020), Issue 7, Auteurs : Gerzhova, N., Blanchet, P., Dagenais, C., Ménard, S. et Côté, J.

Chapitre 6 : « *Fire risk of green roofs to adjacent buildings* », sous évaluation pour publication dans le *Journal of Building Engineering*. Auteurs : Gerzhova, N., Dagenais, C., Ménard, S., N., Blanchet, P. et Côté, J.

Finalement, les conclusions générales sont présentées.

Les travaux de cette étude ont également été présentés dans les conférences et activités suivants :

- Présentation orale, 26e Expo Contech Bâtiment (Québec, Canada), octobre 2017
- Présentation orale, 33e Expo Contech Bâtiment (Montréal, Canada), novembre 2017
- Présentation par affiche, CitiesAlive (New York, États-Unis), septembre 2018

  « Meilleure affiche scientifique »
- Présentation orale, Colloque facultaire FFGG (Faculté de foresterie, de géographie et de géomatique) (Québec, Canada), mars 2019
- Présentation orale, cours SBO 8001, Séminaire II (Québec, Canada), avril 2019
- Présentation par affiche, Colloque SQP (Société québécoise de phytotechnologie) : Innovation Phytotechnologique (Montréal, Canada), mai 2019

  « Bourse de recherche 2019 »
- Présentation par affiche, 87e Congrès de l'ACFAS (Association Canadienne-Française pour l'Avancement des Sciences) (Gatineau, Canada), mai 2019

Les présentations par affiches sont reproduites à l'Annexe B.

Introduction

Les systèmes de toitures végétalisées (TV) gagnent de plus en plus en popularité dans le monde. L'inclusion de zones végétalisées dans les projets de construction améliore considérablement leur intérêt visuel. Ces systèmes, qui à première vue semblent faciles à mettre en œuvre, sont des technologies complexes qui peuvent être utilisées pour aider à résoudre divers problèmes dans un bâtiment en tant qu'outils efficaces grâce à leurs performances multifonctionnelles. L'utilisation à grande échelle apporte un avantage significatif à l'environnement et à la vie urbaine. Malgré leur coût d'installation et de main-d'œuvre au départ, ces systèmes peuvent représenter des investissements raisonnables si l'on utilise au maximum tous leurs avantages. De plus, l'encouragement par les autorités sous forme de différents programmes de soutien financier, réductions d'impôts et de mandats existent dans de nombreuses villes du monde comme incitatifs à implanter ces systèmes dans les bâtiments.

Les TV possèdent une très large gamme d'avantages par rapport aux systèmes conventionnels et peuvent être utilisés avec succès dans toutes les zones climatiques propices à l'habitation et à la végétation. L'un de ses plus grands avantages est la gestion des eaux pluviales qui est particulièrement pertinente pour les villes manquant d'espaces verts, ce qui signifie une forte proportion de surfaces imperméables. De plus, il convient également de mentionner le problème de l'effet d'îlot de chaleur urbain. Habituellement, dans les grandes villes, en raison de la forte densité de construction et de l'augmentation des chaussées, la température moyenne est plus élevée que dans les banlieues, ce qui a un effet négatif sur l'environnement. Les TV vont créer des taches vertes supplémentaires qui, en cas d'utilisation généralisée, peuvent contribuer d'une manière ou d'une autre à maintenir le niveau de température ambiante. Ils contribuent également à améliorer la qualité de l'air, car les plantes ont la capacité d'éliminer une certaine quantité de polluants. Une autre zone d'application de ces toits comprend l'agriculture urbaine, qui tend à devenir de plus en plus courante dans les grandes villes. L'espace supplémentaire qu'une TV fournit est raisonnablement utilisé pour les jardins soutenant des voisinages avec des produits frais locaux. La TV est un moyen pour enrichir et préserver la biodiversité locale. L'introduction des TV dans les villes est une création de refuges permettant l'hébergement de différentes espèces d'animaux et d'insectes.

Enfin, les jardins urbains attirent les gens et face au manque d'espace dans les villes, les TV peuvent servir de zones récréatives lorsqu'elles sont autorisées à l'accès et spécialement aménagées. Ceci, en conséquence, apporte plus de valeur au bâtiment et améliore son apparence. En ce qui concerne les avantages pour le bâtiment lui-même, la grande contribution sera de réduire la demande en climatisation et d'améliorer l'environnement interne. Les couches de tels toits, en particulier la couverture de plantation et le sol, exercent une fonction d'isolation particulièrement utile dans les climats chauds où les toits ne sont généralement pas isolés. Ces couches sont capables non seulement de protéger contre les fluctuations de température la structure du toit, mais également la membrane imperméable contre les intempéries. Comme la membrane est une partie essentielle du toit qui la protège des fuites et des petits dommages, elle devrait être suffisamment durable. Les couvertures végétalisées la protègent de l'exposition directe à l'extérieur et assurent ainsi un service plus long de cette partie du toit (Snodgrass and McIntyre, 2010). Les avantages énumérés sont loin d'être une liste complète, mais ils démontrent suffisamment que les TV méritent l'attention et l'importance de leur promotion.

Tirer pleinement parti du potentiel des TV est réalisable à la condition de bien connaître toutes ses possibilités. Sensibiliser la population à tous les avantages peut réduire le scepticisme existant quant à leur valeur. De plus, l'intérêt des autorités envers cette technologie est un moyen efficace et nécessaire à son développement. Dans le cas contraire, ce développement n'aura pas beaucoup de succès s'il se base uniquement sur les efforts des passionnés ou des spécialistes des TV (Erik van Lennep, 2008). Le manque de connaissances de la plantation sur les toits conduit souvent à une mauvaise compréhension de sa fonctionnalité, de sa rentabilité et surtout de sa sécurité. En conséquence, dans certains endroits, les discussions sont interminables entre les fabricants et les autorités, afin d'ouvrir des portes pour que ces systèmes progressent.

L'installation de TV est de plus en plus présente dans plusieurs villes et pays du monde. Leur expérience est un bon exemple pour d'autres qui souhaitent mettre en œuvre cette technologie. L'adoption de leurs pratiques plutôt que le développement de nouvelles pratiques est parfois un meilleur choix, puisque le principe de fonctionnement est le même et que les matériaux y sont communs et largement disponibles. Les conditions climatiques locales ne détermineront que partiellement le type et la composition des composants

principaux. Toutefois, d'autres facteurs, tels que les règles et les normes de construction locales existantes, peuvent parfois influencer les processus de conception et d'installation. La province de Québec a sa propre spécificité et donc ses propres règlements quant à la sécurité. Pour les TV, l'une des questions importantes est un problème de sécurité incendie, notamment si elles sont utilisées sur le toit d'un bâtiment de construction en bois. Il est considéré que les TV sont perçues comme dangereuses si elles sont installées sur des constructions en bois et, par conséquent, elles sont exclues par la RBQ. Une grande attention est portée à une partie sur la protection contre la propagation de l'incendie et l'exigence développée contient un grand nombre de détails qui, malheureusement, compliquent parfois l'installation et dans certains cas rendent même impossible la réalisation d'un projet. Par conséquent, ces règles créent différents types de restrictions qui, bien sûr, entraînent le mécontentement des concepteurs et fabricants. L'ensemble de ces contraintes est assez important et peut affecter à la fois les petits et les grands projets. Ceci démontre qu'en situation de manque de connaissances spécifiques sur le comportement de ces toits lors d'un incendie, le législateur tend à maximiser la sécurité et de prévenir les accidents éventuels en conformité avec son rôle.

Les fabricants effectuent souvent des tests de performance au feu pour démontrer que leurs assemblages ne fournissent aucun risque d'incendie. Cependant, une grande variété d'assemblages et de composants ne permet pas de caractériser tous les TV. Ce qui signifie que chaque fois qu'un test est réussi, il est considéré comme concluant en termes de sécurité incendie jusqu'à ce que l'un de ses paramètres soit modifié, y compris la couleur d'un matériau.

Cette situation démontre une opportunité de recherche du problème. La sécurité incendie dans le bâtiment est une science complexe et il sera donc nécessaire de mettre en évidence les aspects les plus importants et d'évaluer le risque incendie que représente la TV pour les bâtiments. Cette recherche vise à caractériser le comportement au feu de systèmes de TV. Spécifiquement, l'accent est mis sur la caractérisation de matériaux, la contribution au feu de composants de TV et la capabilité de propagation du feu. L'étude contribuera à mieux comprendre les processus lors d'un incendie et à déterminer les paramètres ayant un grand impact.

CHAPITRE 1 :Revue de la littérature

1.1. Types de couvertures

Il existe deux types de couverture de toit utilisés au Québec : conventionnelle et inversée (Fig. 1.1). La différence entre les deux est que dans le type conventionnelle (ou traditionnelle) la membrane d'étanchéité est placée sur une couche d'isolation. C'est une couche supérieure qui est directement exposée à l'environnement. Dans le type inversé la membrane est appliquée à un platelage et recouverte d'une couche d'isolation, qui à son tour est recouverte d'un ballast pour maintenir en place un matériau d'isolation léger. Ce type est également appelé membrane protégée ou isolée. Dans ce cas, une membrane est protégée contre les intempéries et les fluctuations de la température, ce qui permet à la membrane de servir plus longtemps. Les deux types ont leurs propres avantages, et tous deux permettent l'installation de TV au-dessus. Cependant, les toitures inversées ont plus d'avantages pour l'installation des TV et elles sont recommandées par les associations de couvreurs CRCA (*Canadian Roofing Contractors' Association*), surtout pour les systèmes de TV avec une couche épaisse de substrat et les jardins sur le toit (CRCA, 2006). En plus de la protection contre l'exposition directe à l'environnement, la membrane dans ce type de couverture a moins de chance d'être endommagée mécaniquement pendant la construction. Dans les toits conventionnels, où l'isolant est autre que le polystyrène extrudé qui est suffisamment résistant en compression et qui a une bonne stabilité dimensionnelle, la membrane est plus susceptible d'être endommagée que lorsqu'elle est collée directement sur un platelage dans le type inversé. Dans ce cas, si une déchirure se produit, l'humidité du sol pénètre dans l'isolant et sur le toit et peut causer de graves dommages, car les fuites ne sont généralement pas visibles au début et ne sont pas facilement détectables. Au Québec les règles pour l'installation de TV contiennent certaines particularités pour les couvertures inversées, ce qui est décrit dans la section suivante.

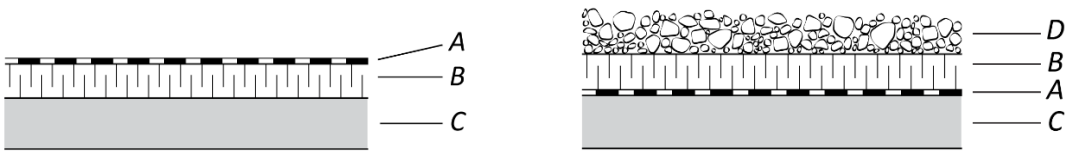

a b

Figure 1.1. Types de couvertures : (a) conventionnelle; (b) inversée : A - membrane, B - isolation, C - platelage, D - ballast.

1.2. Toitures végétalisées

Les TV sont des assemblages composés de plusieurs couches. Ces couches sont placées et fixées directement sur le platelage du toit. Les systèmes typiques n'exigent pas la création de construction supplémentaire en dessous pour maintenir l'ensemble, sauf pour les cas de nécessité de renforcement structurel. Les TV peuvent être installées sur les nouveaux bâtiments ainsi que sur les bâtiments existants avec les toits plats ou en pente. Le matériau de pontage n'est pas limité, le béton, le métal et même le pontage en bois, malgré les inquiétudes générales concernant la pourriture, ont la capacité de bien soutenir.

L'assemblage et les composants de la TV dépend de la conception, c'est-à-dire les fonctions qu'elles doivent servir, et des conditions comme le type d'un bâtiment, le climat, les conditions locales. Cependant, l'assemblage est basé sur le même principe et contient les matériaux communs placés à peu près dans le même l'ordre. Il comprend tout d'abord la végétation et le substrat de croissance, le tissu filtrant, le système de drainage et la barrière anti-racine. La végétation et le substrat sont les composantes principales et sont responsables des avantages d'une TV. La TV est placée sur la couverture, qui comprend principalement un platelage de toit, une isolation et une membrane d'étanchéité. La membrane est une partie importante, puisqu'elle sert de protection au bâtiment.

Il existe plusieurs types de TV, qui se différencient principalement par les espèces végétales (les plantes basses, comme la graminée, ou plus grandes, comme les arbustes ou les petits arbres) et l'épaisseur de la couche de substrat de croissance. Les plantes plus diversifiées exigent plus d'espace et des conditions spéciales. Ainsi, le substrat doit fournir un environnement favorable afin que la végétation survive sur le toit, où les conditions sont plus

sévères. Puisque sur les toits, il est même possible de faire pousser des arbres, le substrat doit, dans ce cas, y être assez profond pour maintenir leurs racines.

Le plus simple et le plus léger est un type extensif. Le substrat de croissance d'environ 5 à 10 cm est suffisant pour supporter des plantes simples, comme les graminées ou les sedums. Une telle végétation nécessite peu d'entretien et d'irrigation. Ces systèmes peuvent être installés sur des toits à forte pente et leur masse surfacique, généralement inférieure ou égale à 150 kg/m^2, permet leur installation sur n'importe quel toit. Ces types sont considérés comme durables et écologiques, car peu de ressources sont nécessaires pour les créer et les soutenir. Après l'établissement des plantes, ce toit a besoin de peu d'entretien et peut pleinement remplir ses fonctions pendant de nombreuses années (Fig. 1.2a).

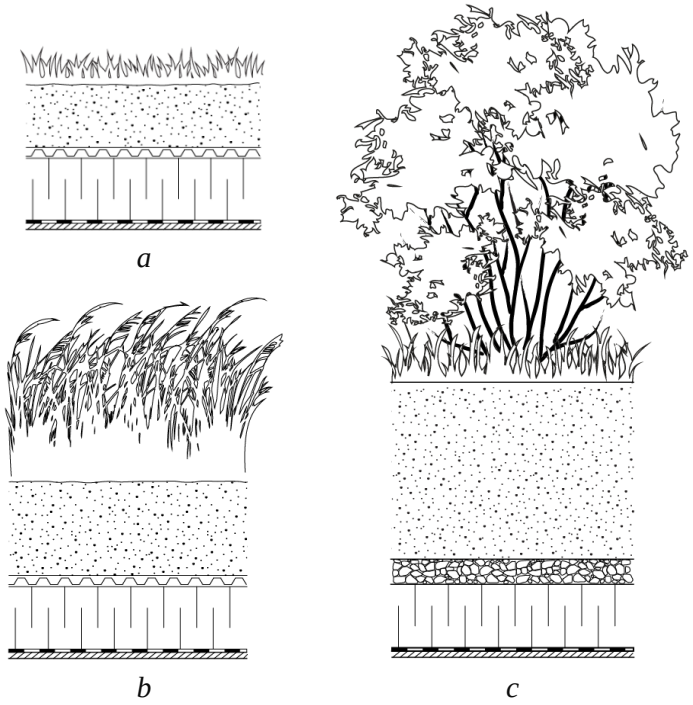

Figure 1.2. Types de TV : (a) Extensive; (b) Semi-Intensive; (c) Intensive.

Un autre type est la TV intensive (Fig. 1.2c). Ce type contient une grande variété de végétation y compris des arbustes et des arbres. Souvent, il représente un jardin ou une terrasse sur le toit. Ces toits ont besoin d'une approche complètement différente. Une vérification minutieuse de la capacité portante au départ et la création d'un plan de maintenance approprié est essentiel pour éviter les défaillances. Contrairement au type extensif, ces toits sont accessibles au public et peuvent servir à des fins récréatives. C'est

pourquoi une grande attention devrait également être accordée à la sécurité. En outre, le processus d'installation nécessite des connaissances spéciales en raison du grand nombre de matériaux et des particularités de la plantation de différentes espèces végétales. Bien sûr, un système d'irrigation permanent doit faire partie du système, et un entretien régulier doit être effectué. Pour toutes ces raisons, de tels systèmes sont beaucoup plus coûteux et laborieux que la TV extensive.

Les toits contenant divers végétaux avec un substrat d'une épaisseur supérieure à 15 cm, mais qui ne peuvent toujours pas être considérés comme des jardins sur le toit en raison de leur masse ou de leur absence d'irrigation, sont entre les types extensif et intensif et se nomment semi-intensifs (Fig. 1.2b).

1.3. Composants

Les deux composants principaux sont la végétation et le substrat de croissance. La possibilité d'installer une grande diversité des plantes donne la liberté de conception et permet de mettre en œuvre des projets incroyables. Cependant, les plantes sont des matériaux organiques et dans des conditions favorables peuvent brûler ce qui engendre un risque pour le bâtiment. L'utilisation des espèces étant considérées de faible combustibilité, pourrait être une solution pour diminuer le risque. Les listes de telles plantes contiennent diverses espèces pour plusieurs climats (Diablo Firesafe Council). Toutefois, il faut comprendre que le terme faible combustibilité signifie que le plant n'est pas très inflammable et par conséquent, sa contribution au feu sera minimale. Ces espèces ont des feuilles possédant une grande teneur en eau, ils contiennent peu de matériaux en résine et ils n'accumulent pas de matériel végétal mort. Cela ne garantit pas que dans les conditions extrêmes, comme lors d'une période de sècheresse, où le taux d'humidité est bas, ces plantes vont retarder la propagation du feu. Pour cela, l'utilisation des espèces à faible combustibilité ne dispense pas du respect des autres mesures de protection incendie pour les TV.

Le substrat de croissance est un matériel complexe nécessitant des connaissances particulières pour préparer un bon mélange. Il doit non seulement fournir un environnement pour la survie des plantes, leur fournir des nutriments et retenir l'eau, mais il doit aussi être conçu pour durer longtemps afin qu'il ne rétrécisse pas avec le temps. Puisque sur le toit les

conditions diffèrent beaucoup de celles au niveau du sol, le substrat de croissance doit répondre à plusieurs exigences communes en plus des considérations particulières selon la situation (climat, pente du toit, espèces de plantes sélectionnées, but d'un projet). Par conséquent, le sol régulier sera impropre. C'est un mélange spécial de sable, d'agrégats et de matières organiques (MO) qui est normalement plus élevé que dans le sol naturel (Fig. 1.3). Une certaine quantité de contenu organique est nécessaire pour maintenir le mélange et fournir une capacité de rétention d'eau. Le compost et la mousse de tourbe sont les matériaux les plus utilisés pour ajouter la MO. La présence de ces matériaux pose également un risque d'incendie, car ils constituent une certaine charge combustible. Il faut noter que le substrat est un matériau assez poreux grâce aux grandes particules de ses composants. Cela donne au substrat une bonne propriété d'isolation.

Figure 1.3. Substrat de croissance typique.

Les autres composants obligatoires de l'assemblage de TV sont le filtre, pour filtrer les particules fines du substrat et de les empêcher d'obstruer le système de drainage, le drainage et la barrière anti-racine.

1.4. La sécurité incendie des toitures végétalisées

On considère généralement qu'en cas de feu, les TV peuvent contribuer à la propagation des flammes et à l'intensité du feu, car les plantes présentent une charge combustible

supplémentaire dans le bâtiment. Dans l'éventualité où les plantes n'ont pas accès à l'eau, elles peuvent sécher, ce qui pose un risque d'incendie (Weiler and Scholz-Barth, 2009). Cependant, dans la réglementation, il n'y a pas de lien direct entre les mesures et le danger réel que ces toits peuvent causer. Il y a eu beaucoup de recherches sur la réponse des plantes aux feux de forêt, la vitesse de propagation des flammes dans les prairies et leur contribution à l'intensité du feu. Ces études peuvent servir de guide pour étudier le comportement des TV. Cependant, il faut prendre en compte que les conditions environnementales sur le toit d'un bâtiment sont différentes de celles de la nature. En effet, les surfaces sont beaucoup plus petites, les toitures sont à une certaine hauteur du sol, le comportement du vent et d'autres conditions peuvent différer des conditions dans la nature. Quant à la charge combustible, dans certaines régions, il existe des listes spéciales de plantes connues pour leur combustibilité ou qui fournissent un certain niveau de combustibilité (Diablo Firesafe Council; FireSmart Canada, 2019; Pacific Northwest Extension publication, 2006). Elles sont utilisées dans les climats propices aux incendies lors de la création de paysages à la maison. Pour les TV, ces listes ne sont pas incluses dans les règlementations, probablement parce que l'entretien est beaucoup plus important, car toute plante qui est sèche ou qui n'a pas été taillée peut augmenter le risque d'incendie. On croit parfois que les TV peuvent retarder la propagation du feu s'ils sont installés professionnellement et, plus importants encore, sont régulièrement irrigués. Les premières TV en Allemagne étaient utilisées comme le moyen de réduire le risque incendie (Green Roofs for Healthy Cities, 2013).

On trouve peu d'information sur l'observation du comportement au feu de TV dans un feu réel. Aucun cas connu d'incendies sur les TV ayant causé des dommages importants ou d'incendies ne pouvant être contrôlés en raison de la présence d'une TV ou de l'un de ses composants n'a été trouvé. Cependant, en 2018 deux petits incendies se sont produits dans des toitures couvertes par de la végétation, qui démontrent l'importance de l'entretien et des règles de la sécurité. À Portland (États-Unis) une toiture avec des graminées s'est enflammée par une étincelle tombée d'un transformateur se trouvant à proximité. Puisque la TV était mal entretenue, les graminées ont pris feu facilement. Le feu a été éteint par les pompiers en moins d'une heure. Dans le rapport d'incident, il est mentionné que la graminée était très haute, trop développée et était sèche (Portland Fire Bureau, 2018). L'incendie a causé des dommages légers. À Londres (Grande-Bretagne) une petite TV extensive s'est enflammée et

le feu s'est propagé à un mur vert. Les détails sur cet incident ne sont pas disponibles, mais il est évoqué que le feu a pris naissance possiblement à cause d'une cigarette ou d'une allumette. Le mur et presque tout le platelage ont été détruits. La Fig. 1.4 montre la végétation brulée, une partie du platelage d'un toit et une partie d'un mur endommagé par le feu. L'incendie a été éteint par les pompiers.

Un cas d'incendie s'est produit en Autriche en 2016. Il est à noter que l'incendie n'était pas sur une TV, mais a commencé, pour une raison inconnue, dans un lierre autour d'une colonne dans une façade d'un ancien bâtiment d'école (Fig. 1.5). Le feu s'est propagé rapidement vers le haut de la colonne et en peu de temps presque tout le toit était en feu. L'accident a causé des dommages énormes. Le montant total des dommages a été évalué à 15 millions d'euros (meinbezirk.at, 2016). Néanmoins, ce cas est un bon exemple du risque de propagation du feu que les plantes peuvent porter, en particulier celles qui sont hautement inflammables comme le lierre. Une attention particulière à la sécurité incendie doit être portée lors de l'aménagement de végétation sur les façades et les toitures de vieux bâtiments.

Figure 1.4. L'incendie sur le toit à Londres, UK,
Source: twitter.com/LondonFire/status/1027435305744261120.

Figure 1.5. L'incendie au château d'Ebenzweier en Altmünster, Autriche, *Source: www.salzi.at.*

1.4.1. Recherches allemandes

Les premières recherches sur la sécurité incendie des TV ont été menées en 1988 en Allemagne avec des tests à grande échelle. C'était un vaste programme de recherche sur la propagation du feu. Les résultats des tests sur l'assemblage avec une couche du substrat de 5 cm d'épaisseur n'ont montré aucune propagation horizontale du feu, ni vers le bas. La température sur la couche filtrante, c'est-à-dire en-dessous de la couche du substrat, était seulement de 40°C après 30 min d'exposition à la chaleur, même si à la surface elle atteignait 300°C. Dans l'essai avec la végétation, les flammes s'étaient auto éteintes après 2 minutes. Des assemblages sur la résistance à la chaleur rayonnante et aux brandons volants ont également été testés (Appl, 2011). Dans un autre essai sur l'inflammabilité, un toit extensif avec de la graminée sèche a été comparé avec une membrane d'étanchéité bitumineuse. Il a été démontré que la TV avait produit 15 fois moins de chaleur pendant la combustion (Breuning, 2008). On retrouve peu d'information sur ces recherches, mais elles ont tout de même servi de base aux règlements de sécurité incendie pour de tels systèmes dans le tout premier guide au monde FLL (*Forschungsgesellschaft Landschaftsentwicklung Landschaftsbau*), lequel est toujours pertinent et dans lequel peu de changements y ont été faits depuis. Une série de règles ont été développées, à la suite de quoi une TV sera considérée

comme un *hard roof*. Ce terme signifie, que le toit est résistant aux brandons volants et à la chaleur rayonnante, indépendamment de la pente du toit (DIN 4102-4 2016, 5. 195). Spécifiquement, ces toits doivent contenir une couche du substrat de la composition minérale spécifique de minimum 3 cm d'épaisseur, être composés de végétation présentant un faible risque d'incendie, avoir les zones de séparations autour de toutes les ouvertures sur un toit d'au moins 0.5 m de largeur, avoir une barrière d'au moins 0.3 m de hauteur ou une zone de séparation de 1 m pour subdiviser le toit en zones, sans qu'aucun côté de ces zones ait plus de 40 m. Ce fut une étape importante, car les TV ne pouvaient être classées et incluses dans la liste des revêtements considérés comme « résistants au feu ». Les règlements comprenaient des limites sur l'épaisseur du sol, les zones de séparation du feu et le pourcentage de constituants organiques.

1.4.2. Recherches britanniques

Une autre recherche a été faite récemment en Grande-Bretagne (Department for Communities and Local Government, 2013). Plusieurs tests ont été réalisés pour évaluer les risques d'incendie en fonction des exigences locales en matière de sécurité incendie. De même, la possibilité d'inflammation a été évaluée ainsi que la pénétration du feu à travers le substrat de croissance. Cette recherche n'incluait pas de couverture végétale; une attention a été portée à un substrat et à une concentration et un type de matière organique dans celui-ci. Des expériences sur l'inflammabilité d'un substrat complètement sec ont démontré que l'inflammation se produisait seulement à plus de 50% du contenu organique, une proportion anormalement élevée pour une TV. Dans les échantillons avec un substrat de composition standard où l'inflammation est apparue, la flamme n'a pas été soutenue. La condition de chaleur dans le test n'est pas indiquée. Un autre test à grande échelle avait pour but de déterminer si le feu pouvait se propager vers le bas à travers un assemblage de TV dans un bâtiment. Les échantillons du substrat de 8 cm d'épaisseur avec différentes quantités de la MO ont été exposés à la chaleur pendant 1 h. Pour les températures en dessous, les substrats enregistrés à la fin d'un essai n'ont pas dépassé 100 °C, sauf le substrat complètement sec constitué uniquement d'humus de feuilles (compost composé de feuilles d'arbustes et d'arbres), où la température était 218 °C. Toutefois, cette température n'est pas suffisante pour affecter les autres couches en dessous dans un assemblage de TV, car le point d'allumage

de ces matériaux est plus élevé. À la suite de cette recherche, quelques recommandations ont été faites pour les zones de séparation, l'épaisseur de la couche de sol et la quantité de matière organique.

1.5. Dégagements contre la propagation de l'incendie pour les toitures végétalisées

1.5.1. Au Québec

De nombreux pays ont pris les règles allemandes comme base pour leurs guides en les ajustant aux réglementations locales pour la construction et aux conditions climatiques. En 2015, la Régie du bâtiment du Québec (RBQ) a élaboré son guide pour le Québec, faisant référence à un ensemble de normes et de règlements locaux et étrangers. La partie sur la sécurité incendie constitue l'une des sections les plus complexes, car elle ne tienne pas seulement compte de l'assemblage de TV, mais aussi des murs adjacents et du type de revêtements sur lesquels elles sont installées, la membrane d'étanchéité, le type de construction, le type de couverture et de la composition d'un substrat de croissance. Selon les intervenants du milieu, ces règles créent toutes sortes d'obstacles, parfois tels que la question de faire ou non un projet se pose, ou encore ces règles ne permettent pas de créer le plan désiré.

Tout d'abord, les zones stériles doivent être disposées autour du périmètre et de toutes les ouvertures, telles que les drains, les évents, les tuyaux, les conduits, les antennes. La distance doit être d'au moins 0.5 m. Il faut également installer une bande d'une largeur de 0.9 m autour de l'équipement mécanique, les trappes d'accès, les cheminées, l'axe d'un mur coupe-feu, les murs extérieurs et toutes les structures sur le toit. De plus, une zone de séparation de 1.8 m de largeur doit exister entre la végétation et les matériaux combustibles, tels que les lanterneaux, et doit également séparer de grandes surfaces de toit couvertes de plantes (maximum 1450 m^2) ou 39 m la longueur maximale de côté. Toutes ces zones doivent être recouvertes de matériaux incombustibles, tels que du gravier ou dalles de béton (RBQ, 2015). Dans le cas d'un petit toit ou d'un toit de forme inhabituelle (forme allongée et étroite, voire en zigzag), ou s'il contient beaucoup de sorties, les zones de séparation peuvent occuper une grande surface, parfois plus grande que celle laissée à la végétation. Évidemment, toute la beauté de la TV sera perdue. Les séparations sont importantes pour l'entretien d'une

membrane et des sorties, cependant, la réduction de taille de ces zones, par exemple autour des trappes d'accès ou le long du périmètre ne devrait pas poser de risque. D'autres limitations incluent la hauteur de la plante et l'épaisseur d'un substrat (10 cm minimum).

Ensuite, le guide de la RBQ contient des règles pour les toits inversés séparément. Il mentionne que dans le cas où une TV doit être installée sur un type inversé et qu'il remplacera le lest (un gravier sur un isolant), seulement deux types d'assemblages sont autorisés, avec des graminées et des plantes succulentes, comme deux systèmes « résistants au feu » selon la norme ANSI/SPRI VF-1 (2010). Si une autre végétation est prévue, une couche de gravier doit être utilisée. Comme les TV sont souvent installées sur un bâtiment existant, le gravier est un poids supplémentaire avec lequel la structure n'a pas été calculée à l'origine.

Si les règles du guide ne sont pas respectées, il faut demander de mesures équivalentes à la RBQ. Par exemple, la preuve que d'autres assemblages empêchent la pénétration de la chaleur dans la structure du toit et la propagation de la flamme. Cependant, cette procédure prend beaucoup de temps et peut être risquée et coûteuse, car la demande peut être rejetée ou des modifications peuvent être exigées.

Enfin, il est interdit d'installer des TV sur de bâtiments de construction combustible (ex : constructions à ossature de bois). L'une des raisons, est l'obstacle au travail des pompiers. Lors d'un incendie dans les structures à ossature de bois, l'une des tactiques de lutte contre l'incendie est de faire des ouvertures dans le platelage pour la ventilation du vide sous le toit. La couche de substrat avec végétation rend cette procédure difficile à faire et ce, peu importe le type de construction du bâtiment (combustible ou incombustible). Peu de choses sont dites à ce sujet, mais les constructions en bois sont de plus en plus populaires, ainsi que les systèmes de TV, et cette limitation empêche la création de nouveaux projets intéressants. La permission peut être obtenue via une demande de mesure équivalente à la RBQ, mais, comme déjà mentionné, cela demande beaucoup de temps et d'efforts.

1.5.2. Aux autres pays et régions

Pour comprendre l'ampleur de ces limitations, la comparaison avec d'autres pratiques devrait être faite. Les règlements au Québec sont décrits plus en détail que n'importe où ailleurs. Le guide allemand FLL inclut des règles pour les zones de séparation, mais les dimensions sont plus petites. Là où la réglementation locale prescrit 0.9 m, le FLL permet 0.5 m. Certains

pays européens suivent les règles allemandes et gardent les mêmes distances, cependant le guide de Toronto et le système de TV FM 1-35 (FM Global, assureur américain) précisent aussi 0.9 m (FM Global, 2011; Toronto Municipal Code, 2017; Guide). De plus, la norme américaine ANSI/SPRI VF-1 requiert 1.8 m autour de toutes les structures et équipements sur le toit, conformément aux exigences du *International Fire Code*, où pour les TV la séparation d'une telle largeur est nécessaire autour des équipements mécaniques, les équipements relatifs au contrôle des fumées, les lanterneaux, les panneaux solaires, les supports d'antenne et l'équipement de service de construction (ANSI/SPRI VF-1, 2010; IFC, 2012). La zone de séparation entre deux zones, qui doit être de 1.8 m, en Allemagne ne peut être que de 1.0 m de large ou remplacée seulement par une barrière de 0.3 m de hauteur. Certains pays, comme la Suisse et l'Autriche, des pays leaders dans l'installation de TV ayant ces couvertures dans les normes nationales de construction (depuis 2013 en Suisse et depuis 2010 en Autriche), ne comprennent pas de dispositions spéciales pour la sécurité incendie sur les TV, se référant aux règles générales de sécurité incendie sur tous les toits.

En ce qui concerne le type de structure de toit, il est mentionné dans le document FM qu'une TV ne peut être installée que sur des platelages en métal ou en béton. D'autres guides, comme le guide allemand, autrichien, français et d'autres villes au Canada et la norme VF-1, permettent les trois types de platelages de toit, soit en métal, en béton ou en bois, ou ne mentionnent pas ce détail (Toitures Végétalisées, 2012; ÖNORM L 1131, 2010; Zelené střechy, 2016; Energie Cités, 2014). Contrairement au guide du Québec, les règlements d'autres régions autorisent l'installation sur des bâtiments de construction combustible ou n'incluent aucune information à ce sujet (Toronto Municipal Code, 2017; The council of the city of Vancouver). À Montréal, par exemple, deux types de TV ont été développées : un premier type avec le substrat de croissance d'au plus 15 cm d'épaisseur (comme le toit extensif) et un deuxième type, qui a plus de 15 cm de substrat (toit semi- et intensif). L'installation de TV sur les bâtiments de construction combustible est permise sous deux conditions :

- l'aire de la partie de toit couverte par végétation ne doit pas dépasser 300 m^2 et
- la TV est de type 1 (c'est-à-dire une TV dont le substrat de croissance a une épaisseur d'au plus 15 cm).

Une faible épaisseur des couches et une petite hauteur des plants n'empêcheront pas le travail des pompiers sur le platelage. De plus, les deux types sont permis dans les constructions incombustibles avec toiture en gros bois d'œuvre. Dans le cas où il y aurait une comble, il faut créer des ouvertures dans le platelage de toit pour permettre l'évacuation des gaz et de la fumée (Ville de Montréal, 2014). Néanmoins, ces règles sont écrites seulement pour les bâtiments qui sont exemptés de l'application de Code de construction et qui tombent sous la juridiction de la Ville de Montréal.

Quant au contenu organique dans un substrat, il est autorisé au Québec jusqu'à 35% pour le type conventionnel et de moins de 20% pour le type de toit inversé. Dans les normes américaines, l'exigence est similaire, 20% en masse pour le type extensif « résistant au feu » selon VF-1, de 8% à 25% dans *FM Sheet* pour le type extensif et jusqu'à 40% pour le toit intensif. En Europe les règles sont les suivants : le guide allemand autorise 90 g/l pour un toit intensif et 65 g/l pour un toit extensif, ce qui est environ 6-9% et 4-6% en masse respectivement. La Suède suit les règles de FLL et suggère de ne pas dépasser 5% de MO en raison d'un risque d'incendie. L'Autriche 5 à 15% pour les toits intensifs et 3 à 5% pour les toits extensifs en masse. En Suisse (Lausanne), il est suggéré d'ajouter 5 à 10%, maximum et 20% est permis au Royaume-Uni (FLL, 2008a; GRÖNATAKHANDBOKEN, 2017; ÖNORM L 1131, 2010; Ville de Lausanne, 2014; GRO, 2011). Par conséquent, au Québec, les exigences relatives à la quantité de matière organique ne sont pas aussi strictes. Cependant, il existe des exigences concernant le type de matière organique.

1.5.3. Sources

Les dispositions dans tous les guides et toutes les normes diffèrent parfois beaucoup, particulièrement entre les guides européens et nord-américains. Cependant, l'analyse du guide du Québec indique qu'il contient plus de règles et plus de détails, rassemblant toutes sortes de mesures de sécurité incendie, qui se superposent les unes aux autres, comme dans le cas de toits inversés. Le guide a été rédigé en référence à de nombreux documents sur la sécurité-incendie, y compris des guides de l'Allemagne, des villes de Montréal et de Toronto, de la norme ANSI/SPRI VF-1 et de FM Global.

Les zones de séparation sont une mesure importante pour empêcher la propagation du feu dans le bâtiment, car à travers les ouvertures sur le toit, le feu peut entrer dans le bâtiment.

Comme la végétation est considérée comme un matériau inflammable, elle doit être isolée de toutes les parties du bâtiment susceptibles de prendre en feu. Les guides européens acceptent des dimensions plus petites pour ces zones que les guides américains. Il n'est pas étonnant que le guide québécois suive les règles américaines de FM Global, car le climat européen est très différent. Entre autres, parce que la végétation est placée directement sur le toit, pas dans des pots, la TV est considérée comme une couverture. Dans les règlements de construction l'exigence pour toutes les couvertures est qu'elles doivent être d'une certaine classe de résistance au feu, A, B ou C. Comme les TV ne peuvent pas être classées, l'exigence concerne seulement la couverture sur laquelle les couches de TV sont installées et cette couverture doit avoir une classe A uniquement. Cela permet d'éviter de faire des tests pour chaque assemblage de TV.

1.5.4. Normes pour les couvertures

Au Canada, la classe de couverture doit être conforme à la norme CAN/ULC-S107 « Méthode normalisée d'essai de résistance au feu des matériaux de couverture ». Il y a trois classes A, B et C, où la couverture de classe A est plus résistante que les couvertures de classes B et C. Cela signifie qu'elle doit être efficace dans le cas d'exposition à un incendie intense. Ce test contient trois parties pour déterminer trois caractéristiques différentes d'une couverture. Elles ne doivent pas s'enflammer facilement, doivent offrir un degré assez élevé de protection du platelage de toit, demeurer en place et résister à la production de brandons volants. La première partie est le test d'inflammation par flammes intermittentes. Dans ce test, la flamme est appliquée de façon intermittente, avec les intervalles entre les applications. Pour la classe A, la flamme est appliquée pendant 2 minutes, puis est retirée pendant 2 autres minutes. La température moyenne de la flamme doit être de 760 °C. Il y a 15 cycles pour cet essai. L'échantillon passe ce test s'il n'y a pas d'apparition de flammes soutenues à la sous-face du platelage. La deuxième partie est un essai de résistance à la propagation de la flamme. L'essai consiste à allumer une flamme à l'extrémité de la maquette avec l'application de courants d'air par un ventilateur, puis à observer la distance à laquelle la flamme se propage. Pour la classe A, cette distance ne doit pas être plus de 1.80-1.83 m. C'est pourquoi dans les règles, il faut arranger cette distance entre le recouvrement végétalisé et tout matériau combustible et entre les parties de TV. De plus, la couverture ne doit pas former de brandons

enflammés ou de particules qui continuent à brûler. La dernière partie est un test de résistance aux brandons. Les blocs de bois enflammés sont placés sur la surface de la maquette. Les dimensions de brandons pour la classe A sont plus grandes 30 x 30 x 5.7 cm (Fig. 1.6). L'essai se termine lorsque le brandon est entièrement brulé. Pour passer ce test, le platelage ne doit pas être affecté (CAN/ULC-S107, 2010).

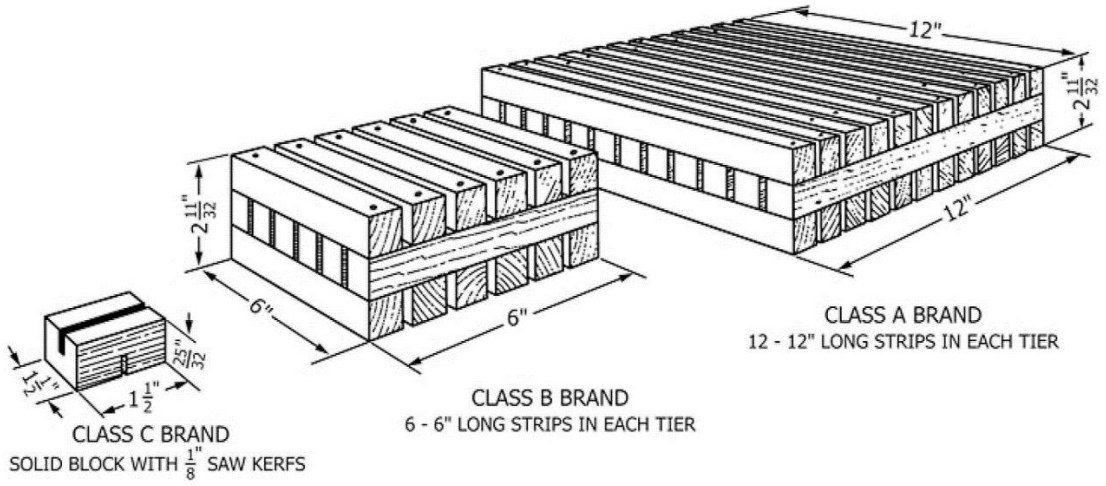

Figure 1.6. Les brandons normalisés (tirée de ASTM E108, 2017).

Au Québec, les deux types de toits (inversés et conventionnels) sont largement utilisés. Parce qu'ils diffèrent de manière significative dans leur comportement, le guide spécifie des exigences différentes pour ceux-ci. Pour un type inversé, certains détails ont été pris à partir de la norme VF-1 dans un cas particulier seulement, lorsque le lest de gravier est retiré. Sans le lest, la couverture n'est plus considérée comme classe A. Comme le gravier est un matériau incombustible qui protège bien le toit, il est présumé qu'il n'y a pas de danger qu'un toit recouvert de graviers s'enflamme à l'extérieur et propage le feu (FM Global, 2012). Sans une couche de gravier, les matériaux combustibles d'un revêtement (isolant, membrane) sont adjacents aux couches de TV, qui sont également combustibles (panneaux de drainage en plastique, sol contenant des matières organiques, couverture végétale). Cela crée un risque que l'assemblage qui brûle contribue à l'intensité du feu, à sa propagation à travers la surface et à la pénétration sur le toit. Mais à la différence des couvertures typiques les TV ne peuvent pas être classées de résistance au feu et doivent être testées dans chaque cas individuel. Dans les documents de FM Global, la solution consiste à interdire l'installation d'une TV sur un platelage en bois. Au Québec il est interdit d'installer les TV sur les bâtiments de construction

combustible. De plus, l'épaisseur d'un sol doit être supérieure à 10 cm. Bien que cette règle ne soit pas liée à la sécurité incendie, mais aux conditions nécessaires à la survie des plantes dans le climat local, il s'agit probablement d'une couche assez épaisse pour protéger de la pénétration de la chaleur, contre seulement 3 cm exigé en Allemagne, qui est directement lié à la sécurité incendie selon leurs recherches. D'un certain point de vue, les exigences sont doublées. Une autre chose dans ce cas concerne la propagation du feu à la surface, lorsque seulement deux types de systèmes végétatifs décrits par VF-1 sont autorisés parce qu'ils sont résistants au feu. Cette règle peut être considérée comme en super-imposition sur une règle quant aux distances de séparation. Néanmoins, alors que des règles de sécurité doivent être établies sur la base de sources fiables, telles que des normes ou des documents de recherche, il n'y a pas eu suffisamment de recherches pour des situations spécifiques de TV en feu.

En résumé, cette description des règles n'est qu'une comparaison superficielle de quelques dispositions exclusivement pour les TV. Pour connaître la taille des restrictions au Québec par rapport à d'autres villes ou pays, il est nécessaire de connaître les codes du bâtiment nationaux et provinciaux, et non seulement pour les TV, mais également les procédures d'obtention de permission pour l'installation de structures non spécifiées dans les règles. Le plus grand obstacle est la durée de la procédure d'obtention de permission. Mais indépendamment de cela, les règles locales entravent le développement de ces systèmes, et cette situation démontre qu'il est nécessaire d'étudier davantage le comportement des TV lors d'un incendie.

1.6. Objectifs

L'objectif principal du projet est d'approfondir les connaissances sur les systèmes de toitures végétalisées en termes de sécurité incendie.

Les objectifs spécifiques de recherche sont :

1. Déterminer les paramètres thermiques du substrat de croissance.
2. Analyser la propagation du feu à travers des systèmes de toitures végétalisées par modélisation.
3. Déterminer les propriétés d'inflammabilité d'un toit végétalisé.
4. Analyser le risque d'incendie des toitures végétalisées pour les bâtiments adjacents.

CHAPITRE 2 : Rétrospective méthodologique

2.1 Caractérisations des Risques

2.1.1. Transfert thermique

Dans la construction, l'un des moyens pour réduire le risque d'incendie vise à contrôler le déplacement du feu et de prévenir l'effondrement causé par les hautes températures (NFPA, 2012). Ainsi, dans la conception de bâtiment il est important de s'assurer que certains éléments structuraux et séparatifs sont capables de résister à la propagation du feu et de maintenir l'intégrité structurale lorsqu'ils sont exposés au niveau de la sévérité du feu spécifié pendant un certain temps. Pour cela, la résistance au feu d'un élément doit être plus grande que la sévérité en la comparant dans l'un des trois domaines : le temps, la température et la résistance mécanique. La comparaison dans le temps est la méthode la plus utilisée dans la construction. Cela signifie que le temps de défaillance d'un élément doit être plus grand que la durée de l'incendie standard. La résistance au feu d'un élément dépend notamment de sa capabilité de transfert de la chaleur. L'une des étapes d'évaluation de ce paramètre est l'analyse thermique, c'est à dire la détermination d'un profil de température développé dans un élément pendant l'exposition à des températures élevées.

Dans la construction, la résistance au feu pour les toitures est évaluée pour l'exposition au feu provenant du côté intérieur. Cependant, si une TV sur le bâtiment prend feu, elle présente un risque provenant de l'extérieur. Puisque la TV est installée directement sur la structure du toit, dans le cas d'incendie sur sa surface cette structure peut être endommagée par les hautes températures, c'est-à-dire la chaleur qui est transférée à travers les couches de TV. Pour cette raison, l'analyse de transfert de la chaleur à travers une TV peut démontrer s'il y a un risque pour la structure d'un toit et dans quelle condition ce risque peut survenir. Cette analyse est présentée dans le Chapitre 4.

2.1.2. Propriétés thermiques

Dans les matériaux solides, la chaleur est transférée par la conduction. L'analyse thermique de l'assemblage de TV nécessite les propriétés thermiques et physiques des matériaux telles que la conductivité thermique, la capacité calorique spécifique et la masse volumique. Le substrat de croissance est un matériau composite et complexe pour lequel ces données

peuvent varier en fonction des propriétés des composants et de leurs proportions dans le mélange. De plus, ces propriétés peuvent changer en fonction de la température. Ainsi, il y a une nécessité de préalablement déterminer les propriétés du substrat pour les utiliser comme paramètres d'entrée dans l'analyse de transfert de la chaleur. Le test de validation peut assurer que les valeurs obtenues sont appropriées pour l'utilisation. Cette partie de la recherche est présentée dans le Chapitre 3.

2.1.3. Combustible

Pour analyser le risque d'incendie dans un bâtiment, il faut comprendre la nature du feu, le dommage qu'il peut causer et ses méthodes de propagation. La combustion est une réaction chimique en chaîne, qui nécessite trois composants dans les proportions nécessaires pour sa soutenance : le combustible, le comburant (oxygène) et la chaleur (Fig. 2.1). En retirant l'un des composants, la réaction est arrêtée et le feu s'éteint.

Le combustible est un matériau qui brûle et qui nourrit le feu. Ses propriétés comme la densité, la teneur en eau, la distribution, la composition chimique, le pouvoir calorique, ainsi que la quantité (masse) sont importants pour caractériser et prédire le développement d'un feu. Dans la construction, les paramètres des objets combustibles, comme les meubles, les éléments de finition intérieure et de la structure, peuvent fournir une information sur la gravité de l'incendie possible et sur les actions nécessaires pour la protection. Cela peut aussi être utilisé pour la prédiction du développement de la température et de la durée de l'incendie. Les paramètres principaux sont la charge combustible et la densité de la charge combustible, qui sont le contenu énergétique et sa quantité par unité de surface. Un autre paramètre est le débit calorifique, qui est un indicatif de la vitesse à laquelle la réaction de combustion se produit. Il est exprimé en quantité d'énergie par unité de temps (Babrauskas, 2016b).

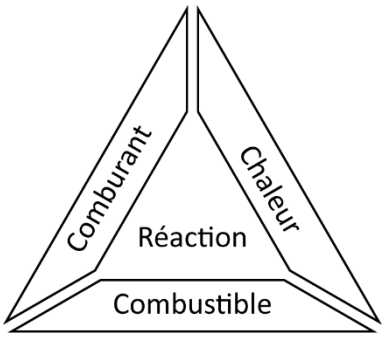

Figure 2.1. Les composants du feu.

C'est pour cela que dans cette étude une attention particulière est accordée à la caractérisation de l'inflammabilité des matériaux de l'assemblage de TV, tel que présenté au Chapitre 5. Les composants de TV sont majoritairement des matériaux combustibles. Cependant, seulement les couches supérieures, le substrat de croissance et la végétation, doivent être analysées. Il est possible de calculer la charge combustible en connaissant la quantité et le pouvoir calorifique d'un matériau. Le débit calorifique peut également être déterminé à partir du pouvoir calorifique et de la vitesse de perte de masse du matériau pendant la combustion. Les données standards peuvent être trouvées dans les listes pour les matériaux communs. Cependant, la MO dans le substrat peut être un mélange de plusieurs matériaux, ce qui rend difficile de trouver les valeurs correctes. De plus, les recherches précédentes sur l'inflammabilité du substrat de croissance ne contiennent pas les données mesurées. Dans cette recherche, les paramètres d'inflammabilité de substrat sont déterminés expérimentalement pour ce qui est utilisé au Québec. Pour la partie végétalisée de TV, l'analyse des données existantes sur l'inflammabilité et la charge combustible de différents types de végétation est faite. Les données sont trouvées dans les recherches sur l'inflammabilité des plants et des différentes espèces.

2.1.4. Propagation du feu

La présence des matériaux combustibles sur un bâtiment, comme la végétation, peut également poser un risque d'incendie pour les bâtiments adjacents. Une fois amorcé, par exemple par une étincelle, le feu peut se développer et se transmettre à d'autres structures dans des conditions favorables.

Il existe trois modes par lesquelles les flammes peuvent se propager. Pendant la combustion, certains matériaux comme les plants, peuvent produire des brandons, des particules d'un matériau qui brûle. Ces particules peuvent être transportées par le vent aux autres surfaces et peuvent causer leurs allumage (Fig. 2.2a).

Un autre mode de propagation du feu est par le contact direct avec les flammes (Fig. 2.2b). Finalement, le rayonnement thermique est un flux de chaleur produit par les flammes pouvant

a

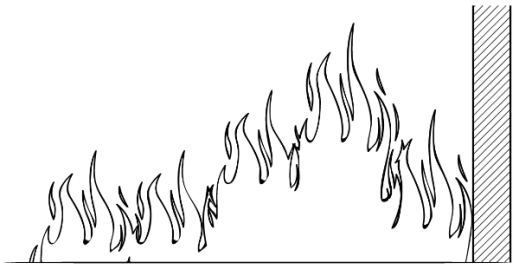

b

c

Figure 2.2. 3 modes de propagation du feu : (a) Brandons volants; (b) Contact direct avec la flamme; (c) Rayonnement thermique.

causer l'allumage d'un objet situé à distance quelconque de la source de chaleur (Fig. 2.2c). Ce mode est le mode principal de propagation du feu aux bâtiments adjacents.

Par conséquent, il est important d'explorer la possibilité d'allumage des façades des bâtiments voisins qui sont exposées au feu dans la TV. La compréhension des possibilités du feu ainsi que de ses paramètres pendant la combustion des plants de TV peuvent être trouvés dans le domaine des feux de végétation. Les méthodes de prédiction de comportement au feu dans la nature peuvent être utilisées pour obtenir les paramètres nécessaires. Ensuite, l'évaluation des risques de propagation du feu par rayonnement thermique peut être effectuée. Les conditions environnementales et le type de plants sont des facteurs importants à considérer. Cette étude est présentée dans le Chapitre 6.

Analyser les risques d'incendie dans les TV est un sujet complexe, qui combine l'étude sur la sécurité incendie dans la construction et le comportement au feu dans la végétation. La caractérisation des propriétés thermiques du substrat de croissance doit être également incluse dans cette recherche. Le problème concerne deux aspects, qui sont le risque pour le bâtiment sur lequel la TV est installée et le risque pour les bâtiments voisins.

CHAPITRE 3 : A Conceptual Framework for Modelling the Thermal Conductivity of Dry Green Roof Substrates

BioResources, 2019, Vol. 14 (4), 8573–8599

Nataliia Gerzhova[1], Jean Côté[1], Pierre Blanchet[1], Christian Dagenais[1,2], Sylvain Ménard [3]

[1] NSERC Industrial Research Chair on Eco-responsible Wood Construction (CIRCERB), Department of Wood and Forest Sciences, Université Laval, Québec, QC, Canada
[2] FPInnovations, Quebec, QC, Canada
[3] Université du Québec à Chicoutimi (UCAQ), Chicoutimi, QC, Canada

3.1. Résumé

Le comportement au feu des toits verts n'a jamais été évalué numériquement. Afin de simuler son comportement au feu, la conductivité thermique d'un substrat de croissance doit être déterminée comme un paramètre d'entrée important. Cette étude a caractérisé la conductivité thermique d'un substrat sec et sa prédiction en fonction de la température, tout en considérant les effets de la température sur les constituants organiques et inorganiques du substrat. Des mesures expérimentales ont été effectuées pour fournir des informations de base sur les paramètres thermophysiques du substrat et de ses composants. Une analyse thermogravimétrique a été réalisée pour considérer la décomposition de la matière organique. Un modèle existant du calcul de la conductivité thermique a ensuite été appliqué. Les résultats de la conductivité thermique des particules solides calculée et mesurée ont montré des valeurs proches de 0.9 et 1.07 W/(m·K), ce qui démontre que le modèle a fourni une bonne estimation et peut être appliqué pour les calculs de substrats de toit vert. Les données de la littérature sur un effet de la température sur les solides du sol ont été utilisées pour prédire la conductivité thermique sur une gamme de températures. Les résultats ont montré que la conductivité thermique augmentait et dépendait de la porosité et des propriétés thermiques des composants minéraux du substrat. La validation préliminaire de la conductivité thermique en fonction de la température obtenue a été réalisée par des expériences et une simulation numérique.

Mots-clés : Toiture végétalisée; substrat de croissance; substrat de toit vert; conductivité thermique; haute température

3.2. Abstract

The fire performance of green roofs has never been assessed numerically. In order to simulate its fire behavior, the thermal conductivity of a growing media must be determined as an important input parameter. This study characterized the thermal conductivity of a dry substrate and its prediction as a function of temperature, considering temperature effects on soil organic and inorganic constituents. Experimental measurements were made to provide basic information on thermophysical parameters of the substrate and its components. Thermogravimetric analysis was conducted to consider the decomposition of organic matter. An existing model of the thermal conductivity calculation was then applied. The results of calculated and measured solid thermal conductivity showed close values of 0.9 and 1.07 W/(m·K), which demonstrates that the model provided a good estimation and may be applied for green roof substrates calculations. The literature data of a temperature effect on soil solids was used to predict thermal conductivity over a range of temperatures. The results showed that thermal conductivity increased and depended on porosity and thermal properties of the soil mineral components. Preliminary validation of obtained temperature-dependent thermal conductivity was performed by experiments and numerical simulation.

Keywords: Green roof; Growing medium; Green roof substrate; Thermal conductivity; High temperature

3.3. Introduction

The technology of green roofs was developed several decades ago (Dunnett and Kingsbury, 2008). Numerous research studies have investigated the advantages of such roofs over conventional roofs. Installing such roofs on buildings has a positive impact on the urban environment and on the building itself, mainly as a tool to reduce energy consumption (Becker and Wang, 2011; Jaffal *et al.*, 2012; Saadatian *et al.*, 2013). Promoting green roof installation is essential for the development of this technology, as its effectiveness for the improvement of environmental conditions (urban heat island mitigation, purifying air) can

become significant only under the condition of widespread use (Yang *et al.*, 2008; Pompeii II and Hawkins, 2011). However, the security of this technology in terms of fire safety has not been assessed scientifically yet. There is a common belief that a vegetated roof may protect the house, preventing the spread of fire. Although not supported by scientific evidence, such an opinion is not surprising, considering that plants consist of up to 95% water. Moreover, organic soils usually contain some amount of water in natural conditions, and they rarely dry out completely. However, regulations for such roofs in the province of Quebec, Canada, contain extensive provisions for fire protection (RBQ, 2015). Together with the organic part of growing medium, plants compose a fuel load that may contribute to fire propagation. Especially in hot seasons or drought periods, plants, as well as growing medium, may dry out and ignite easily. This poses a risk to a roof deck made of materials that are susceptible to elevated temperatures (*e.g.*, wood, metal). Given the complexity of testing the fire resistance performance of green roof coverings, numerical modelling of heat transfer through the roof assembly can be considered a useful tool. Studies on heat transfer analysis through green roofs were conducted before by many authors (Ouldboukhitine *et al.*, 2011; Tabares-Velasco and Srebric, 2012; Chen *et al.*, 2015; Quezada-García *et al.*, 2017). The models, however, were developed for normal temperatures, assessing the performance of such roofs in real conditions. Also, particular attention was paid to the effect of moisture present in soil and associated mass transfer problem. To study the performance of green roofs in fire by modelling, their response to extreme temperatures should be analyzed considering temperature-induced changes in materials and properties.

Several previous studies predicting temperature distribution in soil under high heat exposure have been conducted and experimentally verified. Campbell *et al.* (1995) modelled various mineral soils differing in mineralogy, bulk density, water content, and texture, with good predictions of temperatures compared to experimental results. However, they noted that the results depend on the thermal conductivity of soil at elevated temperatures, which was assumed to depend mainly on the changes of the air thermal conductivity in pores. Thermal properties of solid components were assumed to be independent of temperature (Campbell *et al.*, 1994). To determine the temperature distribution in several volcanic soils, Antilén *et al.* (2006) applied some simplifications for the mathematical model, which fitted the measured temperatures. The simplified models used two separate values for the thermal parameters,

below and above 100 °C. They concluded that the thermal characteristics of soil were essential in successful modelling. Suggestions were made for considering thermal decomposition of organic matter (OM), which may influence temperature evolution and thus improve the prediction. Two other studies on predicting temperature profiles during extreme surface heating were conducted on dry sands (Pourhashemi *et al.*, 1999; Enninful, 2006). Both studies were in good agreement with the laboratory measurements, provided that temperature-dependent thermal conductivity was used. Linear relationships of thermal conductivity on temperature were established and found appropriate for simulations.

Developing an adequate heat transfer model for the green roof system thus primarily requires the knowledge of temperature-dependent characteristics of its components. The top layer of a green roof assembly is a growing medium, which is usually a mixture (or "mix") of different inorganic (sand, lightweight aggregate) and organic materials (peat, compost). The resulting engineered soil blends differ from natural soils by having a lighter weight and the presence of recycled materials such as fly ash or building waste (Molineux *et al.*, 2009; Carson *et al.*, 2012). Therefore, existing data on thermal conductivity of natural soils and associated property models may not be representative of green roofs. It is thus necessary to properly determine this parameter that constitutes key input data for thermal modelling. Because the risk of fire ignition and propagation is the highest when the plants and growing medium are dry, characterizing the growing medium in this most hazardous case would be considered conservative for simulation purposes.

Thermal properties of green roof growing media have been studied previously by direct measurements at ambient temperatures. Apart from moisture content, which generally has a huge impact, the various components and their proportions in a mix also have a noticeable effect on the experimental results (Coma *et al.*, 2016). Increasing the amount of organic material or using lightweight aggregates reduces the overall density of soil, which results in lower thermal conductivity (Sailor *et al.*, 2008; Sandoval *et al.*, 2017). There is also a strong dependence of the thermal conductivity on the type of aggregates used in the mix (Sailor and Hagos, 2011). Due to this sensitivity to variations in mixing proportions as well as to components themselves, it is of utmost importance to characterize green roof growing media (green roof substrate) that is typically used in the Province of Quebec (Canada), containing certain components and in certain proportions. Additionally, the effect of heat on the organic

and inorganic part has to be taken into consideration. It is generally known that thermal conductivity of most of the minerals and rocks changes inversely with temperature (Eppelbaum *et al.*, 2014). Loss of the organic matter (OM) due to a thermal decomposition leads to changes in proportions in the mix. Lastly, elevated temperatures may induce sufficient thermal gradients in the dry porous space to initiate interparticle radiation which has the potential to greatly increase heat transfer compared to conduction alone (Fillion *et al.*, 2011).

This study predicted the thermal conductivity of a dry green roof growing medium at different temperatures, considering changes induced by heat on its components and structure, for future computer models of green roof assembly in fire. First, thermal conductivity at ambient temperature was determined and validated, adapting an existing thermal conductivity model for dry soils specifically for a green roof substrate. Secondly, having this value as a starting point, the thermal conductivity as a function of temperature was predicted. The prediction was based on the general tendency of thermal conductivity change with temperature for the minerals, the degradation of OM, and the effect of interparticle radiation. Finally, a preliminary validation was performed to illustrate the performance of the thermal conductivity model over the entire range of temperature during fire.

3.4. Framework for Modeling Thermal Conductivity

3.4.1. Thermal Conductivity of Dry Soils

Thermal conduction in soils is a complex process that occurs through solids, fluid phases, and through the contacts between solid particles (Robertson, 1988). This requires taking several factors into account, such as porosity and shape of grains, which may substantially reduce the effective thermal conductivity. Green roof substrate is highly porous, and heat is transferred much less effectively through its voids, especially in a dry state as air thermal conductivity is only 0.024 W/(m·K) (Bergman and Incropera, 2011). Under such conditions, heat transmission is expected to occur mostly through the solid phase. However, presence of contacts between particles has a certain resistivity, which also weakens heat conduction. Due to this, thermal conductivity depends mostly on the contact parameters (Robertson, 1988).

The estimation of the thermal conductivity of a dry soil can be made using existing models for granular materials. This paper uses the model from Côté and Konrad (2009), as it integrates the effect of structure on the effective thermal conductivity in two-phase geomaterials. The semi-theoretical model allows determination of the effective thermal conductivity from the volume fractions (based on porosity n) and the thermal conductivities of solid and fluid phases,

$$\lambda = \frac{\left(\kappa_{2P}\lambda_s - \lambda_f\right)(1-n) + \lambda_f}{1 + (\kappa_{2P} - 1)(1-n)} \tag{3.1}$$

where λ_s and λ_f (W/(m·K)) are the thermal conductivities of solid and fluid phases respectively. In present study λ_f is the thermal conductivity of air, as a fluid component of a dry soil. The variable κ_{2P} is a dimensionless empirical structure parameter that characterizes the density of contact between particles, which mainly depends on their shape and the presence of cementation. In the study, three types of materials were identified by the shape of their particles, namely rounded (providing a small contact area), cemented (with a good contact), and angular (somewhere between rounded and cemented). For each type of material, the dependency of κ_{2P} on the ratio λ_f/λ_s was experimentally determined. Fig. 3.1 shows that the smaller the thermal conductivity ratio, the lower the values of κ_{2P}. Low values of κ_{2P} in Eq. 3.1 lead to lower values of thermal conductivity. Fig. 3.1 shows that rounded particles have lower values of κ_{2P} and thus greater particle to particle contact resistance compared to angular and cemented particles. Also, decreasing thermal conductivity ratios leads to increased dependency on the particle shape. Structure effect reduces to none at values of κ_{2P} higher than 1:15.

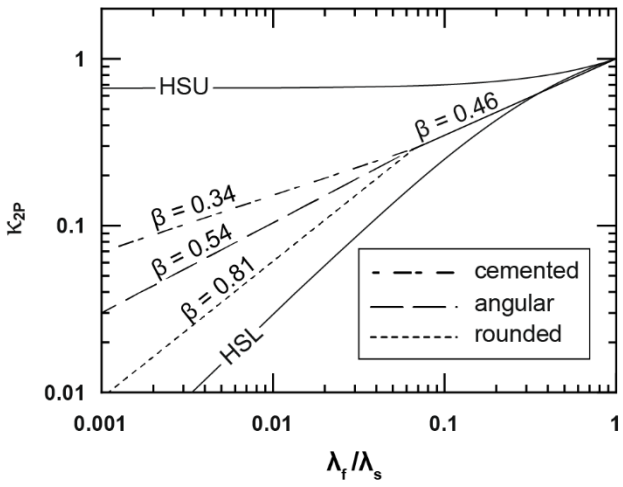

Figure 3.1. Dependence of structure parameter κ_{2P} on the λ_f/λ_s ratio and on the structure (redrawn from Côté and Konrad 2009).

β represents an empirical parameter for the slopes for each type of material, with which κ_{2P} is determined in Eq. 3.2.

$$\kappa_{2P} = 0.29(15\frac{\lambda_f}{\lambda_s})^{\beta} \tag{3.2}$$

All the values of κ_{2P} lay within Hashin–Shtrikman bounds (HSU and HSL) (Hashin and Shtrikman, 1962) applied to thermal conductivity, which represent the upper and the lower bounds of an effective thermal conductivity of a composite material. They are derived based on the shape, volume, and arrangement of particles of one phase with respect to the other. In Fig. 3.1, the upper bound characterizes a material with a continuous solid phase, while the lower bound is for a continuous fluid phase (Côté and Konrad, 2009).

As the presented model was developed for the rock materials without OM, this research laboratory work needs to be carried out first to obtain several thermo-physical parameters of the growing medium. Some results of soil conductivity measurements will also serve to verify the accuracy of the model.

3.4.2. Thermal Conductivity of the Solid Phase

For the model, thermal conductivity of a solid phase is required. For materials consisting of several components, the geometric mean method gives relatively accurate results using thermal conductivities of each mineral components (λ_i) and their volume fractions (x_i).

$$\lambda_s = \prod \lambda_i^{x_i} \quad (3.3)$$

This method is also suitable for soil saturated with water,

$$\lambda = \lambda_s^{1-n} \cdot \lambda_w^n \quad (3.4)$$

where λ is a total thermal conductivity of a soil (W/(m·K)), λ_s is the thermal conductivity of solid material (W/(m·K)), λ_w is the thermal conductivity of water (W/(m·K)), and *n* is the porosity (from 0 to 1). Eq. 3.4 is particularly interesting when the thermal conductivity of the solid phase needs to be assessed when no solid parent rock cores are available for direct measurements. Instead, the thermal conductivity of the solids can be easily back-calculated from the global thermal conductivity (λ) of a mix of solid and water (fully saturated) and by knowing the thermal conductivity of water and by solving Eq. 3.4 for λ_s. This technique will indeed be illustrated later in the paper.

3.4.3. Effect of Temperature

3.4.3.1. Solid particles

Due to several processes taking place simultaneously during burning and the need for fire and temperature proof measuring devices, direct measurements of thermal properties at high temperatures are extremely difficult to conduct. Therefore, this study will rely on existing data from the literature to predict the changes in these properties with temperatures.

Literature contains large amounts of data on thermal properties of rocks and minerals as functions of temperature (Clark, 1966; Cermak and Rybach, 1982; Robertson, 1988). However, as green roof soil is a mixture of different components of different origins, it is difficult to associate it to a particular rock. In this case it would be better to use generalized values.

Variations in thermal conductivity studied by Vosteen and Schellschmidt (2003) were given at temperatures between 0 and 300 °C and showed similar decreasing behavior with temperature for magmatic, metamorphic, and sedimentary groups. Based on the results, they formulated a general equation for temperature dependence for all groups of rocks. Research of Clauser and Huenges (1995) has analyzed existing data for rocks at different temperatures

from several researches on rocks and minerals. They developed curves for four basic groups of rocks for a temperature range from 0 to 800 to 1200 °C. Another study is of Zoth and Haenel (1988), who also collected and examined existing data on rocks, and sorted the results in six groups (salt rocks, limestone, metamorphic rocks, acid rocks, basic and ultrabasic rocks). For each group, a simple formula was given as a mean curve of the results,

$$\lambda(T) = \frac{A}{350 + T} + B \tag{3.5}$$

where constants A and B were provided for each group and T is the temperature (°C). However, if normalizing all groups of rocks with Eq. 3.6, the same slope is obtained and is shown in Fig. 3.2,

$$\lambda_n = \frac{\lambda_T - \lambda_{T2}}{\lambda_{T1} - \lambda_{T2}} \tag{3.6}$$

where λ_n is the normalized value (from 0 to 1), λ_T is the value at a certain temperature (W/(m·K)), and λ_{T1} and λ_{T2} are values at 0 °C and 800 °C (W/(m·K)).

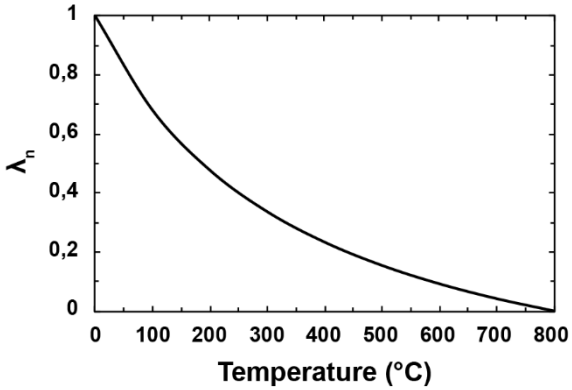

Figure 3.2. Normalized thermal conductivity (λ_n) as a function of temperature.

This normalized relation can be applied for predicting the thermal conductivity of growing medium solids at a given temperature range. However, it requires knowledge of its starting and ending points. Solid thermal conductivity at a reference temperature as a starting point can be modeled with Eq. 3.3. For λ_s at 800 °C, the ratio of thermal conductivities at 0 °C and 800 °C from Zoth and Haenel (1988) may be taken. In their study, the mean curve for all groups of rocks, except rock salts and ultrabasic rocks, was obtained with A and B constants

equal to 770 and 0.7, respectively. From that, λ_{T1} and λ_{T2} are 2.9 and 1.37 W/(m·K), respectively, which gives the ratio of 2.2.

3.4.3.2. Fluid component

As air is a fluid component of soil, changes in its thermal conductivity (λ_f) with temperature must be considered. It increases from 0.024 at room temperature to 0.71 at 800 °C, which is shown in Fig. 3.3 (Bergman and Incropera, 2011).

3.4.4. Effect of Radiation

Another factor that can influence heat conduction in the growing medium may be taken into consideration. Elevated temperature can induce interparticle radiation heat transfer, which flows in the same direction as conduction heat transfer. Howell and Siegel (2010) proposed to mathematically express this process through the diffusion approximation of the Fourier conduction law.

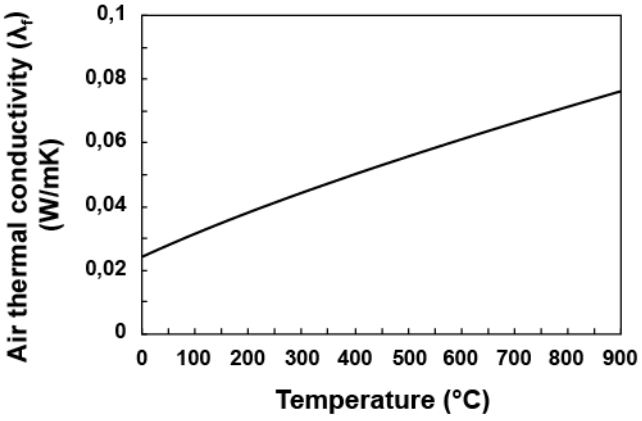

Figure 3.3. Temperature dependence of air thermal conductivity (λ_f).

The effective thermal conductivity λ_e was defined as the sum of the contributions from interparticle radiation λ_{rad} and that from pure conduction λ_c (Tien and Drolen, 1987; Kaviany, 1995).

$$\lambda_e = \lambda_c + \lambda_{rad} \tag{3.7}$$

where λ_{rad} is given by,

$$\lambda_{rad} = 4Ed_{10}\sigma T^3 \tag{3.8}$$

where E is the exchange factor, d_{10} is the particle diameter (m), σ is the Stefan–Boltzman constant equal to 5.67×10^{-8} (W/(m²·K⁴)), and T is the temperature (K). The exchange factor depends on the particle emissivity ε_p (Fillion *et al.*, 2011). Using the equation of Argo and Smith (1953) yielded good prediction (Fillion *et al.*, 2011):

$$E = \frac{\varepsilon_p}{2 - \varepsilon_p} \tag{3.9}$$

3.5. Experimental

To obtain the parameters required to model the thermal conductivity of green roof substrate, several experimental measurements were made. Thermal decomposition analysis was needed to be able to account for the degradation of the organic part of the soil during calculation of the total soil conductivity at elevated temperatures. Also, for the determination of porosities of materials, the densities of solid particles of each component and a soil mix were measured, which then were used to evaluate thermal conductivities of solids. Porosity was determined as,

$$n = 1 - \frac{\rho_{total}}{\rho_s} \tag{3.10}$$

where ρ_{total} is the bulk density (g/cm³) and ρ_s is the density of solid particles (g/cm³).

Finally, measurements of thermal conductivities of growing medium and each of its components were performed.

3.5.1. Materials Preparation

For the laboratory work, a commercially available green roof substrate, commonly used in the Province of Québec, was studied. A typical mix consists of sand, lightweight aggregate (with porous granules), and organic product (in the form of composting material). The total amount of OM is around 20±4% by mass. The mix was tested as is and for some experiments, each component of this mix was tested separately in dry and saturated states. Before experiments in a dry state, soil was placed in an oven at 105 °C for 24 h or until it reached a

constant mass. Afterwards, the soil was placed in plastic bags, sealed, and stored until it was analyzed.

3.5.2. Thermal Decomposition Analysis

To characterize the decomposition behavior of the organic components of the soil, an experimental thermal decomposition analysis was conducted. This test serves to determine the variation of mass with temperature (Todor, 1976). The sample was heated in a furnace at a constant rate under controlled conditions and its mass was continuously recorded yielding a continuous mass-temperature relationship.

Before the analysis, soil was first dried in the oven, and then it was ground into powder in a laboratory sample grinder. The weight of samples was between 17 and 22 mg. The tests were performed by thermogravimetric analyzer Mettler Toledo TGA/DTA 851e (Schwerzenbach, Switzerland). During each test, furnace temperature was raised from 25 to 900 °C with a heating rate of 10 °C/min under air. The experiment was conducted three times with the same conditions.

3.5.3. Density of Solid Particles

Prior to thermal conductivity measurements, it was necessary to know densities of the particles of each material. Small amounts of all samples were saturated with water. Knowing volumes and masses of the sample and water, as well as the density of water, the volume of material can be calculated, from which it is possible to find out the density of solid material ASTM D854-14 (2014).

3.5.4. Thermal Conductivity

3.5.4.1. Sample preparation

The following materials were taken for the experimental part: soil mix and each of its separate components (sand, lightweight aggregate, and compost). Additionally, some modifications were made to these materials, except the sand. First was the removal of the OM from soil mix and compost in a furnace. Soil mix samples in stainless-steel molds were placed into a muffle furnace. Afterwards, the temperature inside the furnace was gradually brought from 25 to 700 °C at a rate of 3 °C/min, and then kept stable for 2 h. Then the samples were taken

out from the furnace, cooled, and sealed. The same procedure was done with the compost following standard test method ASTM D2974 (2014) Method C. A second modification is for the lightweight aggregate. Its granules contain voids. In order to remove them and obtain solid particles, aggregate was pulverized into a powder in a grinder.

3.5.4.2. Equipment

Two different testing methods of measuring thermal conductivity at a given temperature were used for different materials. The choice of method to be used depends on the parameter to be measured and on the type of material as well as sample preparation (effect of structure, saturated *vs* dry conditions, *etc*.). Although the focus of this study was on dry growing medium, testing in a saturated state allowed indirect assessment of the thermal conductivity of solids using Eq. 3.4. A list of all materials, conditions, measurement techniques, and characteristics to determine is presented in Table 3.1.

For the steady state method, the equipment is designed to create one-dimensional heat flux through the specimen by placing it between plates at constant different temperatures. After reaching a steady state for a specimen, the thermal conductivity is then obtained from Fourier's law. Experiments were conducted in a heat transfer cell equipped with heat flux meters that was first described by Côté and Konrad (2005). A cylindrical specimen of approximately 100 mm in diameter and between 50 and 75 mm in height is placed between two heat exchangers. The heat exchangers are connected to an independent temperature-controlled bath. Heat fluxes were measured at both flat ends of the specimen using thermoelectric heat flux meters from Captec, Lille, France. The heat flux meters were equipped with five independent thermocouples for simultaneous temperature measurements on the top and the bottom of the specimen. The heat transfer cell was placed in an insulated box which was kept at a mean temperature of the tested sample. The whole equipment was placed in a cold room, where, for the tests, a temperature of around 4.5 °C was kept (Fig. 3.4). For each analysis, temperatures of the top and bottom plates were set at 12 °C and 2 °C, respectively. The duration of each conductivity test was 24 h.

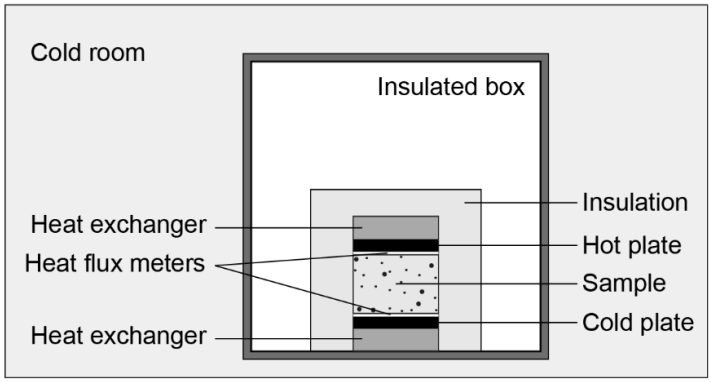

Figure 3.4. Steady state measurement.

Soil mix was tested in saturated and dry states. Samples for a dry state were compacted manually at four different densities. To ensure that proportions of components were kept the same and for easier compaction, soil was moistened first. After filling a mold and compacting it, the mold was then placed in an oven at 105 °C to remove all the moisture. Depending on the density, the time in the oven took from 2 to 5 days. Then, while keeping the sample in the mold, it was installed and insulated in the heat transfer cell to measure its thermal conductivity. All the procedures were also performed for a soil mix without OM.

Tests on lightweight aggregate were carried out in a saturated state. Due to the large size of some of its particles, a soft and compressible sheet made of highly conductive silicone with a thickness of 3 mm was used to create a smooth surface for a better contact between the sample and the upper plate. Such practice was also successfully used by Clarke *et al.* (2016) to reduce interface resistance between the sample and the plates during the measurement of the thermal conductivity of green roof substrates. Compost without OM was tested in a saturated state only.

Measurements of sand, ground aggregate, and compost in a saturated state were conducted by a single needle probe method using the Hukseflux TP02 probe (Delft, Netherlands). It is a standard technique (ASTM D5334-14, 2014) where the needle is inserted in a soil and acts as a heat source, being heated for a certain period of time. The heat dissipates into the surrounding medium, and a thermocouple inside the needle registers its temperature response and the time. Plotting the temperature against logarithm of time, thermal conductivity is calculated. In this test a polyvinyl chloride (PVC) mold in the form of a long cylinder with a

height of 185.7 mm and an inside diameter of 75 mm was used (Fig. 3.5). Saturated material was poured into the mold and then a needle was vertically inserted. The samples were then left for 24 h for measurements. Each material was tested twice to obtain mean values. After the experiments, samples were placed in an oven at 105 °C for 24 h or until they reached a constant mass. Samples were then weighed in order to determine the amount of water and solid material.

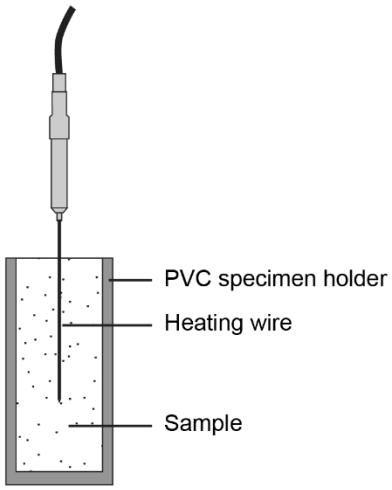

Figure 3.5. Needle probe method.

Table 3.1. Summary of Samples and Test Conditions

Material	Condition	Test Method (Conductivity)	Properties to Determine
Total			
Soil mix	saturated	steady	λ_S
	dry		λ_C, κ_{2P}
Soil mix without OM	saturated	steady	λ_S
	dry		λ_C, κ_{2P}
Components			
Sand	saturated	transient	λ_S
Aggregate	saturated	steady	λ_S
Aggregate (ground)	saturated	transient	λ_S
Compost	saturated	transient	λ_S
Compost without OM	saturated	steady	λ_S

3.6. Results and Discussion

3.6.1. Thermal Decomposition Analysis

The results of the thermal decomposition analysis are shown in Fig. 3.6. The mean curve presents the decomposition of a soil mix at several stages. At the beginning of the test, between 40 and 150 °C, there is a small mass loss of 1 to 1.5%, which is related to a dehydration process in the samples. It is probable that not all water was removed by drying the soil in the oven. Also, the material could have absorbed some amount of moisture from the air in the period between drying and thermal analysis when storing or grinding samples. At the second stage, a considerable mass loss of 12.5 to 13.5% was observed between 250 and 440 to 500 °C due to a combustion process. Lastly, above 500 °C the remaining 1 to 1.5% of OM was removed. After about 700 °C no change in mass was observed in the samples. The remaining amount of the material shows that only 16.4% of OM was present in the soil mix.

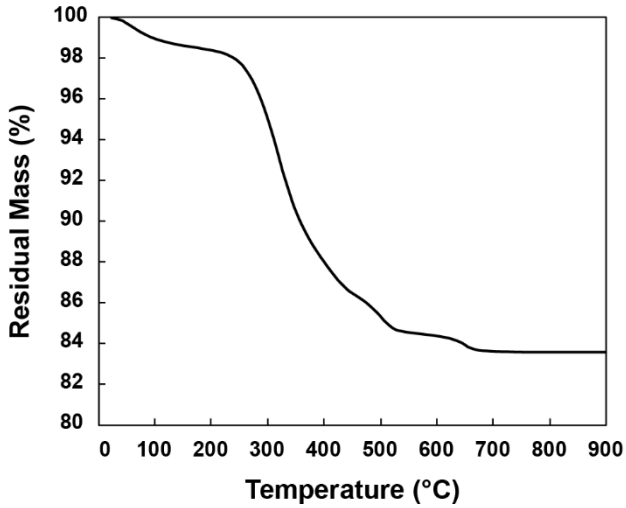

Figure 3.6. TG curve of the soil mix decomposition.

3.6.2. Density of Solid Particles

Results for the determination of solid densities are presented in Table 3.2. The soil with OM had a smaller density than that without OM, 2.22 compared to 2.47 g/cm³. The same is true for the compost with the density of its solid particles of 1.76 g/cm³ and 2.39 g/cm³ after removing of OM from it.

Table 3.2. Densities of Solid Particles.

Material	ρ_S (g/cm^3)
Soil mix	2.22
Soil mix without OM	2.47
Sand	2.69
Aggregate particle	2.10
Aggregate solids (ground)	2.91
Compost	1.76
Compost without OM	2.39

3.6.3. Thermal Conductivity

Results for porous soil mix (with and without OM) and for the solid materials are given. Values obtained from measurements by steady state and by transient method are presented.

3.6.3.1. Effect of porosity

Test results of soil mixes with and without OM in a dry state and at different porosities (n) are presented in Table 3.3. Thermal conductivities for both materials show an increase with a decreasing porosity, with the values from 0.128 to 0.21 W/(m·K) for the soil mix and from 0.25 to 0.33 W/(m·K) for the mix with no OM. It has to be noted that the mix without OM is more compactible. The minimum porosity obtained by manual compaction was 0.42, while for the original mix it was only 0.49. On the opposite side, the presence of OM allowed a much higher porosity (0.69) due to the bulky nature of the composting material.

Table 3.3. Results of the Thermal Conductivity Measurements (λ_c) in a Dry State and Porosities of Samples.

Material samples	n	λ_c of the sample W/(m·K)
Soil mix		
1	0.49	0.210
2	0.59	0.180
3	0.61	0.135
4	0.69	0.128
Soil mix without OM		
1	0.42	0.330

2	0.46	0.300
3	0.49	0.312
4	0.52	0.250

3.6.3.2. Solid particles

The results of thermal conductivities of each material obtained in the experiments in a saturated state are presented in Table 3.4. Thermal conductivities (λ_c) are given together with the porosities (n) that were obtained using Eq. 3.10 knowing ρ_s from Table 3.2 and dry density of the sample (ρ_{total}). From this data solid thermal conductivity λ_s was calculated with Eq. 3.4, using thermal conductivity of water equal to 0.58 W/(m·K) at 7 °C, which is mean temperature at which samples were tested.

The measured value of λ_c of 0.73 W/(m·K) for the soil mix (Table 3.4) is close to the range of values found in the literature (between 0.5 and 0.7 W/(m·K) for the saturation level equal to 1 (Sailor and Hagos, 2011). Low values of λ_s for soil mix with and without OM can be explained by a presence of porous aggregate particles with low thermal conductivity.

Table 3.4. Test Results in a Saturated State.

Material	ρ_{total} g/cm^3	n	λ_c W/(m·K)	λ_s (from Eq. 2.4) W/(m·K)
Total				
Soil mix	0.83	0.63	0.73	1.07
Soil mix without OM	1.36	0.45	1.05	1.70
Components				
Sand	1.72	0.36	2.03	4.12
Aggregate particle	0.98	0.53	0.68	0.82
Aggregate solids (ground)	1.74	0.40	0.92	1.26
Compost	0.26	0.85	0.66	1.35
Compost without OM	0.71	0.70	0.81	1.80

3.6.4. Modelling Thermal Conductivity

3.6.4.1. Thermal conductivity of solid phase

The thermal conductivity of solids of the total soil mix may be calculated from its constituents using the geometric mean method (Eq. 3.3). Because the loss of OM occurs with increasing temperature, it is better to consider it as a separate constituent with its own properties. Using

the same equation (Eq. 3.3), λ_s of OM can be evaluated from the results of λ_s for soils with and without OM (Table 3.4). For that, mass fractions of soil's organic and inorganic parts, obtained from the thermal decomposition analysis and divided by the densities of each of the parts, were transformed into the volume fractions (x) resulting in 0.27 and 0.73 respectively. The density of OM (1.3 g/cm³) was taken from the literature (De Vries and de Wit, 1954). As a result, the indirectly assessed thermal conductivity of OM was 0.31 W/(m·K). This value is close to values from the literature: De Vries and de Wit (1954) reported a value of 0.25 W/(m·K) for humus, while Campbell *et al.* (1994) obtained a value of 0.29 W/(m·K) for solid peat moss.

Obtaining the thermal conductivity of OM is also possible from the compost. However, due to high porosity of samples in the experiments (Table 3.4) the proportion of OM may vary a lot. This remarkably reduces precision in the calculation and thus is not suitable.

Typical growing medium for extensive green roofs contains a large proportion of lightweight aggregate, reaching up to 100%. Pumice, expanded clay, shale, and slate are common materials used. Modeling the thermal conductivity of dry substrates with such materials is complicated by the porous structure of their particles. In the present study, the application of the model (Eq. 3.1) for prediction of λ_s of a porous particle is verified. The maximum value of 0.67 for κ_{2P} must be taken, as it corresponds to a spongy-like structure. Knowing the porosity of a particle from Eq. 3.10 and previously measured λ_s of aggregate solids (ground), thermal conductivity of its particle is modeled, resulting in 0.81 W/(m·K). It has about a 1% difference from the measured value equal to 0.82 W/(m·K) (Table 3.4), which shows the suitability of the model for lightweight aggregate characterization. This verification also gives confidence in measured values and allows to safely use the test results in modeling of thermal conductivity of a growing medium.

Thermal conductivity of solids of soil mix and for soil mix without OM may be calculated from their constituents using Eq. 3.3, which may then be verified with test results. Mass fractions of each component were first converted to volumetric proportions (x) knowing the densities of their solids from Table 3.2. From the data available from the manufacturer on the soil mix recipe, mass proportions of sand, lightweight aggregate, and the inorganic part of compost are 12, 42.6, and 29% respectively, while OM content is 16.4%, as shown in

thermogravimetric analysis. Table 3.5 presents the obtained volume fractions of components. Considering the decomposition of OM and thus changing proportions of each component, results for the substrate without OM are presented as well.

Table 3.5. Volume Fractions (x) of Components.

Component	Volume Fraction (x)	
	Soil Mix with 16.4% of OM	Soil Mix without OM
Sand	0.09	0.12
Aggregate	0.41	0.55
OM	0.25	-
Compost without OM	0.25	0.33

With these values, the calculated λ_s of the soil mix is equal to 0.9, which is 15.9% lower than the measured value of 1.07 W/(m·K) (Table 3.4). For the soil without OM, λ_s is equal to 1.29, which is 24% lower than the experimental result of 1.7 W/(m·K) (Table 3.4). The difference may be explained by the uncertainty in the right value of moisture content of organic product during soil blending that leads to some changes in proportions. The presence of highly conductive sand, in comparison to other components, can make the results very sensitive. Considering these aspects, the comparative results presented herein are satisfying.

3.6.4.2. Thermal conductivity of porous dry green roof soil at a reference temperature

In this study, the reference temperature is set equal to 7 °C, the average of tested samples. Fig. 3.7 presents measured thermal conductivity values of soil mix and soil without OM at four different porosities each (Table 3.3). The fitted curves, also shown in the figure, were obtained using Eq. 3.1, which gave structure parameters κ_{2P} equal to 0.218 for the soil mix and 0.173 for the soil mix without OM. At n=0 and n=1, values calculated for the solids (top part of Table 3.4) and the air were taken correspondingly. The figure illustrates the changes in thermal conductivity with increasing porosity for studied materials.

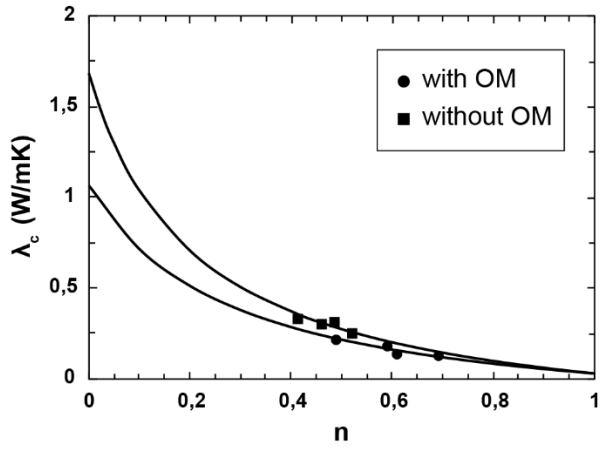

Figure 3.7. Change in thermal conductivity (λ_c) with porosity from experiments and fitting curves for the soil mix and soil without OM.

κ_{2P} values calculated for both materials are shown as functions of the λ_f/λ_s ratio in Fig. 3.8. It can be seen that the values lay slightly higher than the slope presenting cemented types of rocks. Although sand and aggregate are more of a rounded shape, the closeness to cemented type may be explained by the specificity of the organic product, which may act as a thermal bridge between particles. It is speculated that in a moist sample that was compacted and then dried, OM created a good contact between particles comparable to cemented rock materials. According to these results, separate values of β may be established to characterize the tested growing medium. As κ_{2P} for both soils with and without OM are close to each other, a common β value of 0.30 can be preliminarily used as obtained with Eq. 3.2. The thick full line shown in Fig. 3.8 represents the slope for new β.

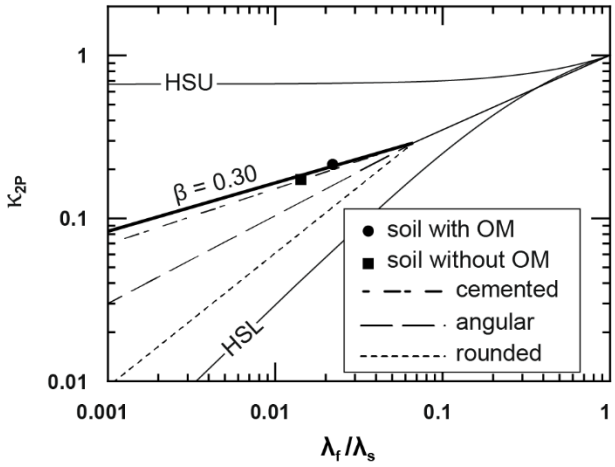

Figure 3.8. κ_{2P} values for soil mixes.

3.6.4.3. Thermal conductivity as a function of temperature

The laboratory was equipped to analyze the decomposition curve as a function of temperature. Unfortunately, thermal properties (conductivity and radiation) could not be assessed at elevated temperature, so existing models had to be used to describe the effect of temperature (*T*).

3.6.4.4. Normalized thermal decomposition analysis curve

The OM content of typical green roof substrates usually ranges between 3% and 20%. The content reduces to 0 at temperatures close to 600 °C, as shown in Fig. 3.6. To be able to account for this variation using a model for any type of substrate, the OM content to *T* relationship can be modeled using a normalized form. It may be seen from the thermal decomposition analysis that the decomposition curve resembles the curve for soil water characteristic, which can be described using a modified version of the equation developed by Van Genuchten (1980), where the normalized amount of OM (m_{OMn}) be modelled as follows,

$$m_{OMn} = \frac{1}{\left[1 + \left(\frac{T}{\alpha}\right)^{n}\right]^{m}} \tag{3.11}$$

where *T* is in °C; α, *n*, and *m* are curve fitting parameters obtained by fitting with the least squares method, equal to 362.26, 5.09, and 1.28, respectively, from the normalized data of Fig. 3.6. The resulting new curve for the thermal decomposition of normalized OM content is displayed in Fig. 3.9.

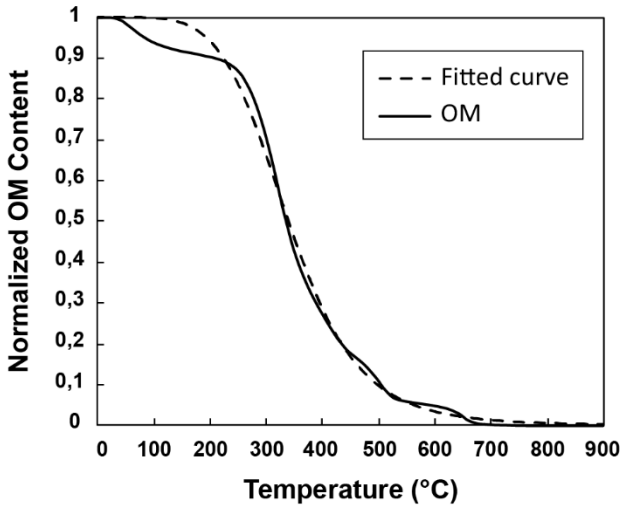

Figure 3.9. Thermogravimetric analysis curve of OM and best-fit curve.

3.6.4.5. Temperature dependence of thermal conductivity of substrate's solids

Equation 2.3 is used for the prediction of λ_s of soil mix at different temperatures considering separately inorganic and organic parts, as well as variations in their volume fractions with temperature. λ_s of inorganic part of soil mix as a function of temperature is obtained using the normalized curve of Zoth and Haenel (1988), where at 7 °C it is equal to 1.29 W/(m·K), which is the previously calculated thermal conductivity of soil mix without OM. At 800 °C it decreases by a ratio of 2.2 to 0.6 W/(m·K), as it was defined in the framework. The thermal conductivity of OM was assumed to be constant with temperature. Volume fractions of both organic and inorganic parts vary from 0.25 and 0.75 to 0 and 1, respectively (Table 3.5), following the normalized thermal decomposition curve (Fig. 3.9). The resulting temperature dependency of λ_s of soil mix is presented in Fig. 3.10.

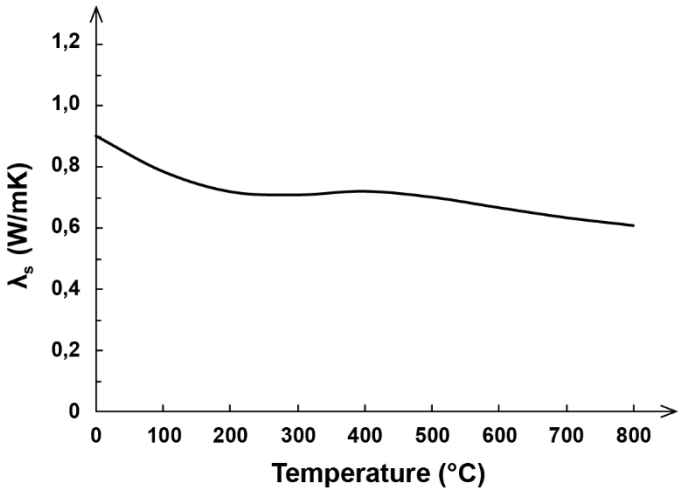

Figure 3.10. Variation of thermal conductivity of soil mix solids (λ_s) with temperature.

3.6.4.6. Effect of interparticle thermal radiation

The radiation contribution to the effective thermal conductivity was determined with Eq. 3.8, assuming particle emissivity equal to 0.9. From the data provided by the manufacturer d_{10} is 2 mm. The results presented at Fig. 3.11 show that the radiative thermal conductivity greatly increases with temperature.

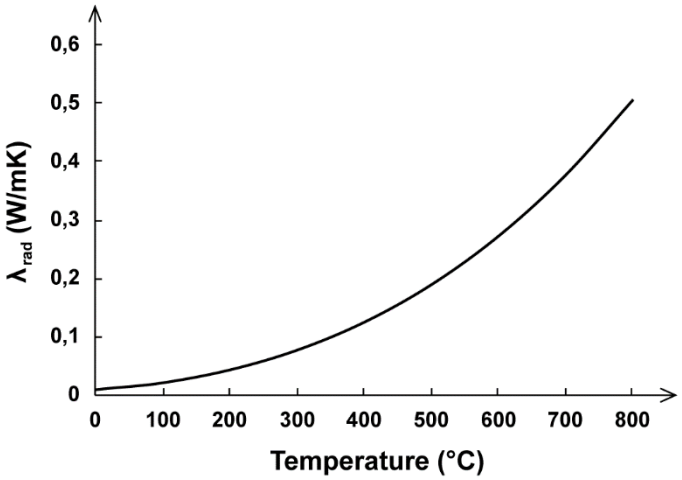

Figure 3.11. Radiative thermal conductivity (λ_{rad}).

3.6.4.7. Global thermal conductivity relationship

Prediction of the thermal conductivity of a dry soil mix (λ_c) at different temperatures is made with Eq. 3.1, knowing temperature dependency of solid and fluid phases. With the limited

data available it is assumed that porosity remains constant with temperature. The decomposition of the OM elevated temperatures can lead to changes in structure of the material and, thus, its porosity. However due to the complex structure of the substrate, its high heterogeneity, it is difficult to predict the exact changes. In some zones it can become more porous, due to a disappearance of OM and creation of larger void spaces. It can also become more compacted in some other zones, where smaller particles can fall and fill in the created void spaces.

Having shown in Fig. 3.8 that the structure parameter is about the same before and after decomposition of OM, it is assumed that the dependency of κ_{2P} to temperature is only owed to changes of the λ_f/λ_s ratio. This relationship is obtained with Eq. 3.2 and is shown in Fig. 3.12.

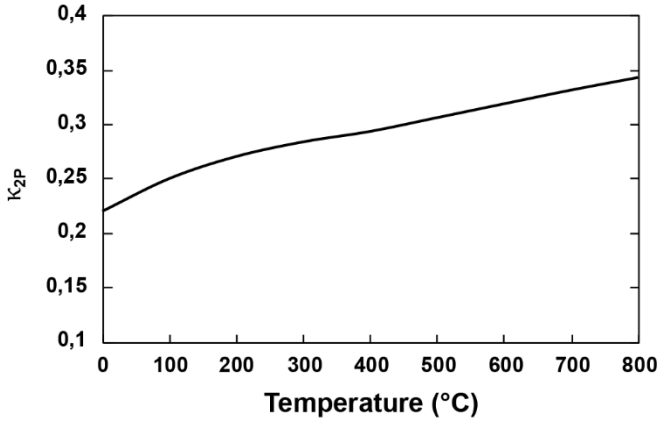

Figure 3.12. Structure parameter κ_{2P} change with temperature.

Figure 3.13 presents thermal conductivity of the growing medium with a porosity of 0.6 predicted for a range of temperatures from 0 to 800 °C. And finally, the effective thermal conductivity, that includes the radiation effect, is displayed in Fig. 3.14. It is seen that contribution from radiation to thermal conduction at elevated temperatures is noticeable.

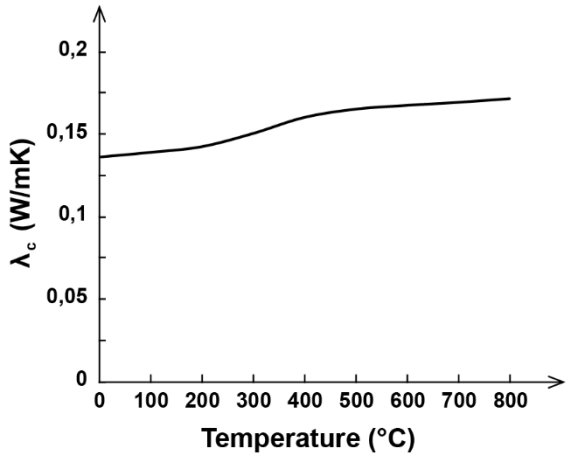

Figure 3.13. Temperature dependence of thermal conductivity (λ_c) of soil mix.

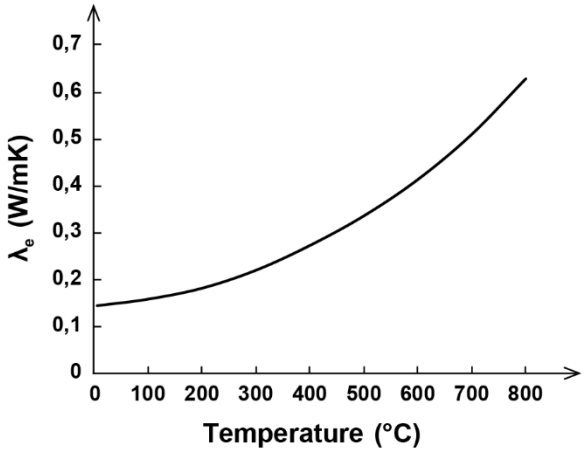

Figure 3.14. Temperature dependence of effective thermal conductivity (λ_e) of soil mix.

3.6.4.8. Thermal conductivity model application over a range of temperatures

The scheme on Fig. 3.15 shows the application of the model for calculating green roof dry substrate thermal conductivity and prediction for the elevated temperatures.

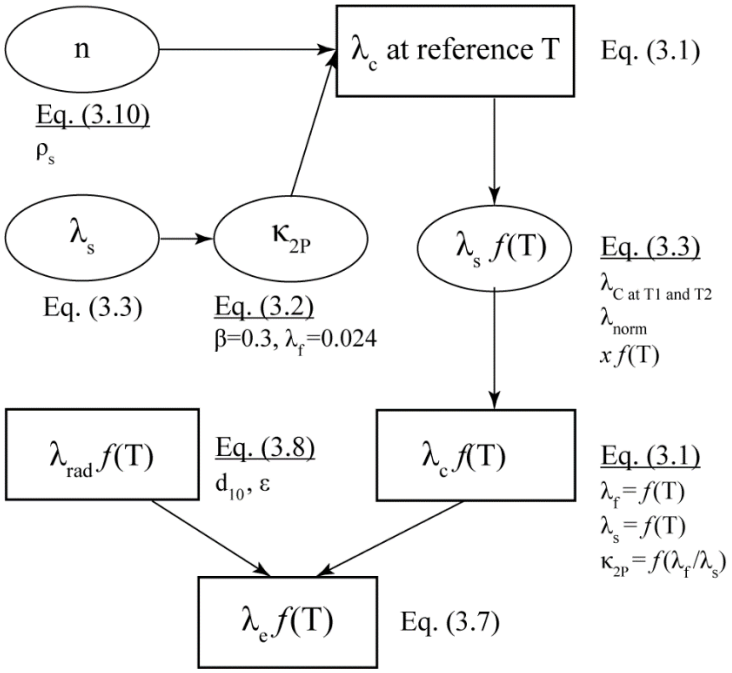

Figure 3.15. Scheme for predicting the thermal conductivity.

3.6.5. Validation

3.6.5.1. Testing Procedure

For the validation of the results of calculated thermal conductivity, the heat transfer test and the numerical solution were performed. Despite the absence of standard verification tests for the thermal conductivity at high temperatures, several authors have previously performed experiments on recording the evolution of temperatures in soil during extreme heating (Aston and Gill, 1976; Campbell *et al.*, 1995; Antilén *et al.*, 2006; Enninful, 2006). They elaborated mathematical models of heat conduction to simulate the test conditions.

In this research, the test conditions were inspired by the work of Enninful (2006) for the ease of applying heating load on a soil surface, using a cone calorimeter. This apparatus was designed to test material flammability characteristics (Babrauskas, 2016a). A small sample with a surface of 100 × 100 mm is exposed to a certain radiant heat, which is emitted by an electric resistance cone-shape heater. The distance between the base of the heater and the top of a sample was 25 mm. The heat emitter is calibrated according to ISO 5660-1 (2015) to establish a uniform incident heat flux over the sample surface.

A special sample holder was constructed to hold the growing medium. The holder consisted of 4 walls and a bottom, made of rigid non-combustible high temperature insulation material of 12.5 mm thickness, constructed so that the internal dimensions of soil samples were 100 × 100 × 80 mm. The wall material was chosen with a low thermal conductivity of 0.1 W/(m·K) to reduce heat loss from the sides. Walls were bonded by a metal frame along the joints. Dried soil sample was placed inside and compacted to a desired density, placing 3 thermocouples at depths of 20 mm, 40 mm, and 60 mm along the center line of the sample (Fig. 3.16). Experiments were conducted for two porosities of the growing medium, 0.66 and 0.61, and repeated twice. The continuous radiant heat flux of 50 kW/m² was applied vertically over the top of the sample by the cone calorimeter (Fire Testing Technology Ltd, East Grinstead, UK) for 1 h. Temperature readings were taken every 10 seconds.

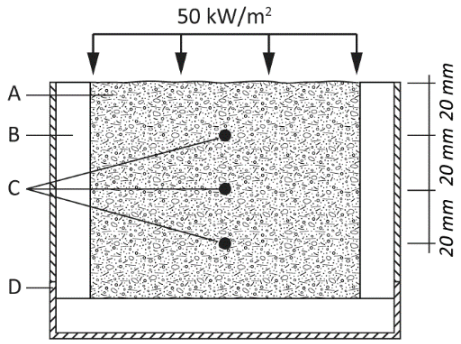

Figure 3.16. Sample: A - substrate, B - rigid insulation, C - thermocouples, D - metal frame.

3.6.5.2. Modelling

In order to simulate the heat transfer test, a simplified one-dimensional transient heat conduction model was created using ANSYS Mechanical (version 18.2) finite element method based software. The analysis was performed solving Eq. 3.12,

$$\rho C_p \frac{\partial T}{\partial t} = \frac{\partial}{\partial z}\left(\lambda_e(T)\frac{\partial T}{\partial z}\right) \tag{3.12}$$

where λ_e is the temperature dependent effective thermal conductivity (W/(m·K)), C_P is soil specific heat (J/(kg·K)), ρ is the density of a sample (g/cm³), z is a soil depth (mm), and T is the sample temperature (K).

For initial (Eq. 3.13) and boundary conditions (Eq. 3.14 and 3.15), the following equations were used:

$$T\,(z, t = 0) = T_0 = 22°C \tag{3.13}$$

$$z = L, t \geq 0, \qquad T = T_0 \tag{3.14}$$

It is assumed that the heat from the radiant emitter is transferred to the specimen surface by radiation only, due to a closeness of both emitting and receiving surfaces. Convection heat losses from the sample surface are neglected, as the air above the surface is not expected to be low. Thus, the boundary condition for the specimen surface is expressed as,

$$z = 0, \qquad -\lambda_e(T)\frac{\partial T}{\partial z} = q''_{net,r} = \varepsilon\sigma(T_S^4 - T_r^4) \tag{3.15}$$

where $q''_{net,r}$ is net radiative heat flux; T_S is source temperature, 751.5 °C; T_r is temperature of a receiving surface of a soil; ε is emissivity, assumed equal to 0.8; and σ is the Stefan–Boltzmann constant, 5.67×10^{-8} W/(m²·K⁴).

In this preliminary validation phase, heat generation caused by the thermal decomposition of OM is not included in a current model due to a complexity of a process itself. Occurring between 150 and 650 °C, the thermal decomposition passes through several stages, as can be seen from the test in Fig. 3.6. Also, composting material itself has a complex shape and composition (composting sawdust with manure and small inclusions of peat moss), which can result in heat releasing at different rates during burning. Finally, in cases of well compacted substrate, the access of the necessary amount of oxygen to the deeper layers may be restricted, causing insufficient burning and thus less energy production (DeBano *et al.*, 1998). Therefore, it is difficult to simulate such process in detail. Separate research should be conducted for better understanding of mechanisms and obtaining necessary parameters for a model.

In the model, substrate of 80 mm depth was divided into 32 uniform linear elements and a time step of 10 s was applied.

3.6.5.3. Substrate properties

Modelling was performed using two different temperature-dependent λ_e that were calculated for porosities of 0.66 and 0.61. Both tested porosities were assumed to be constant with

temperature. The density was obtained from the normalized thermal decomposition of OM, considering that the density of solid particles increases (Table 3.2). Specific heat of a substrate was calculated as a sum of specific heats of its components multiplied by their mass fractions in a mix (Eq. 3.16) (De Vries and Van Wijk, 1963).

$$C_P = \sum_{i=1}^{n} C_{P_i} x_i \tag{3.16}$$

where C_{Pi} is the specific heat of each component (i) in J/(kg·K) and x_i is their mass fractions. Neglecting the air component, mineral and organic parts are considered. The specific heat of OM solids is taken at 1925 J/(kg·K) (De Vries and de Wit, 1954). Extensive literature data for minerals and solid rocks shows that for most of them, specific heat varies within relatively narrow limits between 700 and 800 J/(kg·K) with the average value of 770 J/(kg·K) (Waples and Waples, 2004).

Temperature dependent specific heat for the growing medium is obtained considering the effect of temperature on its inorganic part, as well as on mass fractions. Specific heat of OM is assumed to be constant. Waples and Waples (2004) developed the general equation that describes temperature dependence of specific heat of all minerals and non-porous rocks at a range from 0 to 1200 °C. Using their model, it is possible to predict this property at a desired temperature of a certain material on the condition that its value at a certain temperature is known (Eq. 3.17),

$$C_{P_{T_2}} = C_{P_{T_1}} \cdot C_{Pn_{T_2}} / C_{Pn_{T_1}} \tag{3.17}$$

where $C_{P_{T1}}$ is known specific heat capacity (J/(kg·K)) at a certain temperature T_1 (°C), $C_{Pn_{T2}}$ is the normalized specific heat capacity at the temperature of interest T_2, $C_{Pn_{T1}}$ is the normalized specific heat capacity at a certain temperature T_1. The introduced normalized specific heat capacity is given as:

$$C_{Pn_T} = 8.95 \cdot 10^{-10} T^3 - 2.13 \cdot 10^{-6} T^2 + 0.00172T + 0.716 \tag{3.18}$$

This normalized specific heat represents best-fit curve of normalized specific heat capacities of all studied rocks and minerals. Their normalized values were obtained by dividing the existed values of each material at different temperatures by their values at 200 °C.

Mass fractions for different temperatures are taken from the thermal analysis, where x_{OM} decreases from 0.164 to 0. As a result, the curve for specific heat of soil is obtained as a function of temperature (Fig. 3.17).

3.6.5.4. Validation of results

Results of temperature evolution at three different depths obtained from the experimental work and numerical simulation are shown in Fig. 3.18 for the growing medium of two different porosities. Solid lines present predicted temperatures and the dashed lines are the measured values. It is seen that using effective thermal conductivity calculated as proposed in this study results in smaller values of temperature at all depths and for the whole duration of the simulation. However, all curves follow the similar shapes of the temperature curves from the experiment.

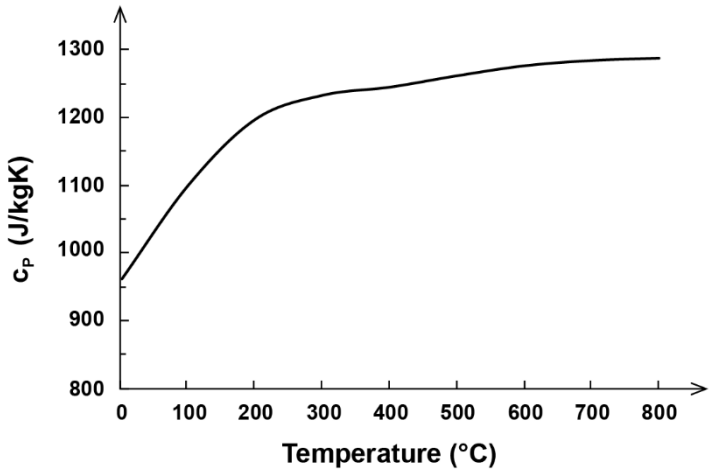

Figure 3.17. Specific heat of soil mix (C_p) changes with temperature.

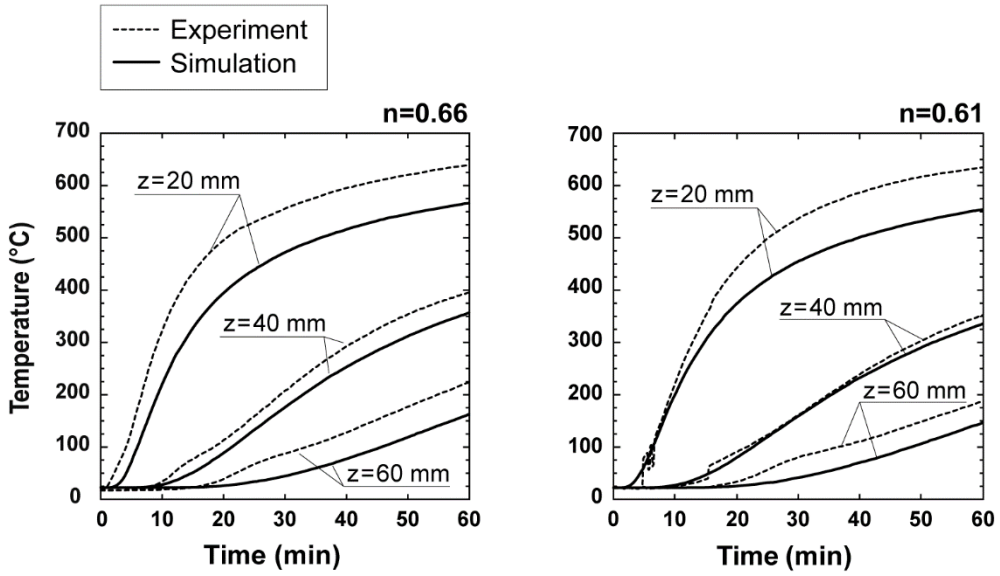

a b

Figure 3.18. Results on calculated and measured temperature developments at depths 20, 40 and 60 mm in soils samples: (a) with a porosity 0.66; (b) with a porosity 0.61.

The main source of discrepancy between results can be the heat generated by the decomposition of OM, which was not considered in the model. Also, the height of the sample, which was limited by the apparatus geometry, may not be sufficient to represent a semi-infinite solid.

3.7. Conclusions

The existing model for the determination of thermal conductivity of two-phase porous materials is suitable for dry green roof substrates at ambient temperature. The model requires taking the parameter β equal to 0.3, which was evaluated specifically for green roof substrate in order to obtain structure parameter.

Experimental results of a dry substrate show the effects of porosity, causing an increase in the thermal conductivity with decreasing porosity.

For the prediction of thermal conductivity at elevated temperatures, the decomposition of organic matter and the effect of heat on thermal properties of solid inorganic part are considered. Together with added interparticle radiation effect, the effective thermal

conductivity of a substrate shows a substantial increase with increasing temperature compared to the thermal conductivity at normal temperatures.

Temperature-dependent thermal conductivity of dry growing medium, obtained as described in present study, can be suitable for the prediction of temperature profiles in fire. Inclusion of a heat generation in simulations is suggested, which can improve the accuracy of the models. Also, attention must be paid to the natural processes occurred on green roofs, such as settlement of a substrate with time. Roofs that have reached maturity have more compacted substrate than newly installed.

3.8 Acknowledgments

The authors are grateful to Natural Sciences and Engineering Research Council of Canada for the financial support through its ICP and CRD programs (IRCPJ 461745-12 and RDCPJ 445200-12) as well as the industrial partners of the NSERC industrial chair on eco-responsible wood construction (CIRCERB).

CHAPITRE 4 : Heat Transfer Behavior of Green Roof Systems under Fire Condition: A Numerical Study

Buildings, 2019, Vol. 9 (9), 206

Nataliia Gerzhova[1], Pierre Blanchet[1], Christian Dagenais[1,2], Jean Côté[3], Sylvain Ménard[4]

[1] NSERC Industrial Research Chair on Eco-responsible Wood Construction (CIRCERB), Department of Wood and Forest Sciences, Université Laval, Québec G1V 0A6, QC, Canada
[2] FPInnovations, Québec G1V 4C7, QC, Canada
[3] Department of Civil and Water Engineering, Université Laval, Québec G1V 0A6, QC, Canada
[4] Université du Québec à Chicoutimi (UCAQ), Chicoutimi G7H 2B1, QC, Canada

4.1. Résumé

Actuellement, les risques d'incendie sur les toits verts ne sont pas clairement définis. En effet, le problème n'est toujours pas bien compris, ce qui soulève des inquiétudes. La possibilité que les plantes s'enflamment, notamment lors des périodes de sécheresse, est l'une des raisons des mesures de protection nécessaires. Le risque d'incendie potentiel des terrasses couvertes de végétation n'a pas encore été entièrement étudié. La présente étude analyse la performance des toits verts dans des conditions de chaleur extrêmes en simulant un processus de transfert de chaleur à travers l'assemblage. Le principal objectif de cette étude était de déterminer les conditions et le temps requis pour que le platelage de toit atteigne une température critique. Les effets de l'épaisseur de la couche de substrat de croissance (entre 3 et 10 cm), de la porosité (0.5 à 0.7) et de la charge thermique (50, 100, 150 et 200 kW/m²) ont été examinés. Il a été constaté qu'un toit vert peut prévenir l'inflammation d'un platelage de toit en bois avec seulement 3 cm de couche de substrat lorsqu'il est exposé à de forts flux de chaleur pendant au moins 25 minutes. La dépendance du temps de défaillance à l'épaisseur du substrat diminue avec l'augmentation de la charge thermique. Il a également été constaté que la porosité du substrat a un faible impact sur le temps de rupture, et uniquement à des charges thermiques élevées.

Mots-clés : toiture végétalisée; feu; transfert thermique; modélisation

4.2. Abstract

Currently, green roof fire risks are not clearly defined. This is because the problem is still not well understood, which raises concerns. The possibility of plants catching fire, especially during drought periods, is one of the reasons for necessary protection measures. The potential fire hazard for roof decks covered with vegetation has not yet been fully explored. The present study analyzes the performance of green roofs in extreme heat conditions by simulating a heat transfer process through the assembly. The main objective of this study was to determine the conditions and time required for the roof deck to reach a critical temperature. The effects of growing medium layer thickness (between 3 and 10 cm), porosity (0.5 to 0.7), and heating intensity (50, 100, 150, and 200 kW/m2) were examined. It was found that a green roof can protect a wooden roof deck from igniting with only 3 cm of soil coverage when exposed to severe heat fluxes for at least 25 minutes. The dependency of failure time on substrate thickness decreases with increasing heating load. It was also found that substrate porosity has a low impact on time to failure, and only at high heating loads.

Keywords: green roof; fire; heat transfer; modeling

4.3. Introduction

The current increase in the use of green roofs requires an assessment of the safety aspect, including their fire behavior. Even though these systems, as a modern technology, have existed for about 40 years, their fire performance is still debated. In an attempt to design safe green roofs, a large experimental research was conducted in Germany in the 1980s. Based on the results, the first fire protection measures were developed and made a part of the German green roof design guideline FLL (FLL, 2008b). There is an opinion that green roofs can protect a building from fire, and it was mentioned that, in the past, some green roofs were installed to resist fire propagation (Köhler *et al.*, 2002). This belief is due to the fact that plants are about 95% of water. However, concerns arise in the case when a green roof has dried up, due to poor maintenance or during hot summer periods. Dried plants and accumulated debris may be easily ignited, and therefore, contribute to fire. This was demonstrated recently by a fire that occurred in the summer of 2018, in Portland (Portland

Fire Bureau, 2018), where a poorly maintained vegetated roof with overgrown plants caught fire from the sparking of a nearby transformer. Although the damages and losses were not substantial, this incident confirms the possibility of fire on green roofs.

To conform to building regulations, roof coverings are evaluated according to test standards CAN/ULC-S107 (2010) in Canada or ASTM E108 (2017) in the United States. The samples are tested for their ability to resist the spread of flame and downward flame propagation through the deck (for combustible decking). Even though green roof manufacturers successfully tested their assemblies following these standards, it is still difficult to conduct the tests on such roofs, due to the specificity of the components. The conditions for testing the assembly are unclear, such as the presence of vegetation, level of compaction of the growing medium, moisture content of the growing medium and plant material, and associated difficulties. The absence of an established test procedure specifically for green roofs makes it difficult to correctly classify their fire performance.

In order to shed some light on the fire safety of green roofs, or factors affecting their fire performance, a necessity emerges to conduct research that will not repeat a standard test but show and analyze a green roof's response to fire in the most severe conditions. This would demonstrate the potential fire hazard that a green roof could pose to a building. For this particular study, a downward heat transfer was analyzed for predicting the possible damages to a roof deck caused by a fire on the roof. Decking materials, such as wood or steel, can be affected by a high temperature, which can lead to the structural failure. A downward heat transfer was chosen due to the risk of damage to a roof deck. This is because a green roof fire was identified as the main concern of some Authorities Having Jurisdiction.

There is limited data available from fire tests previously conducted on green roofs. Large-scale fire tests conducted according to DD CEN/TS 1187 (2012) (analogue to CAN/ULC-S107) in the UK aimed to determine the possibility of fire spreading into the building in the case where a roof surface was exposed to fire (Department for Communities and Local Government, 2013). In the experiment (burning brand test), the specimen consisted of a growing medium layer of 8 cm thickness and no plants on top. It was shown that the temperature measured under the soil layer did not exceed 100 °C — which was insufficient to ignite the layers underneath, and thus, no fire penetration could occur. Similar burn-

through tests were performed on green roof assemblies (Appl, 2011). Specimens consisted of a 5 cm thick growing medium, a 2.5 cm thick drainage layer, and a 0.5 cm thick protection mat, thermal insulation, and steel deck. After the end of the test (which took approximately 30 min), a temperature of 40 °C was registered under the soil layer even though the soil surface reached 300 °C. The drainage and all other layers, thus, remained intact. Even though both tests showed that a substrate layer could protect from fire penetration, no detailed data was provided with respect to the effects of soil moisture level, composition, amount of organic matter (OM), or temperature evolution during the test. Moreover, it is unclear from these results whether the soil thickness is an important parameter that influences heat conduction. Given that a green roof is a multiple-layer assembly, with different characteristics of each component, it is important to understand which factors affect the most the heat transfer in the event of a fire.

Although there are well-accepted methods to carry out full-scale experimental investigations that evaluate possible damages due to fire, conducting tests is a complex, labor- and time-consuming process of creating conditions and specimen preparation. Instead, the heat transfer problem can be successfully solved by numerical simulations. This is a good alternative approach, provided the modeling is verified and validated by test data. This method allows for the analysis of different scenarios in a relatively simple and fast way.

The objective of this research is to assess the fire risk that a green roof can present to a roof structure using numerical simulation. Specifically, it aims to determine under which conditions the roof deck can be damaged if the green roof is exposed to elevated temperatures from the exterior. It also aims to determine which configuration of vegetated roof assemblies or characteristics of its components present a greater fire risk. Due to great variability in factors that affect weather conditions on a roof, some simplifications were made, such as for the heating load. The analysis was, thus focused on the simulations of the worst cases.

4.4. Methodology

4.4.1. Numerical Modeling

Numerical models were developed that could represent heat transfer through green roof assemblies of different geometries, with the purpose to analyze the temperature response of

these roofing systems to extreme heat, and to determine at which conditions a system may fail. Specifically, they determine the moment at which the roof deck reaches its critical temperature (failure time). The model contains simplifications, such as the thermal load is constant for the whole duration of simulation, the condition that the heat transfer occurs by conduction only, and that no heat generation within a soil layer is considered. Although the thermal decomposition of the soil OM can contribute to heat propagation, its content in the substrate for green roofs is usually low, within 3–6% by mass, and thus, neglected.

The one-dimensional heat transfer is described by the following partial differential equation (Eq. 4.1).

$$\frac{\partial}{\partial x}\left(\lambda\frac{\partial T}{\partial x}\right) = \rho C_P \frac{\partial T}{\partial t}, \tag{4.1}$$

where λ, C_P and ρ are the thermal conductivity (W/(m·K)), specific heat (J/(kg·K)) and density (kg/m³) of each material, respectively. x is the depth (m), T is temperature (K) and t is time (s). All material characteristics are temperature-dependent, as presented in the next section.

The initial temperature in the model is 22 °C (295 K). The boundary condition at the soil surface (x = 0) exposed to heat is a combination of convective and radiative heat fluxes:

$$q_1^{"} = q_{rad}^{"} + q_{conv}^{"} = h_1(T_f - T_s) + F\varepsilon\sigma(T_f^4 - T_s^4), \tag{4.2}$$

where q''_1 is the net heat flux, q''_{rad} is the radiative heat flux, q''_{conv} is the convective heat flux, h_1 is the convective heat transfer coefficient equal to 25 W/(m²·K); T_f is the source temperature (K); T_S is the temperature of a receiving surface (K); F is the view factor assumed 1; ε is the emissivity assumed to be equal to 0.8; σ is the Stefan–Boltzmann constant equal to 5.67×10−8 W/(m²·K⁴). For the underside of the roof deck the heat loss is:

$$q_2^{"} = h_2(T_s - T_a), \tag{4.3}$$

where T_a is the ambient temperature set at 295 K, h_2 is the convective heat transfer coefficient equal to 9 W/(m²·K), which, according to EN 1991-1-2 (2003), can be assumed to contain the effect of heat transfer by radiation.

4.4.2. Modeling Parameters

4.4.2.1. Geometry

A typical green roof assembly consists of a soil layer, drainage, insulation (optional) and a roof deck. Other layers, such as filter sheet, root barrier and waterproof membrane are of small thicknesses and will most likely not greatly affect the temperature evolution in the assembly, therefore these components are not included in the numerical models. For green roofs one of the most common insulation materials is extruded polystyrene (XPS), lightweight rigid boards, resistant to water and with good compressive strength. However, XPS is a highly flammable material that softens, then rapidly melts and loses its structure as it reaches 100 °C, which can lead to changes in geometry of the assembly. Therefore, only geometries without insulation are used for the simulations. A granular material forming a 2 cm thick layer is used for the drainage. The description of the material is presented in the next sections. Two different types of roof deck susceptible to heat damage are selected for the modeling. A wooden deck made of plywood of 19 mm thickness and a corrugated steel deck (modeled as a flat steel sheet of 1.5 mm in thickness). In such cases, a gypsum board (Type X, 13 mm) is usually placed on top of the deck to provide fire protection due to the fire resistance properties of such boards. It is also used as a cover board to ensure a flat surface, when installing vegetated roof over the steel deck. To analyze the most severe case, additionally, the assembly installed on a wood deck without gypsum board on top is used. Fig. 4.1a,b and Fig. 4.2 show the green roof assemblies used for the modeling.

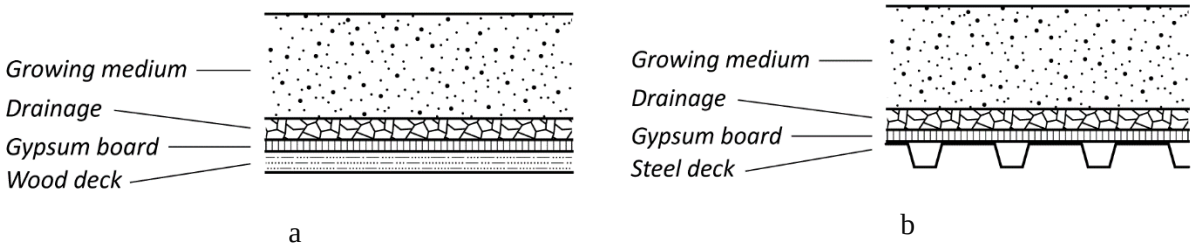

Figure 4.1. Assemblies with the gypsum board installed over a: (a) Wood deck; (b) steel deck.

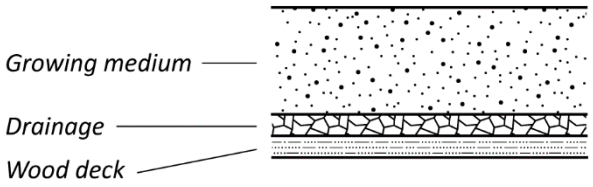

Figure 4.2. Assembly installed over a wood deck, without gypsum board.

Since the objective of the analysis is to identify under which conditions the roof deck can be damaged, the critical temperature for the decking material will be an indicator of roof failure. The critical condition for the plywood deck is a state at which charring is initiated. Thus, a charring temperature of 300 °C is chosen as critical, as per EN 1995-1-2 (2003). For steel, a temperature of 538 °C (1000 °F) is considered a failure criterion according to ASTM E119 (2012) fire resistance test for steel structures.

4.4.2.2. Growing Medium

Substrate thermal and physical properties are determining factors in heat conduction and therefore their impact needs to be examined. As this study focuses on the analysis of the most severe conditions, only dry soil is considered. Moisture causes a delay in temperature increase in soil at about 80–100 °C until almost all water vaporizes, whereas the temperature rise in dry soil is smoother at all depths and reaches higher values (DeBano *et al.*, 1998). Temperature profiles of dry natural soils during fires have been experimentally studied in the past (DeBano *et al.*, 1979; Valette *et al.*, 1994; Raison *et al.*, 1986; Frandsen and Ryan, 1986). It was shown that dry soil is a poor thermal conductor and prevents the heat from propagating downwards, causing a large temperature gradient to appear. Measurements during wildfires showed that dry soil, reaching high temperatures at the surface, over 700 °C, stayed in the range of 43 to 54 °C at a depth of 5 cm (DeBano *et al.*, 1979). Another study showed that the temperature at a depth of 1 cm increased to only 46 °C, while the surface reached 362 °C during a fire of low intensity (Valette *et al.*, 1994). Other studies have provided the following data: the temperature of soil during forest fires measured at the surface reached 450 °C, while it reached 45 °C on average at a depth of 5 cm (Raison *et al.*, 1986); a peak temperature of 700 °C at the surface and 440 °C at a depth of 2 cm in dry sand (Frandsen and Ryan, 1986). Therefore, the soil layer can greatly reduce the heat penetration down to the roof elements below. Similar behavior is expected from green roof growing medium, as it contains large

amount of porous aggregate with low thermal conductivity. The minimum thickness of growing medium for green roofs in Canada is usually 10 cm (Toronto Municipal Code, 2017; RBQ, 2015). However, German FLL guideline contains a description of a green roof that is considered resistant to radiant heat (hardroof) when substrate depth is at least 3 cm. Thus, several models need to be performed to determine the depths of the growing medium sufficient to resist the propagation of heat down to the roof deck. In view of the objective of this research to model the response of green roof assembly to extreme heat in most severe cases, the smallest growing medium thickness required in Canada, 10 cm, was chosen for the simulations. Simulations of green roof assemblies with smaller thicknesses of growing medium were performed, namely with 3, 5 and 7.5 cm to investigate the effect of substrate thickness on time to failure of a roof structure.

Another factor affecting soil heat transfer performance is porosity. Growing media on green roofs can have different levels of compaction, which, among other factors, depend on the age of roof, since the soil naturally settles and becomes denser with time. This parameter directly affects thermal conductivity. In dry soil, heat is transmitted by conduction mainly through the solid particles because air, contained in pores, has a very low thermal conductivity. A smaller porosity means more solid particles per unit volume of soil and thermal conductivity therefore increases (Farouki, 1981). A typical growing medium was characterized in a previous work (Gerzhova *et al.*, 2019). Maximum and minimum possible porosities of dry samples reached by manual compaction were 0.7 and 0.5.

4.4.3. Material Characteristics

4.4.3.1. Growing Medium

The heat transfer in granular materials such as soil is a complex process. Previous work on the prediction of the effective thermal conductivity (λ_e) of dry green roof substrate as a function of temperature has been conducted specifically for application in numerical simulations (Gerzhova *et al.*, 2019). In the present study, λ_e was calculated for different temperatures using the same method and data, but for a growing medium containing 5% OM by mass, which is typical for extensive green roof systems. The effective thermal

conductivity is a sum of the thermal conductivity of a dry substrate (λ_c) and the contribution of interparticle radiation (λ_{rad}):

$$\lambda_e = \lambda_c + \lambda_{rad} \tag{4.4}$$

where λ_c is calculated with the Côté and Konrad (2009) as:

$$\lambda_c = \frac{\left(\kappa_{2P}\lambda_s - \lambda_f\right)(1-n) + \lambda_f}{1 + (\kappa_{2P} - 1)(1-n)} \tag{4.5}$$

where λ_s and λ_f are the temperature dependent thermal conductivities of soil solids and air respectively in W/(m·K), *n* is the porosity, which is assumed constant, and κ_{2P} is a structure parameter. λ_f was taken from the literature (Incropera and Dewitt, 2007). λ_s as a function of temperature was taken from Gerzhova *et al.* (2019) considering 5% OM and the loss of OM with increasing temperature according to the thermal decomposition curve shown in Fig. 4.3.

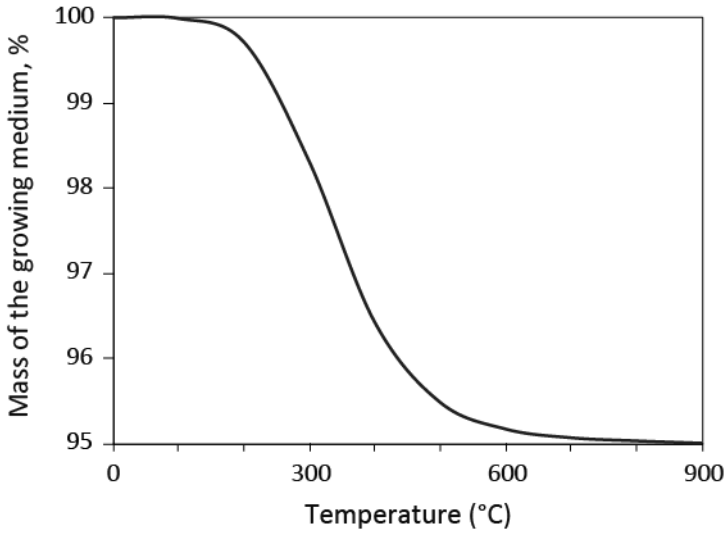

Figure 4.3. The loss of organic matter (OM) in the growing medium with respect to temperature.

The structure parameter was obtained with the equation of Côté and Konrad (2009):

$$\kappa_{2P} = 0.29\left(15\frac{\lambda_f}{\lambda_s}\right)^{\beta} \tag{4.6}$$

where β was determined in the previous study for green roof soils and is equal to 0.3. The radiation contribution to λ_e was calculated as:

$$\lambda_{rad} = 4Ed_{10}\sigma T^3 \quad (4.7)$$

where E is the exchange factor equal to 0.82, d_{10} is the particle diameter equal to 2 mm (from the data provided by the manufacturer), σ is the Stefan–Boltzman constant equal to 5.67×10^{-8} (W/(m²·K⁴)), T is the temperature (K). Fig. 4.4 shows the effective thermal conductivity of the growing medium that was used in the modeling.

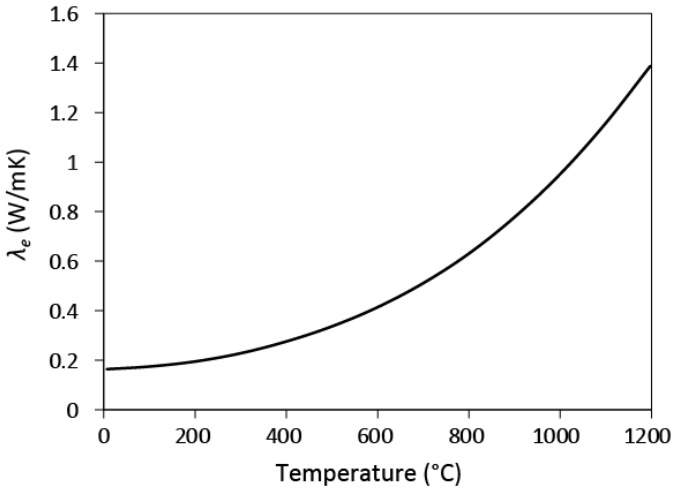

Figure 4.4. Effective thermal conductivity of the growing medium.

The density (ρ) was calculated using porosity (n) and the data on particle densities:

$$n = 1 - \frac{\rho}{\rho_s} \quad (4.8)$$

where n is the porosity, ρ is the bulk density (kg/m³) and ρ_s is the particle density (kg/m³). The loss of OM, that has low ρ_s, at high temperature leads to changes in proportion of the components of the substrate, and therefore, changes in the substrate mean particle density and bulk density. In the previous study on the same substrate, ρ_s of its inorganic part was measured and was equal to 2470 kg/m³. ρ_s of the substrate with 5% OM is 2400 kg/m³, which is obtained taking ρ_s of OM equal to 1300 kg/m³ (De Vries and Van Wijk, 1963). It has been verified with a furnace test that the soil porosity of 0.6 remains the same before and after burning. For simplicity, it is assumed that other porosities used in the modeling do not

change. Fig. 4.5 shows temperature dependent densities for each porosity, which slightly increase after the loss of OM.

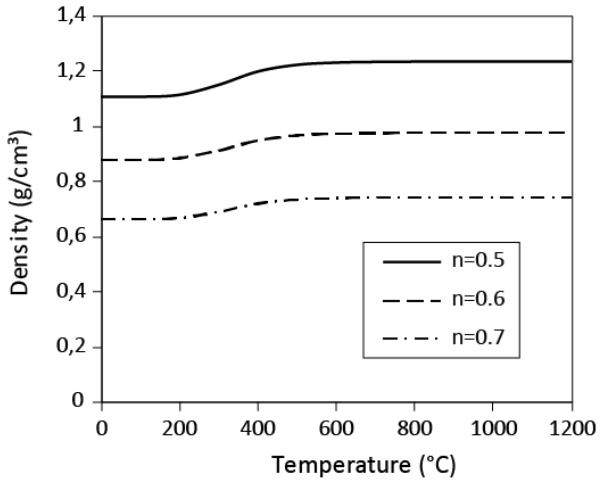

Figure 4.5. Temperature dependent densities of the growing medium according to porosities (*n*) 0.5, 0.6, and 0.7.

Specific heat at different temperatures was obtained as a sum of specific heat of mineral and organic parts multiplied by their mass fractions (De Vries and Van Wijk, 1963):

$$C_P = \sum_{i=1}^{n} C_{P_i} x_i \tag{4.9}$$

where C_P is the specific heat in J/(kg·K), x is the mass fraction, and i is the component. Specific heat of OM is kept constant and equal to 1925 J/(kg·K). The specific heat of the mineral component is, however, a temperature-dependent property and can be predicted with the equation proposed by (Waples and Waples, 2004):

$$C_{P_{T2}} = C_{P_{T1}} \cdot C_{Pn_{T2}} / C_{Pn_{T1}} \tag{4.10}$$

where $C_{P_{T1}}$ is the specific heat at normal temperature equal to 770 J/(kg·K) (Waples and Waples, 2004). C_{Pn_T} is the normalized specific heat capacity at a certain temperature (T) obtained with:

$$C_{Pn_T} = 8.95 \cdot 10^{-10} T^3 - 2.13 \cdot 10^{-6} T^2 + 0.00172T + 0.716 \tag{4.11}$$

where T is in °C. Fig. 4.6 is the resulting curve of the specific heat that was used for the simulation.

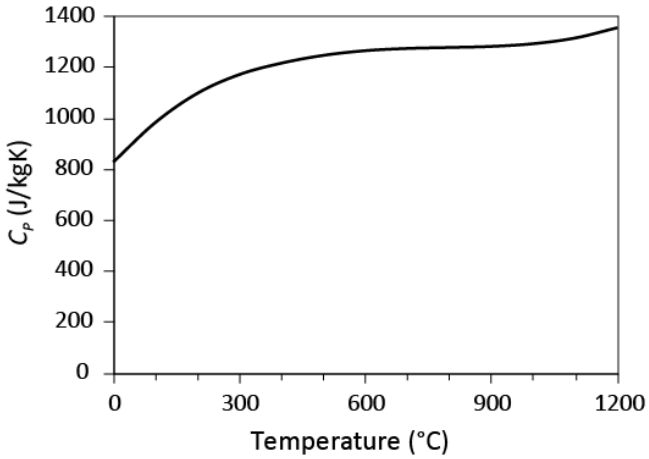

Figure 4.6. Specific heat of the growing medium at different temperatures.

A simplified validation test using a cone calorimeter apparatus was performed in the previous study on the thermal properties of the same green roof substrate (Gerzhova *et al.*, 2019). It was concluded that the thermal properties used in the model are suitable for simulation purposes.

4.4.3.2. Other Components

It is considered that the drainage layer is made of a granular material, a porous lightweight aggregate that serves to drain water. Its thermal conductivity can be obtained by the same method as for the growing medium (Eq. 4.4-4.6). As it is used as one of the components in the growing medium, several of its physical characteristics are known from the previous study (Gerzhova *et al.*, 2019). The λ_s of the aggregate particles was measured and is equal to 0.82 W/(m·K). κ_{2P} is obtained by taking β equal to 0.54 for materials with angular shaped particles, according to Côté and Konrad (2009). Assuming λ_s is constant with temperature and n is equal to 0.5, λ_c can be determined with Eq. 4.5. The radiation contribution to the thermal conductivity is similar to that of the growing medium since d_{10} is 2 mm (laboratory analysis provided by the manufacturer) and E is assumed to be 0.82. The effective thermal conductivity for a drainage layer is therefore obtained and presented in Fig. 4.7.

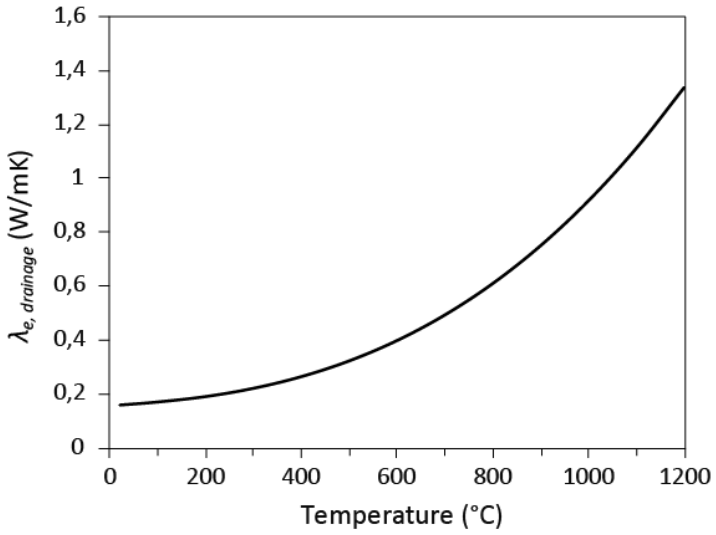

Figure 4.7. Effective thermal conductivity of the drainage layer.

The density of the drainage layer is 1050 kg/m³, which is obtained from Eq. 4.8 using the data on the measured particle density of 2100 kg/m³ and assuming a porosity 0.5. It is noted that the material itself is steel slag. The specific heat of slag at different temperatures has been studied by Gil *et al.* (2014). The results of this research were used for the simulations and are presented in Fig. 4.8.

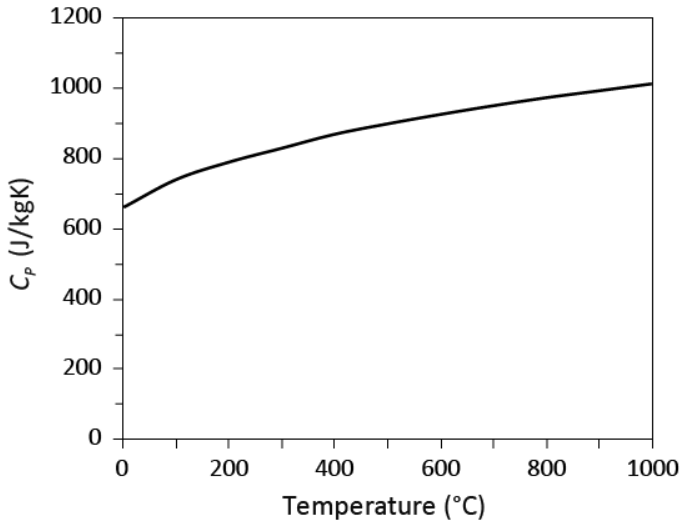

Figure 4.8. Specific heat of the drainage layer with respect to temperature.

The temperature dependent properties of other components in the assembly used in the numerical modeling are presented in the literature by standards and research documents. Properties for the wood are presented in Fig. 4.9a-c (EN 1995-1-2, 2003). Type X gypsum board properties are shown in Fig. 4.10a-c (Benichou *et al.*, 2001) with the density equal to 836.4 kg/m³ at 20 °C (Ang and Wang, 2009).

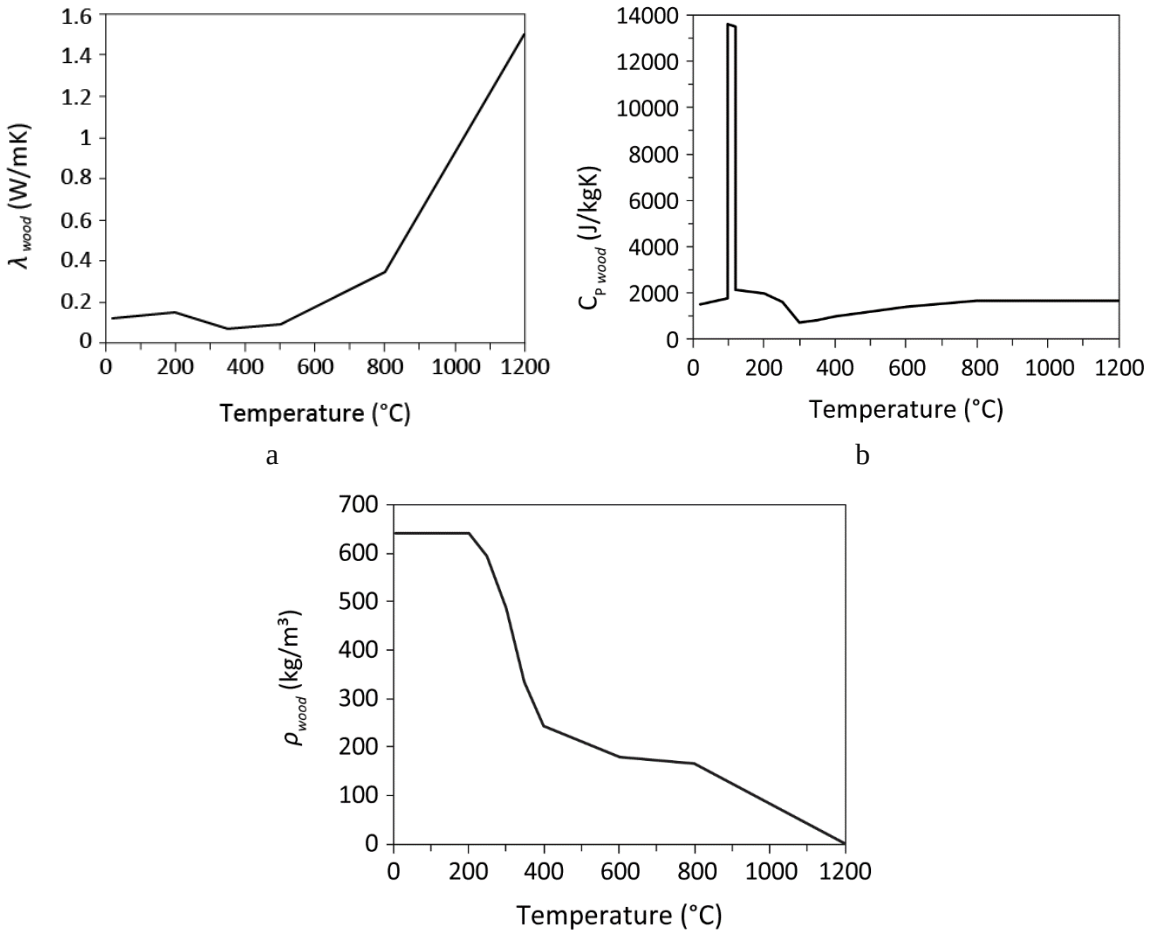

Figure 4.9. Temperature dependent properties of wood: (a) Thermal conductivity; (b) specific heat; (c) density.

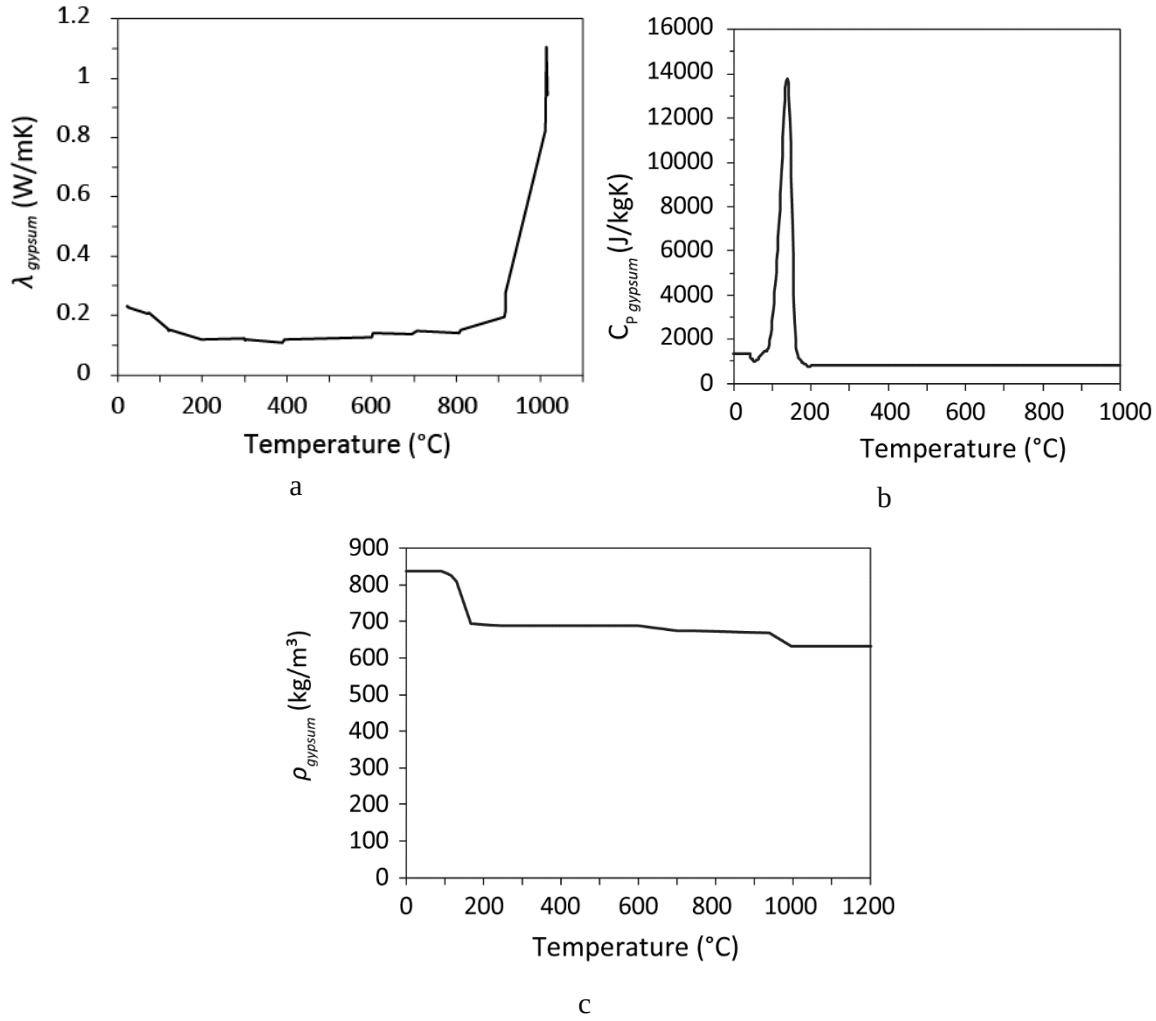

Figure 4.10. Temperature dependent properties of type X gypsum board: (a) Thermal conductivity; (b) specific heat; (c) density.

Steel density is kept constant and is equal to 7850 kg/m³. Thermal conductivity of steel as a function of temperature can be obtained with Eq. 4.12 for a temperature range between 20 and 800 °C, keeping a constant value of 27.3 W/(m·K) above 800 °C (EN 1993-1-2, 2005).

$$\lambda_{steel} = 54 - 3.33 \cdot 10^{-2} T \qquad (4.12)$$

where *T* is the temperature (°C). The specific heat for steel is calculated with Eq. 4.13.1 (for *T* between 20 and 600 °C), Eq. 4.13.2 (for *T* between 600 and 735 °C) and Eq. 4.13.3 (for T between 735 and 900 °C). For a temperature range between 900 and 1200 °C, the specific heat of steel is equal to 650 J/(kg·K) (EN 1993-1-2, 2005).

$$C_{P,steel} = 425 + 7.73 \cdot 10^{-1}T - 1.69 \cdot 10^{-3}T^2 + 2.22 \cdot 10^{-6}T^3 \quad (4.13.1)$$

$$C_{P,steel} = 666 + 13002/(738 - T) \quad (4.13.2)$$

$$C_{P,steel} = 545 + 17820/(\mathrm{T} - 731) \quad (4.13.3)$$

4.4.4. Thermal Load

The thermal response of a structure is largely dependent on the heating load applied, or fire intensity. In the research on fire spread in wildlands, a peak radiant heat flux of 51 kW/m² was registered ahead of the fire front and suggested as a representative value in wildfires (Silvani and Morandini, 2009). Larger heat fluxes of up to 200 kW/m² were measured in forest fires (Butler *et al.*, 2004). Four thermal loads were used in the modeling: 50, 100, 150 and 200 kW/m² for a duration of four hours. In order to describe the thermal loads, a correspondence of heat flux to a temperature is shown using a time-temperature curve of a standard fire resistance test CAN/ULC-S101 (2014). The dashed line in Fig. 4.11 shows the evolution of temperature with time in the furnace during the standard CAN/ULC S101 test.

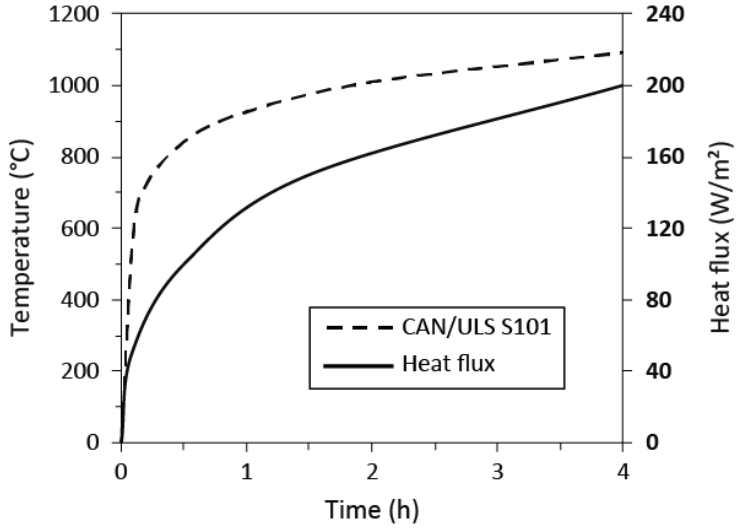

Figure 4.11. CAN/ULC S101 standard fire curve and corresponding heat flux.

The heat flux curve (solid line) was obtained with Eq. 4.2 and is the sum of the radiative and convective heat fluxes. The correspondence to temperature (T_f) was determined by taking the convective heat transfer coefficient (h_1) equal to 25 W/(m²·K) for the net convective heat

flux component according to EN 1991-1-2 (2003) in order to describe standard temperature-time curve. For the net radiative heat flux component, the configuration factor (F) is chosen to be equal to 1 and the emissivity (ε) equal to 0.8, following the same standard. Table 4.1 contains temperatures used in the modelling that are set to represent certain heat fluxes, where, for example, a heat load of 200 kW/m² corresponds to a 240 minute standard fire-resistance test, time at which the temperature inside the furnace is 1110 °C. This relationship also corresponds to the measured values from Sultan (2006).

Table 4.1. Heat flux characterization.

Load (Heat flux) kW/m³	Temperature °C	CAN/ULC S101 time minutes
50	623	7
100	850	33
150	1000	112
200	1110	240

After performing several preliminary simulations, a time step of 20 seconds was elected for all simulations. The mesh for the assemblies with a wooden deck was composed of linear elements of 5 mm each for the soil and the drainage layer, and four elements for a wooden deck. For the assembly that contains gypsum board and a metal support, the mesh included equal elements of 5 mm for the soil and the drainage layers, six elements for the gypsum board and one element for the steel deck. The sensitivity test was performed for a mesh size of the substrate and drainage layers. The results of simulations with 2 mm elements showed the difference in temperature profiles of less than 1 °C. The elements of these layers were set to 5 mm for all simulations to reduce calculation time. The transient heat transfer calculations were performed in ANSYS Mechanical (version 18.2), finite element analysis software.

4.5. Results and Discussions

4.5.1. Temperature Profiles

Several models were performed to simulate the response of green roof assemblies to fire. Fig. 4.12a,b and 4.13 show temperature profiles for the different assemblies with a 10 cm thick growing medium and a porosity of 0.6 during exposure to a heat load of 50 kW/m² for four

hours. It can be seen that the heat slowly penetrated the growing medium layer, creating a smooth temperature gradient, especially after a long period of heating. The temperature below the growing media started to rise after 40 minutes and at a very slow rate. No temperature increase was observed at the roof deck after the first hour. Further, these layers were still not affected after the second hour of exposure, not exceeding a temperature of 50 °C. In all cases, the critical temperature at the deck was not reached during the 4 h heating period. The temperature at the top of the wooden deck not covered by a gypsum board reached only 110 °C, and 178 °C under the substrate (10 cm depth) (Fig. 4.13). In the case of the presence of a Type X gypsum board, the wooden deck reached only 86 °C, while the metal deck temperature was only slightly increased to 69 °C (Fig. 4.12). The temperatures at a 10 cm depth were comparable to values given in the literature for temperature profiles of soils during forest fires. For example, after two hours the temperature reached 79 °C (Fig. 4.12b) and 73 °C (Fig. 4.13). In the research by Busse *et al.* (2005) about 80 °C was registered in dry mineral soil (ρ = 1000 kg/m³) at a 10 cm depth after two hours of fire. However, the heat load at the surface decreased with time, which led to smaller values at durations of more than two hours. Campbell *et al.* (1995) recorded about 260 °C at a depth of 3.6 cm in dried natural soil during exposure to a heat flux between 39 and 54 kW/m². A temperature of 270 °C at the same depth and for the same heating time was found in the present study.

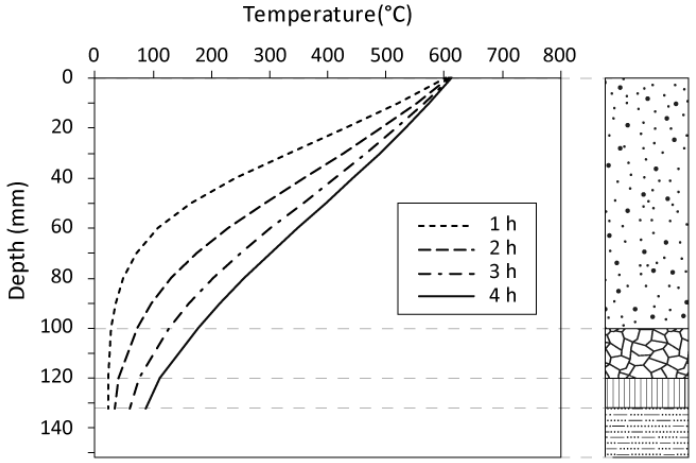

a

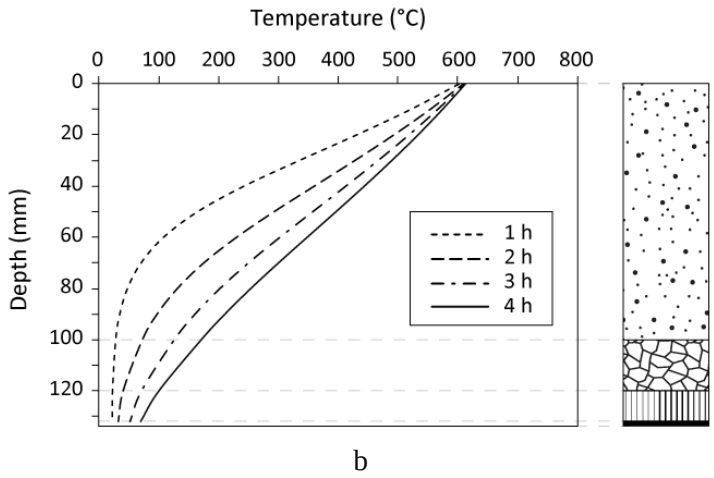

b

Figure 4.12. Temperature distribution in green roof assemblies: (a) With wooden deck; (b) with steel deck.

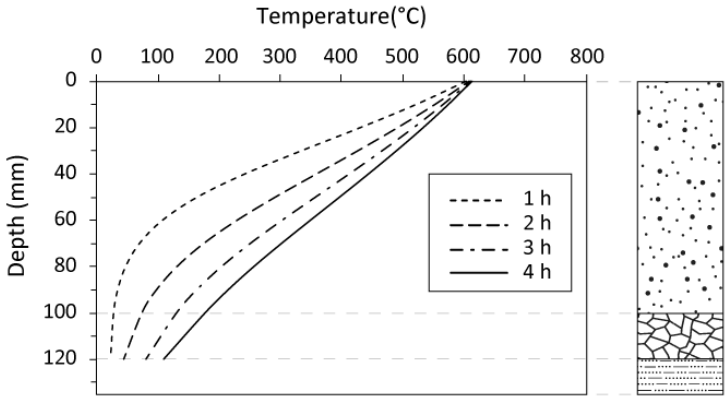

Figure 4.13. Temperature distribution in a green roof assembly installed over a wood deck and without gypsum board.

While exposed to a heat load of such intensity, the roof structure remained intact when covered by a 10 cm thick dry growing media of medium porosity. An increased duration of heating caused a temperature rise at the depths of interest. However, the critical temperature under these conditions will not probably be reached in all assemblies since the temperature profile curves are almost linear after four hours of exposure (Fig. 4.12a,b and 4.13), which indicates the approaching of a steady state. Therefore, increasing the exposure time at such a heat load for more than four hours is not reasonable.

4.5.2. Thermal Load Effect

While a low heating load does not greatly affect the deck temperature and roof failure does not occur even after four hours, the increase of the imposed heat flux at the surface can influence the evolution of temperatures in the assembly. This is shown in Fig. 4.14, where the green roof assembly without gypsum board was subjected to heating loads of different intensities. The temperature underneath a substrate layer remained almost the same after one hour of exposure to higher thermal loads (Fig. 4.14a). However, the difference was noticeable after two hours. The temperature increased almost twice when the thermal load was twice as high — 124 °C with a heat load of 100 kW/m², and 73 °C when applying 50 kW/m². When applying 200 kW/m² the temperature was more than three times higher than when applying 50 kW/m², 256 °C compared to 73 °C. It was the same for temperatures at the top of the deck (Figure 4.14b). After two hours, the deck was at 43 °C under 50 kW/m², while under 200 kW/m² it reached 115 °C. The critical temperature was attained after 3 h 13 min, which is 45 min earlier than when exposed to 150 kW/m². Smaller heat loads did not lead to a failure under such conditions.

Thus, the results suggest that the effect of thermal load is significant under such conditions, even though the growing media has low conductive characteristics and the layer is thick enough.

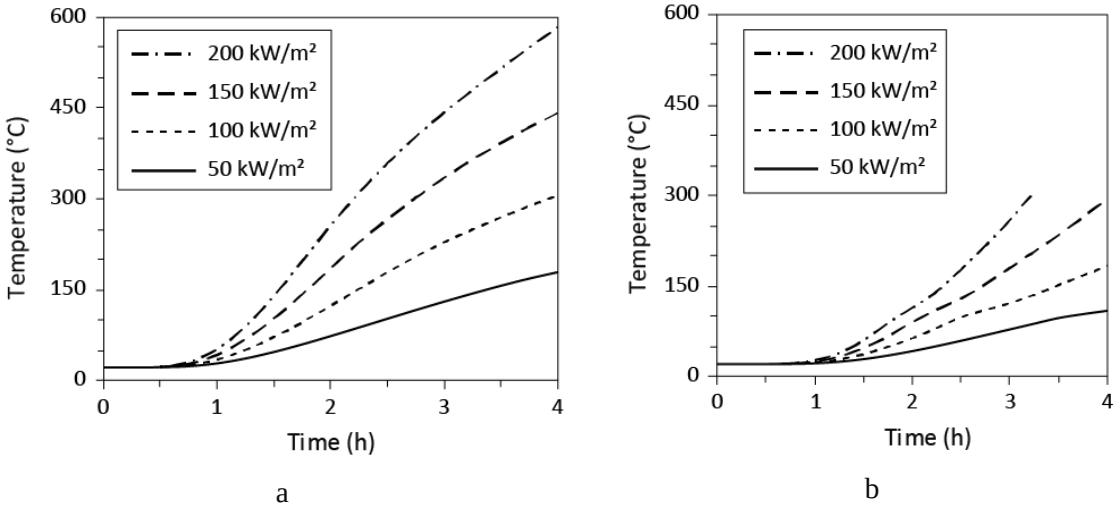

Figure 4.14. (a) Temperature evolution at the depth of 10 cm of a substrate layer within the green roof assembly installed on a wooden deck with no gypsum board; (b) temperature evolution at the top of the wooden deck.

The roof structure made of wood and not protected by a gypsum board (most severe case) is subject to a risk of failure only when the heating load is above 150 kW/m² for a period of four hours.

4.5.3. Substrate Thickness

The above analysis suggests that a 10 cm layer of growing medium insulates the roof by retarding the propagation of heat for at least three hours when exposed to a severe heat load. However, a thinner layer, may not be as effective at protecting the deck from heat damage. Critical temperatures reached at different soil thicknesses and applied thermal loads are presented in Fig. 4.15 and 4.16 for the assemblies installed over the wooden deck with and without gypsum board, respectively. The curves represent the critical temperature reached by the deck at a certain thermal load.

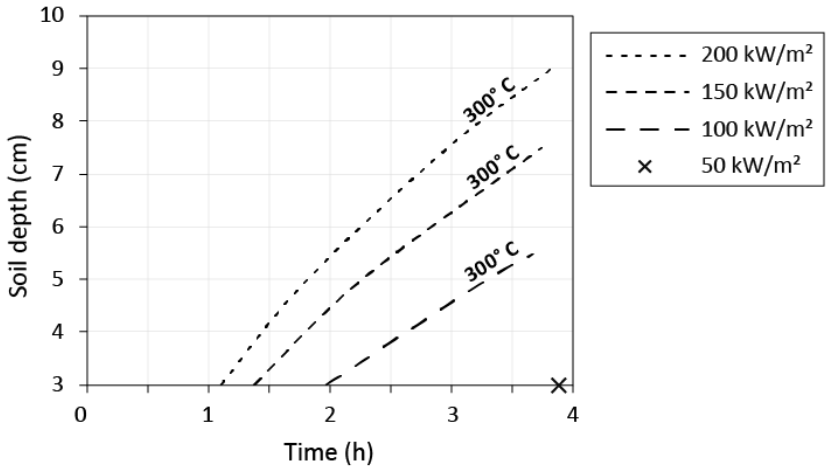

Figure 4.15. Assembly installed over a wooden deck with gypsum board. Relationship of time to failure of the deck (300 °C was reached under different thermal loads) and substrate thickness.

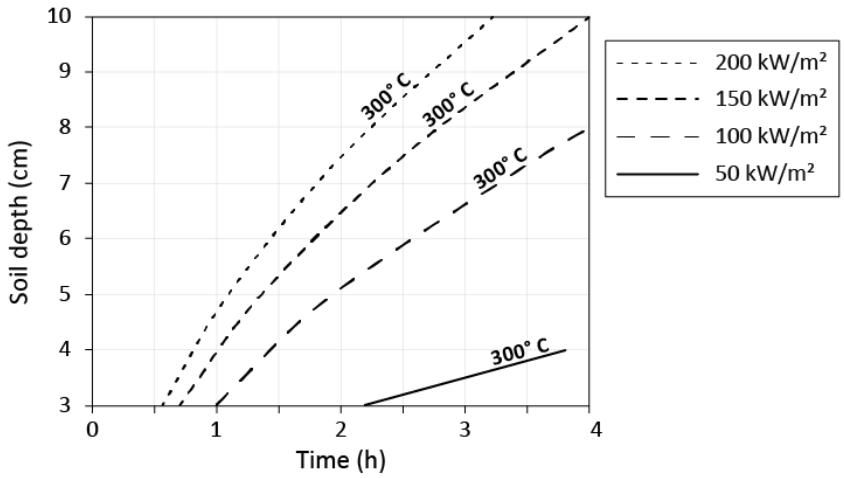

Figure 4.16. Assembly installed over a wooden deck without gypsum board. Relationship of time to failure of the deck (300 °C was reached under different thermal loads) and substrate thickness.

As expected, critical temperature was reached earlier as the thickness of soil decreases. When comparing the applied thermal loads, it was seen that in all cases the time to failure increases greatly for every additional cm of soil, especially for thermal loads of low intensity. For example, when imposing 100 kW/m², a deck, covered by a 5.5 cm soil layer and a gypsum board, reached 300 °C after 3 h 40 min, which is 1 h 40 min later when compared to the same assembly but with 3 cm of soil. A similar situation was observed for the assembly without gypsum. Under the same heat flux, the deck reached 300 °C at 2 h 15 min when protected with 5.5 cm of soil, while removing 2.5 cm led to much earlier failure, i.e. after one hour. At the same time, results show that with increasing thermal load the curves become steeper, which means lesser influence on dependence of time to failure on soil thickness. For instance, under 150 kW/m² the difference in failure time was 1 h 30 min when comparing assemblies with 7.5 and 5 cm thicknesses of growing media (Fig. 4.15). A greater increase in heating intensity to 200 kW/m² for such thicknesses resulted in a smaller difference in time to failure, namely 1 h 10 min. For the assembly without gypsum board, the dependency of time to failure of the roof deck on thermal load intensity was less pronounced. Again, comparing soil coverages of 7.5 and 5 cm, the difference in the effect was 70 and 55 minutes, for 150 and 200 kW/m² respectively (Fig. 4.16).

Considering the effectiveness of the growing media layer in protecting the roof from fire damage, it can be seen that, with decreasing thickness, the influence of heat load intensity on

the time to roof failure becomes significantly smaller. Fig. 4.15 shows that for the assembly with a 3 cm thick soil cover, the deck reached its critical temperature between 1 h 5 min and 2 h when exposed to thermal loads between 200 and 100 kW/m². Whereas, for the assembly with 5.5 cm of soil the critical temperature is reached between 2 h and 3 h 40 min for the same thermal exposure range. This effect is more evident for the assembly with no gypsum board (Fig. 4.16). Comparing applied thermal loads of 100 and 200 kW/m², in the assembly with 3 cm of soil, the deck reached the critical temperature after 60 and 35 minutes respectively, which is a 25 minute time difference. Whereas in case of 8 cm of soil, the difference in failure time is 1 h 45 min, with failure occurring after 4 h and 2 h 15 min respectively for each thermal load.

When comparing the two assemblies with the wood deck it can be seen that the presence of gypsum board helps to greatly increase failure time, especially under low thermal loads. For example, the delay is one hour when applying 200 kW/m² for the roof with a 7.5 cm soil layer. For a smaller load of 150 kW/m², the delay is 1 h 15 min for the same assembly. Gypsum delays the deck failure in the assembly with the thinnest soil layer by 32 minutes for the maximum thermal load applied in the model and by 1 h 40 min for the minimum thermal load applied.

Failure is not expected, even with the shallowest growing media and under maximum thermal load, for the assembly with a steel deck. Fig. 4.17 shows the roof deck temperature development where each curve represents the assembly with different soil layer thicknesses exposed to 200 kW/m². The better performance of such assembly in terms of time to failure compared to the assembly installed over a wooden deck is due to the higher critical temperature of steel. For example, the wood deck protected with gypsum board and 10 cm of soil reached a temperature of 235 °C after 4 h at 200 kW/m² while the steel deck reached 202 °C. Similar shape curves were obtained for all substrate layer thicknesses. It can also be seen that, at certain points, the 3 and 5 cm thickness curves show a slowing down of the temperature increase. The same model run for the assembly with 3 cm of soil and a 6 h duration does not show a significant increase in deck temperatures between 4 and 6 h of exposure to heat (results not shown). The reason is the approaching to reach steady state, as (not presented in the figure) the temperature under the substrate also slows to increase after about 2.5 h reaching 970 °C.

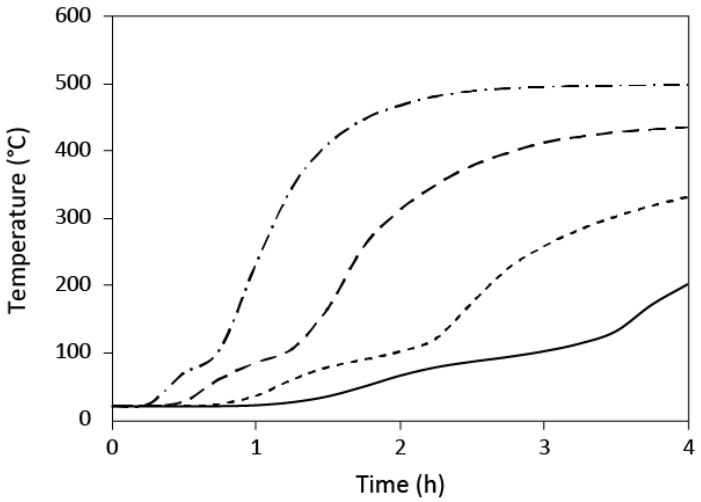

Figure 4.17. Temperature evolution at the deck (steel) level in the assembly exposed to 200 kW/m².

4.5.4. Substrate Porosity

Soil compacted to different porosities does not show great differences in reaching critical temperatures. Fig. 4.18a,b shows the results of the deck temperature evolution with a 7.5 cm substrate layer and exposed to a heat load of 200 kW/m².

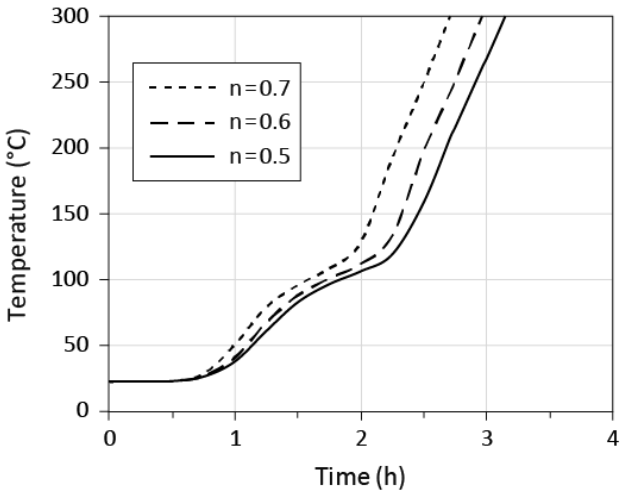

a

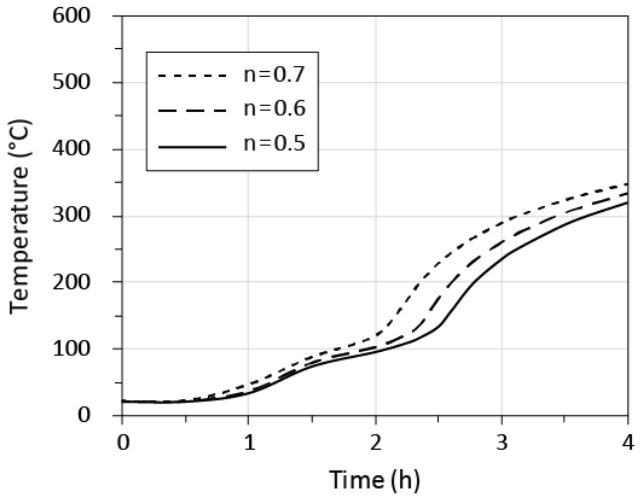

b

Figure 4.18. Temperature evolution at the top of a deck with a 7.5 cm growing medium layer at three different porosities (*n*): 0.5, 0.6, and 0.7 when exposed to 200 kW/m²; (a) wooden deck; (b) steel deck.

The smallest porosity of 0.5 (better compacted soil) retards the time to failure for the wood deck by 25 minutes compared to the assembly with a substrate porosity of 0.7, i.e. 3 h 9 min compared to 2 h 43 min (Fig. 4.18a). For the assembly with the steel deck it can be seen that the porosity is not an important factor in roof failure because the critical temperatures are never reached, even at the shallowest soil layer (Fig. 4.18b). Nevertheless, substrate shows the same behavior. Higher porosity leads to faster heating. For example, substrate of 0.7 porosity reached 100 °C 20 minutes earlier than the substrate of 0.5 porosity. The difference increases to 30 minutes when reaching 300 °C. The difference is smaller to insignificant at heating loads of lower intensity. When imposing 50 kW/m² temperature curves of the roof deck differ only by a few degrees (not shown).

Generally, soil compaction in green roof assembly determines, to some extent, heat propagation, especially in the case of severe fires, but not greatly.

4.6. Conclusions

This research explored the behavior of green roof systems when exposed to fire through the use of numerical modeling. A heat transfer analysis through the roof assembly was performed

to predict the time to failure of a roofing deck in most severe fire cases. Only systems with a shallow growing media in completely dry conditions were examined.

Green roof substrate, sufficiently different from natural soils by composition and more bulky structure, still is comparable with some literature data for dry natural soils in temperature distribution along the depth when exposing to extreme temperatures. Due to its insulation characteristics, other layers in the assembly and a roof deck appeared to be effectively protected from damages by heat.

Near linear relationships were obtained between growing media thickness and time to failure of the roof when exposed to different heat fluxes. Greater substrate layer thicknesses delayed heat penetration through the assemblies. Also, an increased heat load had a smaller influence on the relationship between soil thickness and time to failure.

Assembly installed on a metal roof deck showed better performances in fire in terms of time to failure, namely due to a higher critical temperature of steel (538 °C) when compared to that of wood (300 °C).

Gypsum board greatly improved the performance of green roof installed over a wooden deck in fire by increasing the time to reach critical temperature for the whole range of heat load intensities. A delay in reaching the critical temperature by the deck of at least 30 min can be attained in the roof assembly having at least 3 cm of substrate when exposed to intensive thermal load.

Substrate porosity had a small effect on the time to failure and only at high heat loads, which means that matured green roofs with settled growing media can have a slightly better performance under fire conditions than newly installed.

The present study examined green roof temperature responses to fire under idealized conditions. The scenarios studied are improbable since maintaining such high heat fluxes for a long period of time is not reasonable when taking into account only the vegetation as a fire load. Nevertheless, such an approach permitted the generalization of the behavior of such roofs during extreme heating. It was shown that the thicker the soil layer the better protection it provides for the roof deck when exposed to a heating load of any intensity, considered in this study, and at different compaction levels.

The limitation of these models is using the worst-case scenario in order to investigate conditions at which a structure failure is reached. Such idealizations can lead to overestimations of some results compared to real fires. Analyzing heat transfer in the assembly while taking into consideration several factors reflecting real fire conditions can be a subject for future research. These factors include boundary conditions on top, because the heat load is not uniform in its intensity in real fires and lasts for a shorter period. Also, the standard value for convective heat transfer coefficient taken for the boundary conditions for the underside of the roof deck may be slightly greater and thus, can affect the results. A lower value of 6.13 W/(m²·K) can be used, that is suggested in ASHRAE (2017) for the downward heat flow for horizontal surfaces. Another factor is the heat generation produced by OM combustion. Even though the amount of this material is small to negligible, including this portion of heat can improve the accuracy of the model. This can pose a challenge, as, in addition to collecting necessary information, understanding that incomplete combustion occurs at a certain depth due to a restriction of air access, adequate adjustments must be made. Developing a model that includes moisture in the growing medium would more realistically describe the fire performance of green roofs. The main effort in such model should be paid to the effect of water evaporation on the temperature development inside the assembly.

Another limitation is the lack of validation tests for the results due to the complexity in conducting such experiments. This is because of the absence of a standard method and equipment for providing 1D conduction that ensures the large scale application of controlled uniform heat loads downwards. A small-scale fire test in previous study (Gerzhova *et al.*, 2019) was conducted with a separate substrate layer to validate the heat transfer model and to verify the applicability of the thermal conductivity of a substrate determined in the study. Special arrangements and sample preparation were made to create modeled conditions as accurately as possible. Based on the satisfying test results of a previous research, simplified models were developed in this study with assemblies of green roof containing similar substrate and typical materials (structure, gypsum) with known properties.

Nevertheless, an intermediate-scale fire testing protocol should be developed to assess the fire behavior of realistic green roof assemblies, namely as it relates to heat transfer through the assembly based on similar failure criteria to those presented here. As an example, for a

one hour fire resistance rated roof assembly, the time to reach its critical temperature should not be reached before one hour.

4.7. Acknowledgments

The authors are grateful to Natural Sciences and Engineering Research Council of Canada for the financial support through its IRC and CRD programs (IRCPJ 461745-18 and RDCPJ 524504-18) as well as the industrial partners of the NSERC industrial chair on eco-responsible wood construction (CIRCERB).

Authors also acknowledge the Green Roof Working Group of the Green Building Council of Canada, Quebec's section for technical data and mobility funding.

CHAPITRE 5 : Flammability Characteristics of Green Roofs

Buildings, 2020, Vol. 10 (7), 126

Nataliia Gerzhova[1], Pierre Blanchet[1], Christian Dagenais[1,2], Sylvain Ménard[3] Jean Côté[4]

1 NSERC Industrial Research Chair on Eco-responsible Wood Construction (CIRCERB), Department of Wood and Forest Sciences, Université Laval, Québec G1V 0A6, QC, Canada
2 FPInnovations, Québec G1V 4C7, QC, Canada
3 Department of Applied Sciences, Université du Québec à Chicoutimi (UCAQ), Chicoutimi G7H 2B1, QC, Canada
4 Department of Civil and Water Engineering, Université Laval, Québec G1V 0A6, QC, Canada

5.1. Résumé

L'évaluation du risque d'incendie des TV comprend la détermination de sa contribution possible au feu. Les composants de la TV, tels que les plantes et le substrat de croissance, sont des matières organiques et représentent un combustible pouvant contribuer à la propagation du feu. Les caractéristiques d'inflammabilité de ces composants ont été analysées et comparées à une couverture de toit typique. Le substrat de croissance contenant 15% de matière organique a été testé à l'aide d'un calorimètre à cône. La charge combustible et le débit calorifique ont été mesurés pour les échantillons à l'état humide (30%) et à l'état sec. Il a été constaté que le substrat humide ne présente pas de risque d'incendie, atteignant un débit calorifique maximal de 33 kW/m². Pour le substrat sec, cette valeur est de 95 kW/m² atteinte en moins d'une minute et diminue rapidement durant une seconde minute à 29 kW/m². Lorsque comparé à une membrane de toit en bitume modifié, le substrat a montré une meilleure performance au feu même à l'état sec. Les résultats montrent également que les types de TV extensives et intensives présentent 22% et 95% de densité de charge calorifique additionnelle lorsqu'ils sont installés sur une membrane de bitume modifié, soit 19.7 et 85.8 MJ/m² respectivement.

Mots-clés : toiture végétalisée; feu; inflammabilité; débit calorifique

5.2. Abstract

Assessing the fire risk of vegetated roofs includes the determination of their possible contribution to fire. Green roof components such as plants and growing media are organic materials and present a fuel that can catch and support the spread of fire. The flammability characteristics of these components were analyzed and compared to a typical roof covering. Growing media with 15% of organic matter were tested using cone calorimeter apparatus. The fuel load and heat release rate of the growing media were measured in both moist (30%) and dry conditions. It was observed that growing media in a moist condition do not present a fire risk, reaching a maximum heat release rate of 33 kW/m². For dry substrates, a peak heat release rate of 95 kW/m² was recorded in the first minute, which then rapidly decreased to 29 kW/m² in the second minute. Compared to a typical bitumen roof membrane, the green roof showed a better fire performance. The literature data report more severe results for plant behavior, reaching peak heat release rates (HRRs) of 397 kW/m² for dried and 176 kW/m² for a green material. However, a rapid decrease in HRR to much lower values occurs in less than 2 min. The results also show that extensive and intensive types of green roofs present 22% and 95% of the additional fire load density when installed on a modified bitumen membrane, 19.7 and 85.8 MJ/m², respectively.

Keywords: green roof; fire; flammability; heat release rate

5.3. Introduction

Currently, plants are being successfully used as an environmental improvement tool. One of the examples of this contemporary technology is the installation of vegetation on roofs and walls of buildings, which helps to improve the ecology and social life in urban areas. This has been demonstrated by numerous scientific studies on various aspects, such as reduction of water runoff, increased energy efficiency of buildings, bringing aesthetic value and increased biodiversity by providing a natural habitat (Stovin *et al.*, 2012; Yio *et al.*, 2013; Jaffal *et al.*, 2012; Jungels *et al.*, 2013; Brenneisen, 2003). Studies make a great contribution to the development of these systems and to the promotion of the installation. The safety of green roofs, however, is poorly studied, namely in terms of the fire hazard. It is still debated whether the presence of such roofs possess a risk to the building and to what extent. The

primary concern is the combustibility of green roof components, such as plants and soil organic matter (OM), which are claimed to present an additional fuel load that can contribute to fire (Meacham *et al.*, 2013; RBQ, 2015). In fire design, little attention is paid to roofs, because as non-living spaces they pose a very low risk of fire exposure for the occupants. This conforms to the primary objective of the building code for fire safety NRCC (2015), to limit the risk for the occupants. Moreover, unlike the interior of the building, these spaces are not confined, and the amount of stored combustible materials on top of the roof is restricted. However, green roofs fully covered by vegetation, especially in cases of intensive greening, appear to store some amount of fuel continuously distributed on their surface, presented by the organic material in soil and plants. The possibility of such fuel to be ignited and to develop a fire was confirmed by the recent small green roof fires that happened in Portland (OR, USA) and London (UK) in the summer of 2018 (Portland Fire Bureau, 2018; LFB (London Fire Brigade), 2018). From the available information, dried overgrown grass caught on fire from a spark in the first case. In the second, low extensive greening was ignited, possibly by a cigarette. Sustained flaming appeared, which spread over a roof deck and a wall nearby. Both fires were extinguished by firefighters.

The flammability characteristics of organic materials, such as peat (Lin *et al.*, 2019), leaf litter (Scarff and Westoby, 2006), forest litter in the form of pine needles (Jervis and Rein, 2016), ornamental vegetation (Weise *et al.*, 2005) and various plant species (leaves and twigs) (Dimitrakopoulos and Papaioannou, 2001) have been reported. However, studies on organic soil flammability or green roof substrates are difficult to find. A British report on the fire safety of green roofs investigated the behavior of dry green roof substrates in terms of ignitability and heat release rate (HRR) at a small scale using a cone calorimeter (Department for Communities and Local Government UK, 2013). The document concluded a good performance for a standard mix showing either no ignition, or in the case of ignition, no sustained flaming. The report contains general conclusions and no details were given as for the tested samples (composition and amount of OM in the soil blend), test procedure and the description of results. Moreover, only dry material was tested, assuming the most dangerous case. Comparisons with a substrate containing some amount of moisture, as in real conditions, can provide a better idea of the fire hazard of the substrate. Another interesting comparison is given in the literature as for the advantages of a green roof over a conventional

one in fire performance. It was stated that a dry extensive green roof with dry grass releases much less heat (3 kWh/m²) than a typical bituminous roof membrane (50 kWh/m²) (Breuning, 2008). A description of the experiment was not given and therefore it is not clear what the test conditions (test method) and the parameters of the green roof assembly were (soil organic product, the amount of vegetation material, moisture content).

Additional information on combustible characteristics of green roof substrates, as well as a summary of the fire load, composed of substrates and vegetation, can contribute to the knowledge on the fire hazards of these systems. The objectives of this study are to determine the potential amount of fuel that is presented by a green roof, the heat release rate produced by green roof materials in case of fire, and to compare this to a conventional type of roof.

5.4. Background

5.4.1. Fuel Load

The protection of a building from fire by a safety design involves the development of fire scenarios that may occur in the building. Necessary information includes the characterization of the building in terms of the quantity of combustible materials (fuel) that presents a certain fire load (Hadjisophocleous and Mehaffey, 2016). The fire load in buildings is usually expressed as the amount of energy per area (fire load density, MJ/m²), which can be calculated by knowing the mass of fuel per area (fuel load) (kg/m²) and the energy content of this fuel (MJ/kg). The amount of fire load is necessary in the prediction of temperatures during a fire inside a compartment. It is also one of the parameters that influences HRR, which is the main characteristic of fire severity in buildings (Fontana *et al.*, 2016). In vegetation fires, or wildfires, the prediction of fire behavior differs from that of the building, concerning not only the intensity of fire but also its rate of spread, which depends on multiple factors. The fuel load presented by various plant materials is one such factor.

When estimating fuel load, it is important to consider its availability. For example, the moisture of a plant material reduces the availability of fuel. Its increased content in live plants makes them act as a heat sink, rather than a source of fuel (Burgan, 1979). Dead plant material with a low moisture content burns more easily. The difficulty in estimating the amount of

available fuel presented by vegetation in wildlands is that it always changes due to the transition of plant parts from live to dead, provoked by a seasonal fluctuation in moisture.

Another indicator of the fuel availability is the direct disposition to flames (fuel density, fuelbed porosity) and fuel thickness (fuel surface-to-volume ratio) (Fontana *et al.*, 2016). For example, grass, leaves and small shrubs are fine fuels, which are considered highly susceptible to fire. Their high surface-area-to-volume ratio and the small size of their particles allow them to dry out during hot periods, increasing the risk of being ignited and contributing to fire (Bond and Van Wilgen, 2012). Such material burns quickly and can be expected to be consumed completely in fire. Moreover, since it does not require much heat input to lose moisture, in the case of an existing fire, live herbaceous plant material cannot always effectively resist the flame spread. Plants with particles of lower surface-area-to-volume ratio (particle diameter over 0.25 in) require more time to be completely burned, releasing energy more slowly. The moisture presented in such fuels requires a lot of energy input to be driven out. Another example of fuel availability is organic material in soil, which, for green roof growing media, is usually in the form of peat and compost, which are mixed with mineral components and packed. In soil, the access to air is limited, and thus the combustion occurs mostly at the surface layer, whereas incomplete combustion occurs underneath, which means that not all fuel will be consumed. Both large plants and organic soil are considered thick fuels (Rein, 2016).

5.4.2. Vegetation

A large amount of data on vegetative fuel load exists in the literature. This can be found in the default data for different types of wildlands as input parameters for wildfire modeling. Several sets of fuel models have been elaborated in the USA (Rothermel, 1972; Bradshaw *et al.*, 1983; Scott and Burgan, 2005) and Canada (Wotton *et al*., 2009) that describe fuelbed parameters, such as the amount of dead (fine, medium, large) and live fuel load per area, type of vegetation, fuel depth (height) and energy content. Fuel data are also available for Australian and some European and African wildlands to be used in the models (Anderson et al., 2015; Dalgleish *et al*., 2015; Marsden-Smedley and Catchpole, 1995; Cheney *et al*., 1993; Rossiter *et al*., 2003).

Fuel load can also be presented as the amount of biomass (organic part of a plant, typically dry weight is taken). In wildfires, plant biomass is not always regarded as a total fuel, because of a reduction in fuel availability. However, each green roof is unique, which means their fuelbed parameters are different in each case. Assumptions of the most hazardous case can show the potential contribution of different types of green roofs to fire, and therefore the data on the biomass can be considered as a total fuel load.

There are several categories of green roofs (Figure 5.1) that differ mostly by the type of vegetation and the thickness of the growing medium necessary to support the plants. Extensive green roofs with a shallow layer of substrate are planted with low-growing herbaceous plants, grasses, Sedums and mosses. A 10-cm thickness of growing medium with low organic matter (OM) content (2–5% by mass) is usually enough to support such plants. Semi-intensive roofs have a greater variety of plants, including small shrubs. Intensive green roofs are usually roof gardens with diverse vegetation, from simple grasses to shrubs and small trees. A growing medium rich in OM (up to 20%) and a larger thickness is required. Each of these categories of roofs thus stores a certain range of fuel load. It must be noted that succulents, typically used for simple extensive green roofs, do not carry fire easily, unlike other plants, because of their ability to store great amount of moisture. Their specific structure does not allow for the loss of water at a high rate. This helps them to survive even in severe drought periods. Their contribution to fire risk therefore can be neglected. Trees (installed on roof gardens) can also be excluded from fuel estimation due to the large diameter of their particles. Thus, only some fine fuels, herbaceous plants and shrubs with branches of small diameters should be considered.

a b c

Figure 5.1. Green roof categories: (a) extensive (with low grass); (b) semi-intensive (with tall grass and low shrubs); (c) intensive (with tall shrubs).

To have an idea of the amount of fuel load presented by each of the categories of green roofs, existing data on the biomass of species grown on roofs can be used. Moreover, each category can be associated with a certain wildland (or fuel model). Existing data on the fuel parameters (biomass) of vegetation can be sorted into three categories: extensive greening (low grass, that is, up to 0.5 m height); semi-intensive (includes tall ornamental grasses of 0.5–1.5 m height, and small shrubs of less than 1 m); intensive (includes tall shrubs of more than 1 m height). For shrublands, data are sometimes given at a certain percentage of cover (between 10% and 99% in the literature), which is acceptable, since intensive green roofs contain only inclusions of tall vegetation, not being covered completely. Thus, the percentage of vegetation cover may not be considered. Wildland types or fuel models can be ascribed to each category.

Tables 5.1–5.3 present the data on fuel load for vegetation of each roof category. Fuel types were collected from sources of the models and measured values of specific wildlands vegetation from other studies on fire behavior in wildlands and on the aboveground biomass accumulation. Models include fine dead fuel, which is presented by particle diameters of less than one inch (2.5 cm), also called 1- and 10-h fuels. They also include live herbaceous material. Other fuels, such as dead fuels with more than one-inch diameters, and live woody fuels, are not considered.

Table 5.1. Fuels chosen for extensive green roofs.

Fuel	Total fuel load (kg/m²)	Reference

1 (Short grass)	0.18	(Albini, 1976)
A (Western annual grass)	0.13	(Bradshaw *et al.*, 1983)
L (Western perennial grass)	0.19	
GR-1	0.10	(Scott and Burgan, 2005)
GR-2 (Sparse or grazed grass)	0.27	
O-1a, O-1b (Grass)	0.30	(Wotton *et al.*, 2009)
Understorey of native grasses	0.39	(Rossiter *et al.*, 2003)
Grasslands	0.40	(Cheney *et al.*, 1993)

Table 5.2. Fuels chosen for semi-intensive green roofs.

Fuel	Total fuel load (kg/m²)	Reference
3 (Tall grass)	0.74	(Albini, 1976)
5 (Short shrub cover)	0.86	
N (Grass prairie)	0.75	(Bradshaw *et al.*, 1983)
T (Sparse shrubs and grass)	0.50	
GR 3-4 (Grass)	0.49 to 0.53	(Scott and Burgan, 2005)
GS 1-4 (Grass-Shrub)	0.17 to 1.41	
SH 1-3, 6 (Brush)	0.16 to 1.11	
Ornamental grass (Sideoats grama, Green needlegrass, Indian grass)	0.37 to 0.75	(Jefferson *et al.*, 2002; Bosworth and Kelly, 2013)
Tall grass species	0.80 (average)	(Kidnie, 2009)
Moorland (Low young shrubs)	0.24 to 1.53	(Marsden-Smedley and Catchpole, 1995)
Button grass moorland	1.10 to 1.60	(Anderson *et al.*, 2015)

Table 5.3. Fuels chosen for intensive green roofs.

Fuel	Total fuel load (kg/m²)	Reference
7 (Brush)	0.83	(Albini, 1976)
D (Southern rough)	0.81	(Bradshaw *et al.*, 1983)
SH-5 (Chaparral)	1.41	(Scott and Burgan, 2005)
SH-7 (Brush)	2.17	
Shrub-steppe	0.95	(Li *et al.*, 2017)
Shrubland	0.78 to 1.51	(Dalgleish *et al.*, 2015)
Moorland (High density, 1 m height)	2.00	(Marsden-Smedley and Catchpole, 2001)
Mediterranean shrubs	1.1 to 2.4	(González-González *et al.*, 2017)
Heathland	1.4 to 2.47	(Anderson *et al.*, 2015)
Shrubs (heath, gorse, broom)	1.90 to 2.63	(Viana *et al.*, 2012)

In the studies on plant biomass, descriptions of a type of vegetation and its height are usually given. No division by the diameter size or live and dead material of plants could be found. However, from the description in the studies used, it is clear that the vegetation does not present thick fuel. For the most hazardous case, it can be assumed that the live woody material of these plants can also present the fuel load. Thus, the total biomass was included. Data on the biomass of separate species of tall ornamental grasses such as Switchgrass (*Panicum virgatum*), Big bluestem (*Andropogon gerardii*), Little bluestem (*Schizachyrium scoparium*), Mammoth wildrye (*Leymus racemosus*) and Western wheatgrass (*Pascopyrum smithii*), which are used on green roofs (Torrance, 2013; Sutton *et al.*, 2012; GNPC), can be found in other studies. These values, however, may not be realistic for green roofs, as the studied areas present tall and dense stands, and therefore do not represent the accumulation of fuel load on a roof. For example, for mammoth wildrye, switchgrass and big bluestem, the range of maximum values found is 1.58–1.7 kg/m², with a mean value of 1.64 kg/m² (Jefferson *et al.*, 2002; Heaton *et al.*, 2004). For Little bluestem and Western wheatgrass it is 1.2–1.25 kg/m² (Zilverberg *et al.*, 2016).

5.4.3. Growing Medium

The growing medium for a green roof usually contains some amount of OM in different forms, such as peat, compost and sawdust. The proportion of organics in the soil mix varies between 2–3 and 20–25% by mass. The thickness of a substrate layer varies depending on the type of vegetation it supports. The minimum thickness is usually not less than 5 cm. Typically, for extensive greening, 10 cm is taken; for intensive green roofs, a greater depth is needed. Because soil is a thick fuel, only its available part (organic matter in the combustion depth) can be considered in fuel loading. During wildfires, heat does not usually penetrate deep into the soil, because soil in the dry state is a poor heat conductor, and the in moist state, a lot of energy needs to be applied to evaporate the water first. Measured temperatures in natural fires rarely exceed 100 °C at a depth of 5 cm. For example, temperatures were recorded in the range of 49 and 66 °C at a depth of 5 cm; at a depth of 2.5 cm, temperatures varied between 57 and 174 °C for dry soil in chaparral fires (DeBano *et al.*, 1979). Higher temperatures are given by Beadle (1940) and Busse *et al.* (2005) for a 2.5 cm depth, 250 and 370 °C, respectively. Because of the absence of record temperatures reached

in green roof soils in fires, which also differ from natural soils, it can be assumed that a layer of 2.5 cm in depth can contribute to fire. Growing media fuel parameters can be determined experimentally.

In addition to the vegetation and substrate, the assembly of a green roof contains other combustible materials, such as drainage panels (recycled polyethylene), a filter cloth (geotextile) and a root barrier (high-density polyethylene). As they are covered by a layer of soil, usually not less than 5 cm thickness, it can be assumed that they cannot present a fire load, as their availability for combustion is limited.

5.5. Materials and Methods

5.5.1. Flammability Characteristics

In fire engineering, the combustion performance of materials is usually investigated using the cone calorimeter apparatus. It is a standard method of measuring the flammability properties of a material, such as HRR, time to ignition, mass loss rate, smoke and toxic gas production (Babrauskas, 2016a). In the experiment, a small sample is exposed to a uniform radiant heat flux of a constant intensity (up to 100 kW/m²) and, with a spark igniter, the surface of the sample is ignited.

To evaluate the hazard that a green roof substrate represents in terms of its fire response, its performance was experimentally investigated with this method. For a better understanding of the scale of the risk, the obtained results were compared to existing data on waterproofing membranes tested in the same conditions. The following properties of the green roof substrate were measured: total heat released, HRR and time to ignition.

Few studies have been conducted on the fire properties of typical roof-covering materials using a cone calorimeter. In conventional types of roof coverings, the top layer is a waterproof membrane, which is made of combustible materials. One of the most common waterproof membranes used under green roof systems is polymer-modified bitumen (PMB). Data on its flammability parameters, such as HRR, average and peak HRR (pHRR), time to ignition, as well as the effect of ageing and fire retardant additives on these parameters, are available in the literature (Thureson and Nilsson, 1994; Bourbigot *et al*., 2013).

5.5.2. Testing Procedure

The growing media were tested using a cone calorimeter fabricated by the Fire Testing Technology company (UK). Experiments were performed to determine HRR, as one of the most significant indicators of the fire hazard of materials (Babrauskas and Peacock, 1992). Ignitability, pHRR and average HRR parameters were also measured. Tests were carried out in accordance with ISO 5660-1 "Reaction-to-fire tests—Heat release, smoke production and mass loss rate" (ISO 5660-1, 2015). In the absence of guidance on choosing a heating load specifically for green roof substrates and a lack of information on real fires on such roofs, a mean radiating heat flux of 50 kW/m² was used in the experiments. Such an irradiance level can represent small-scale fires (Babrauskas, 1995). The duration of each test was 15 min or until no heat was released. For each substrate in wet and dry conditions, the test was repeated three to five times or more to obtain reliable data.

5.5.3. Materials and Sample Preparation

Two commercial growing media mixes that are used in Quebec for extensive green roofs were taken for the study (Substrate 1 and 2), shown in Figure 5.2a,b. The OM content of both materials was 20 ± 3% by mass. The two substrates were different in the composition of their components. The inorganic part of the first mix was in the form of a lightweight aggregate (slag) and a small amount of sand; the second mix contained expanded shale and perlite. Organic products were the composting material and peat moss in different proportions for each substrate.

To evaluate the effect of presence of moisture in the substrate on its fire behavior, samples were tested in both dry and moist conditions. In natural conditions, the moisture content (MC) of soil can vary greatly depending on multiple parameters such as season, time of day, weather and irrigation. It also depends on soil composition, soil particle characteristics and the ability of its components to absorb certain amounts of water. Because of this, analyzing the effect of a whole range of MC will be representative only of the substrates tested. This study focuses on general comparison of the fire hazard in the most severe case (dry state) and real conditions (with a certain level of MC). Therefore, only one moisture condition (30% of MC), which was chosen arbitrarily, was considered for the analysis. To eliminate water from

the substrates, samples were placed in an oven at 105 °C for 24 h. Moist samples were prepared by adding water to an oven-dried soil, and then sealing them in plastic bags for 1 week. The dry weight of a substrate was the same for dry and moist samples, and was equal to 80 ± 5 g.

The standard specimen holder of the cone calorimeter was used for the test, consisting of a metal sample pan of 100 × 100 mm and a metal edge frame of 50 mm in height. When installing it into in the holder, the substrate was manually compacted, and the surface was flattened. Figure 5.2c shows a sample of a dry substrate in a specimen holder.

a b c

Figure 5.2. (a) Substrate 1; (b) Substrate 2; (c) sample in a holder.

5.6. Results and Discussion

5.6.1. Fire Load Density of Green Roofs

The total fire load density of vegetated roofs includes vegetation fuel and the top of the growing media. Fire loads of the two types of growing media in the dry state were determined in the cone calorimeter. The obtained values of total heat released were calculated for a 2.5 cm thickness of each sample (with 15% of OM) and were equal to 36.9 and 14.1 MJ/m² for Substrate 1 and Substrate 2, respectively. It is assumed that fire loads of substrates with smaller amounts of OM can be obtained from these values by calculation per percent of OM.

The fire load densities of vegetation were calculated by multiplying fuel loads by their energy (heat) content. Studies on the heat content of vegetation showed that it depends largely on plant species. For example, for tall grasses, the reported range of values is 16.8 to 19.1 MJ/kg (Sampson, 2012; Parmar, 2017). The averaged value of 17.3 MJ/kg was found by Kidnie

(2009) for different tall grasses. From the experimental research on several Mediterranean shrub species (tested twigs and leaves), the heating value was between 19.9 and 22.9 MJ/kg (Madrigal *et al.*, 2011). However, in fire prediction systems, usually one value is used for all fuel models, such as 18.6 MJ/kg in the U.S. (Scott and Burgan, 2005) and 18 MJ/kg in Canadian Forest Fire Behavior Prediction (FBP) System (Hirsch, 1996).

Table 5.4 presents fire load densities for three types of vegetation cover in each of the green roof categories, and for the growing media. The energy content for vegetation was assumed to be 18.6 MJ/kg. The obtained values for the vegetation are given in the ranges, while, for the growing media, the higher result of Substrate 1 was taken, which presents a higher risk. Extensive and semi-intensive green roofs included substrates with 5% OM, intensive roofs included substrates with 15% OM.

When comparing these data with a conventional roof covering made of a modified bitumen membrane, which is composed of 90.4 MJ/m² (Thureson and Nilsson, 1994), it can be seen that the green roof with extensive greening presents about 22% of the additional fire load, semi-intensive presents up to 47% and intensive greening up to 95%.

Table 5.4. Fire load density of green roof and its components.

Components	Fire Load Density (MJ/m²)
Vegetation	
Extensive	1.9 to 7.4
Semi-Intensive	3.2 to 29.8
Intensive	15.1 to 48.9
Growing medium (Substrate 1, 2.5-cm combustion zone)	
5% OM	12.3
15 % OM	36.9
Green roof category	
Extensive	14.2 to 19.7
Semi-Intensive	15.5 to 42.1
Intensive	52.0 to 85.8

5.6.2. Combustibility

5.6.2.1. Growing Media

Figure 5.3 presents HRR curves obtained in the experiment for two commercial substrate mixes (Substrate 1 and 2) with 15% of OM in dry and moist conditions. It is seen that moist substrates release much less heat than in the dry state, reaching pHRRs of 33 and 24 kW/m² and only after 8 min, which presents a very low risk. In dry substrates, pHRRs are reached in the first few seconds and are equal to 95 and 64 kW/m², which is three times higher than those for the moist substrates. However, after only about a minute, these values decreased to 29 and 22 kW/m² and, until the end of the test, did not exceed 40 and 30 kW/m² for each substrate, respectively. In Figure 5.3, the curve for a typical roof covering, from a study by Bourbigot *et al.* (2013), is shown for comparison. The material is a roof membrane made of PMB with fire retardants. Peak HRR is not much greater than that of dry substrates at the first peak. However, it does not decrease much, continuing to release heat for a much longer period, increasing to 162 kW/m² at the second peak after 10 min.

A comparison can also be made to a membrane of the same material but without fire retardants. The results from another study show that the pHRR of such a material reaches 498 kW/m², staying at more than 100 kW/m² at first 6 min (Thureson and Nilsson, 1994). The mean HRRs of dry Substrates 1 and 2 in the first 5 min are equal to 37 and 27 kW/m², respectively. Compared to the membrane from the same study with the result of 260 kW/m² in the same period, it is more than seven times lower.

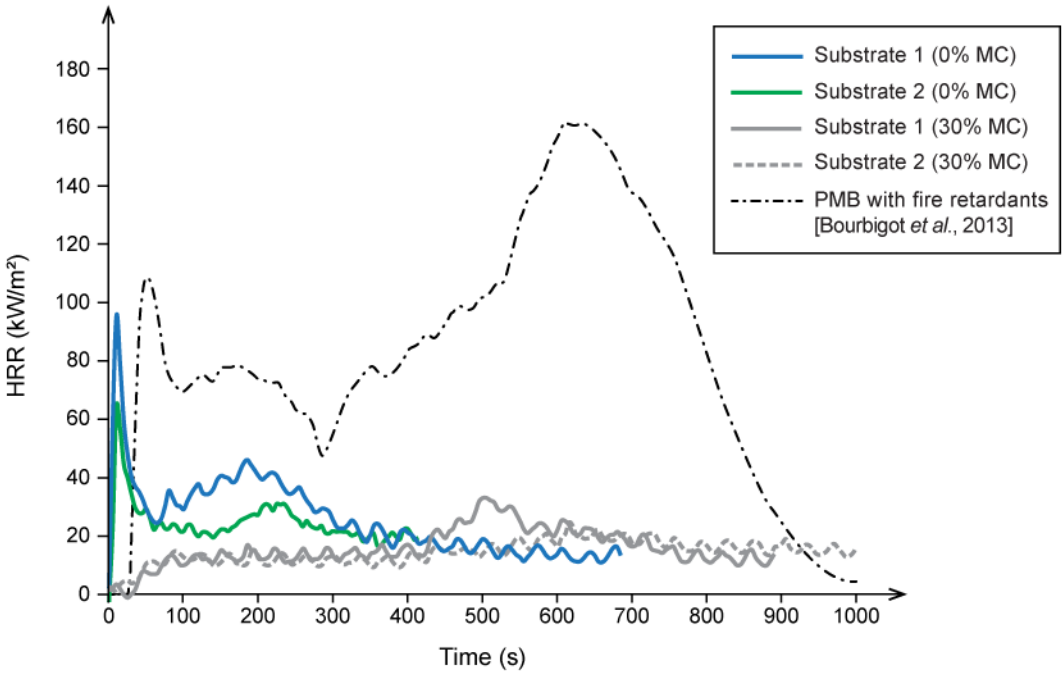

Figure 5.3. Comparison of heat release rate (HRR) of green roof substrates at dry and moist state with typical roof covering: (a) Substrate 1 (0% moisture content (MC)); (b) Substrate 2 (0% MC); (c) Substrate 1 (30% MC); (d) Substrate 2 (30% MC); (e) polymer-modified bitumen (PMB) membrane with fire retardants (redrawn from Bourbigot *et al.* (2013)).

There is a small difference in the results of two types of dry substrates, which is explained by the difference in the organic products and their proportions (compost and peat), which burn differently. Compost is presented in Substrate 1 in much larger proportions than peat. This can also explain the flaming in moist substrates, which for Substrate 2 was not observed, as shown in Table 5.5. Moreover, the maximum duration of flames observed in soils was about 5 min, while, in the membrane, the flaming ceased after 13 min.

Table 5.5. Times to ignition (seconds) and flameout for dry and moist substrates.

Material	0% MC		30% MC	
	Ignition, s	Flameout, s	Ignition, s	Flameout, s
Substrate 1	5	560	462	686
Substrate 2	7	294	-[1]	

[1] no ignition and flameout observed

5.6.2.2. Vegetation

Data on vegetation flammability characteristics tested in a cone calorimeter can be found in several studies (Dibble *et al*., 2007; Weise *et al*., 2005; Madrigal *et al*., 2012). The results show that HRR differs a lot depending on the species and moisture content of plants. Measured pHRRs of different northeastern USA plants were in the range of 30 and 397 kW/m² (Dibble *et al*., 2007). In the research of Weise *et al*. (2005), the pHRR of dried plant material was between 49 and 331 kW/m², and for green material (with high MC) it was between 1 and 176 kW/m². However, in both studies, HRRs of more than 50 kW/m² were observed for no more than two consecutive minutes. The example of the HRR curve produced by vegetation is taken from the experimental study of Madrigal *et al.* (2012) on European gorse (shrub), and is shown in Figure 5.4. Here, the curve is also compared to the results of the bitumen membranes. It can be assumed that vegetation from this research presents intensive greening (the fuel load specified in the study is between 1.6 and 3.1 kg/m²). Figure 5.4 shows HRRs separately for dead (leaves and twigs of small diameters with 25% MC) and live (green leaves with 75% MC) plant material. It is seen that curves of both components rapidly increase, reaching maximum values of 332 and 190 kW/m² for dead and live parts, respectively, but after about 2 min they rapidly decrease to about 25 kW/m² and continue to decrease after this.

When comparing these results to the roof membranes, it can be seen that both membranes release heat at much higher levels and for a much longer period, suggesting a greater potential contribution to the severity of a fire.

Some data can be found in the literature on plant flammability obtained in large and intermediate scale tests, which can be more realistic. For example, the pHRR of a small rockrose shrub (with up 3–20% MC in its leaves) was 228 kW (Tramoni *et al.*, 2018). With a rapid decrease after the peak, the flameout appeared in less than a minute, leaving the sample to be only partly consumed. Overholt *et al.* (2014) studied the fire behavior of tall grass (little bluestem) with a 7% MC, which can be associated with semi-intensive greening. The experiments on the whole plant showed a range of pHRRs from 35 to 75 kW for a single plant. In one minute, on average, the plants were completely burned. For a multiple plant setups with different stand densities, pHRR varied between 45 and 160 kW. In all cases,

pHRRs were reached in the first minute, after which they rapidly fell to values between 0 and 50 kW. The research data on the fire behavior of coniferous trees, known as highly flammable fuels, are also available. A large-scale experimental testing of Christmas trees (Douglas Fir and Noble Pine) was conducted by Damant and Nurbakhsh (1994). It was shown that the pHRR of a whole dried Christmas tree (very dense Douglas Fir) of around 2-m tall can reach 1667 kW, an extremely elevated value. For a cut and partly dried tree, pHRR reached 831 kW. However, it is not expected that a cut Christmas tree would be installed on a green roof. Thus, these results cannot be used for a comparison with the present study. For a freshly cut tree, the measured pHRR was only 11 kW, exhibiting a negligible amount of total heat released. As for other types of vegetation presented in Figure 5.4, the available tree fuel was rapidly consumed by fire, followed by a quick flameout. The experimental study of Jervis and Rein (2016) on pine needles showed pHRRs of 252 kW/m² and 472 kW/m² for live and dead material, respectively. However, the flaming period lasted only 34 s for live and 18 s for dead material. Nevertheless, high HRR of plants, even with a short duration of flaming, can present a risk of fire propagation in the presence of combustible materials nearby.

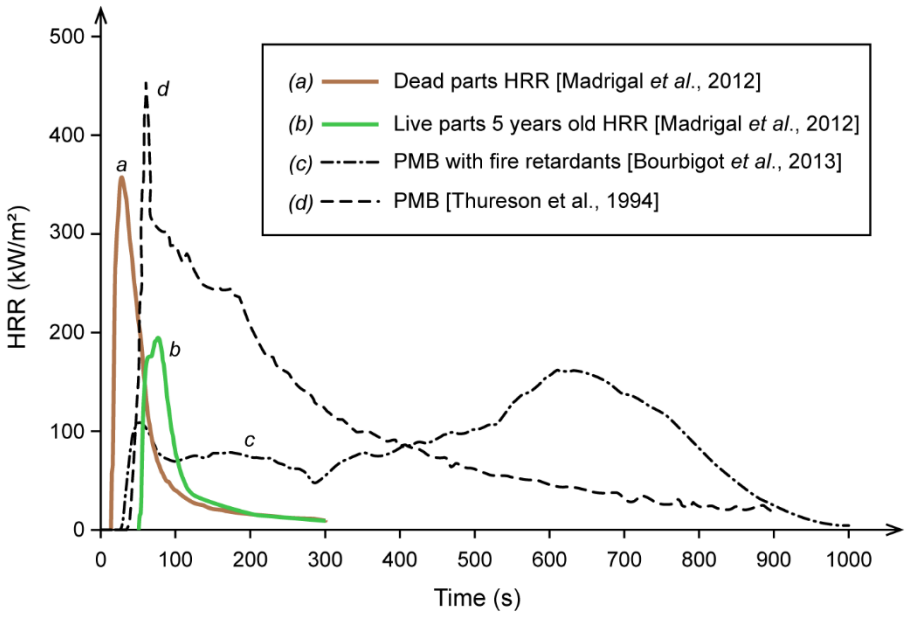

Figure 5.4. Comparison of HRR of vegetation parts of gorse shrub and typical roof coverings: (a) dead parts with dried leaves and twigs (redrawn from Madrigal *et al.* (2012)); (b) green leaves (redrawn from Madrigal *et al.* (2012)); (c) PMB membrane with fire retardants (redrawn from Bourbigot *et al.* (2013)); (d) PMB membrane without fire retardants (redrawn from Thureson and Nilsson (1994)).

It is difficult to match the vegetation components of green roofs against typical roof coverings because of the different spatial arrangement of these materials. However, they still allow us to partially understand the fire hazard that such roofs present on the building in case of fire. It is shown that neither growing media with high OM content nor plants present a higher risk than a roof membrane made of polymer-modified bitumen with or without fire retardants. This means that green roofs can be more advantageous in terms of fire safety in this case. However, compared to other more fire-resistant or non-combustible roof coverings, like PVC or ballasted roofs, such advantages would not be expected.

It has to be noted that vegetation performance in terms of heat release does not fully represent the potential fire hazard, because other characteristics like ignitability, rate of flame spread, sustainability and characteristics of flames produced are important to consider as well (White and Zipperer, 2010).

5.7 Conclusion

The present work characterized green roof flammability characteristics. From the conducted tests on growing media and the available literature data on vegetation and roof membranes, several conclusions can be made.

Green roofs do not add a substantial amount of fire load, even with intensive greening. It is estimated that such roofs present almost the same fuel load as roofs covered by a PMB membrane with no fire retardants, adding up to 95% of the available fuel. Extensive green roofs present a very small amount of fuel, which, in case of fire, will not contribute a lot.

In terms of fire performance, such roofs are comparable to conventional bitumen roofs. The results also show that dry substrates produce a smaller amount of heat during combustion than a bitumen membrane. Experiments on the growing media for intensive greening (15% OM) show a great influence of moisture content. In the dry state (most hazardous case), the growing media is much more ignitable than in the moist (natural) state. However, flames do not last more than 10 min. The limitation of the experimental study was the consideration of only one moisture condition. Testing substrates with a range of possible MC would help us to better assess the effect of moisture. The vegetation components of a green roof can produce

heat at a very high rate, but for a shorter period than bitumen membranes. The peak HRR of dead vegetation material greatly exceeds the value produced by a membrane with fire retardants and is comparable with the value of a standard bitumen membrane.

The fire risk of the vegetation on rooftops must be assessed, including different flammability parameters, which is a challenging task, due to the complexity of plants' structures and the dependence of their parameters on surrounding conditions. Future research on flammability properties and the fuel parameters of vegetation planted on green roofs can give a more realistic understanding of the fire risks of such roofs.

5.8. Acknowledgments

The authors also acknowledge the Green Roof Working Group of the Green Building Council of Canada, Quebec's section for technical data and mobility funding.

CHAPITRE 6 : Fire risk of green roofs to adjacent buildings

Soumis à Journal of Building Engineering

Nataliia Gerzhova [1], Christian Dagenais [1, 2], Sylvain Ménard [3], Pierre Blanchet [1], Jean Côté [4]

[1] NSERC Industrial Research Chair on Eco-responsible Wood Construction (CIRCERB), Department of Wood and Forest Sciences, Université Laval, Québec G1V 0A6, QC, Canada; Pierre.Blanchet@sbf.ulaval.ca

[2] FPInnovations, Québec G1V 4C7, QC, Canada; Christian.Dagenais@fpinnovations.ca

[3] Université du Québec à Chicoutimi (UCAQ), Chicoutimi G7H 2B1, QC, Canada; Sylvain_Menard@uqac.ca

[4] Department of Civil and Water Engineering, Université Laval, Québec G1V 0A6, QC, Canada; Jean.Cote@gci.ulaval.ca

6.1. Résumé

La susceptibilité des plantes à brûler soulève des préoccupations quant au risque d'incendie que les toits végétalisés peuvent poser aux bâtiments. En effet, lorsque les toits sont mal entretenus ou stressés par des conditions de sécheresse, cela conduit au dessèchement des plantes et à l'accumulation de matière organique, ce qui augmente considérablement la charge combustible. Les règles de sécurité incendie existantes visent à empêcher la propagation du feu à travers le couvert végétal. Cependant, la propagation du feu par rayonnement thermique n'est pas prise en compte. Dans cette étude, le risque d'exposition des bâtiments adjacents au flux de chaleur rayonnant produit par le feu sur les toits verts a été évalué. En se basant sur le flux de chaleur rayonnant maximal toléré généralement admis sur les façades exposées de 12.5 kW/m², les distances de séparation minimales ont été obtenues pour différentes conditions. Le modèle de comportement des feux de végétation a été utilisé pour déterminer la longueur des flammes, qui est le paramètre nécessaire pour le modèle de transfert thermique par rayonnement. Plusieurs types de végétation, scénarios de teneur en humidité et vitesses du vent ont été pris comme variables. Il a été constaté qu'en fournissant à la végétation une teneur en eau raisonnablement élevée, le risque d'incendie peut être considérablement réduit, en particulier pour les toits recouverts de plantes herbacées. Le vent a également un effet important sur la distance sécuritaire. Ainsi la prise en compte de l'exposition d'un toit végétalisé au vent peut permettre de mieux comprendre le risque d'incendie pour les bâtiments adjacents. En l'absence de vent et à une teneur en humidité

extrêmement faible, les distances de séparation sont aussi courtes que 3.1 m pour les arbustes denses et 2.4 m pour les graminées hautes et denses.

Mots-clés : Toiture végétalisée; le risqué d'incendie; transfert thermique par rayonnement; distance de séparation

6.2. Abstract

The susceptibility of plants to burn raises concerns about fire hazard that green roofs may pose to buildings. Main concerns relate to cases when such roofs are poorly maintained or stressed by drought conditions which leads to drying out of plants and the accumulation of dead organic material, that greatly increases the availability of fuel load. Existing standard safety measures aim to prevent the spread of fire through the vegetation cover. However, fire spread by thermal radiation is not considered. In this study, fire risk of exposure of adjacent buildings to radiant heat flux produced by fire on green roofs was assessed. Based on generally accepted maximum tolerable radiant heat flux to exposed facades of 12.5 kW/m², the minimum safe separation distances were obtained for different conditions. Wildland fire behavior model was used to determine flame lengths which is the necessary parameter for radiation model. Several vegetation types, moisture content scenarios and wind speeds were taken as variables. It was found that by providing the vegetation with reasonably high moisture content the fire risk can be greatly reduced, especially for grass-covered roofs. Since wind also has a strong effect on flame size, considering the exposure of a green roof to wind can bring better understanding of fire risk to adjacent buildings. At no-wind condition and at extremely low moisture content separation distances are as short as 3.1 m for dense shrubs and 2.4 m for tall dense grass.

Keywords: Green roof, fire risk, radiation heat transfer, separation distance

6.3. Introduction

Adding vegetated zones in building design, such as green roofs and living wall systems, becomes increasingly popular (Sutton, 2015). Together with bringing the aesthetic value these features serve multiple functions to improve urban ecology and social well-being

(Snodgrass and McIntyre, 2010). Numerous design projects showed the possibility to install a great variety of vegetation from simple grass to gardens with small trees and shrubs. Such zones, however, may be vulnerable parts of the building in terms of fire safety. Roofs usually are large open surfaces with no obstacles where a continuous vegetation cover presents a fuel load that can support fire. In case maintenance work on green roofs is neglected, such as removing of debris and dead plant parts, failure or absence of irrigation system where it is necessary, the formation of additional fuel load and reduced moisture make the roof a subject to fire risk. In the presence of wind and favorable moisture conditions the fire can spread and occupy a large area as well as spread to the building and adjacent structures. In the absence of previous researches and evidences of large fires on green roofs it is not clear whether such roofs present a real fire hazard to adjacent buildings.

Fire can spread horizontally by three modes, such as by 1) flying burning brands transported by wind from vegetation in fire, 2) direct contact with flames, and 3) thermal radiation (Carlsson, 1999). It is the radiation that is mostly responsible for fire spread between buildings, because in such mode heat can travel long distances not requiring any solid or liquid material between emitting and receiving surfaces (Buchanan and Abu, 2017). Flames produce a radiant heat flux that reaching an exposed object can cause its ignition. This heat flux received by the surface of the adjacent wall and the ability of a wall material to withstand a certain level of heat flux, critical value of exposure, determines the necessary separation distance between possible fire and the receiving surface.

Green roof design in most of the countries contains provisions to limit the spread of fire and to protect the adjacent walls from fire attack by burning brands and direct flame contact. Requirements of non-combustible wall material (RBQ, 2015), irrigation and regular maintenance, fire walls, fire breaks between large vegetated areas, separation zones around roof penetrations, equipment (RBQ, 2015; ANSI/SPRI VF-1, 2017; FM Global, 2011; FLL, 2008a) and adjoining walls (RBQ, 2015; FM Global, 2011) greatly reduce the fire risk. To some extent, this is confirmed by the fact that no spread of fire was observed where these rules are properly followed such as in the Province of Quebec, Canada. Protection of adjacent structures from radiant heat exposure is, however, not considered. Examining the risk of building damages from possible fire on adjacent green roofs can help to ensure the safety of such roofs.

The objective of this study is to assess fire risk of green roofs to adjacent structures by examining the fire attack by thermal radiation. Specifically, based on the critical incident heat flux to an exposed facade of adjacent building minimum separation distance from a green roof must be determined. Additionally, the effects of parameters, such as wind speed and moisture content, on the minimum separation distance will be explored. The diversity of vegetation will also be considered. For that, several scenarios varying environmental conditions and the vegetation types will be analyzed.

6.4. Methodology

6.4.1. Radiation model

Methods of assessment of horizontal external fire spread between buildings by radiation consider a fire originating inside the building, and heat is emitted by building facade through the openings (e.g. windows). Determination of safe separation distances is based on the knowledge of fire intensity, dimensions of emitting surface and critical radiation heat flux for a receiving surface of opposite building. Commonly accepted value of critical incident heat flux to building facades in Canada and some other countries (US, the UK, New Zealand) is 12.5 kW/m², which is the amount of heat needed for the piloted ignition of wooden materials with the presence of the ignition source, such as burning brands (McGuire, 1965). National Building Code of Canada contains tables on separation distances between buildings in relation to maximum allowed area of openings (NRCC, 2015). Tables were elaborated based on assumption on maximum expected intensity of fire of 180 kW/m² or 360 kW/m² for normal and hazardous cases respectively (Torvi *et al.*, 2005). Even though 12.5 kW/m² is conservative for the piloted ignition (Carlsson, 1999), for this study it was taken as a critical incident heat flux since it is a standard value. Based on the critical heat flux, minimum separation distances to the adjacent facade ($d_{12.5}$) were obtained.

Assessing the risk from fires that are located outdoors, and specifically on the rooftops, is not regulated. Fire sources, parameters and behavior can vary greatly depending on the type and characteristics of the fuel burning, as well as the environmental conditions. Therefore, the level of radiation emitted by such fires is difficult to generalize and must be determined considering a panoply of factors determining the fire intensity.

Generally, methods of determination of safe separation distance from flames include the following steps: characterization of fire, such as burning rate and flame dimensions, determination of thermal radiation from the emitting source, and calculation of the heat flux incident to the receiving surface (Beyler, 2016). Existing methods for determination of heat flux of flames from natural fires propose point source model in which the heat is assumed to be emitted by a single point located at half-height along the flames axis, where it is considered that radiation heat flux has a maximum value (Drysdale, 2011). This model, however, is considered to be very simplistic because it performs well where incident heat flux is below 5 kW/m², such as at large distances between fire and the receiving surface. In other cases, underprediction of the results can occur (Beyler, 2016).

Another more complex method is based on the concept of shape factor, such as solid flame model in which flames are represented as a cylindrical-shaped body that uniformly emits heat (Shokri and Beyler, 1989). The method was developed for pool fires, where the base of flame has rounded shape. Such geometry can be applicable for a spot fire, such as burning tree (Zárate *et al.*, 2008).

A more flexible approach is the rectangular planar (solid planar surface) model that is used for natural wildland fires (Fleury, 2010; Butler and Cohen, 1998; Sullivan *et al.*, 2003; Cohen and Butler, 1998), where flames are presented as a box-shaped body of given dimensions that is projected onto a rectangular vertical (radiant) panel, i.e. the emitting surface. Dimensions of this emitting surface and the distance to the receiving object determine the fraction of radiation that reaches the object, and is called shape factor, also known as configuration or view factor.

For all models incident radiant heat flux can be obtained from the following expression (Mudan, 1984):

$$\dot{q}''_{rad} = E_f \tau F \tag{6.1}$$

where radiant heat flux is in kW/m², E_f is the emissive power (W/m²), τ is the atmospheric transmissivity (unitless), F is the shape factor (unitless). Emissive power is the radiative heat flux produced by flames. It depends on the emissivity of the emitting body and flame temperature, and is expressed as:

$$E_f = \varepsilon \sigma T_f^4 \tag{6.2}$$

where ε is the emissivity (unitless), σ is the Stefan–Boltzmann constant equal to 5.67×10^{-8} W/(m²·K⁴), and T_f is the flame temperature (K). Fig. 6.1 shows a schematic representation of the radiation model, where W_f and H_f are the width and height of the radiant surface (m), d is the distance (m) to the receiving surface.

Emissivity (ε) of the flame can vary greatly and is difficult to calculate due to a complexity of fire process and multiple factors affecting it. Fuel type and moisture, environmental conditions and the type of combustion determine the emissivity and temperature of flames. Due to variations of these factors during burning fluctuations of flame parameters appear. Emissivity also depends on flame dimensions. It was experimentally found that it increases with increasing thickness, or diameter of flames (Pastor *et al.*, 2002; Sudheer and Prabhu, 2012; Àgueda *et al.*, 2010) and may approach to unity. Bushfire models assume that flames are uniform black body and have an emissivity of 1 (maximum value of this parameter), which is an assumption for large wildland fires, namely in condition where the flames are more than 3 m deep (thick) (Sullivan *et al.*, 2003).

Atmospheric transmissivity (τ) is a parameter that takes into account the effect of absorption of radiation by surrounding atmosphere (by water vapour and carbon dioxide) and scattering along the path (distance between fire and receiving surface) (Beyler, 2016). It is unitless and vary between 0 and 1.

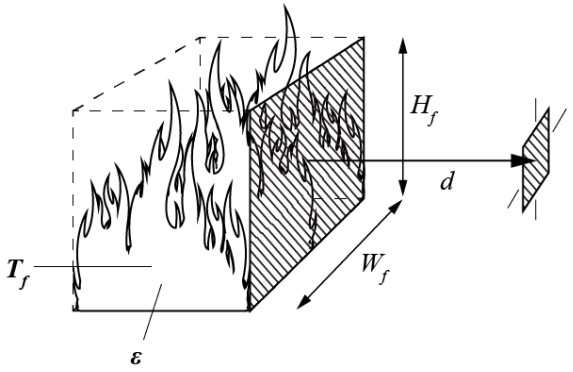

Figure 6.1. Schematic representation of the radiation model.

This parameter can be calculated considering the contribution of atmospheric humidity, the carbon dioxide content and particulate matter weight concentration (Andreucci and Arbolino, 1993). Assuming surrounding conditions are homogenous and constant Fuss and Hamins (2002) proposed an analytical expression, where transmissivity is obtained as a function of flame temperature, temperature of the atmosphere, relative humidity and path length. However, in modelling of heat flux from flames often transmissivity is neglected due to a small effect at small distances (Modak and Croce, 1977). For this study this parameter is taken as unity, which is a reasonable assumption.

Shape factor (*F*) for the solid planar surface model must be calculated for the geometry of the vertical surface, the target placed at half of the height of the radiant surface and the distance at which the target is located from the emitting surface (Fig. 6.1). Thus, from the critical incident heat flux of 12.5 kW/m² and the dimensions of the emitting surface, $d_{12.5}$ can be obtained. Flames are presented as a rectangular panel emitting heat, and a building facade as a receiving target. Therefore, the geometrical parameters of the flame, such as the flame length and width, are necessary for the determination of the incident heat flux. Unlike the flame width, that represents the width of burning area which can be assumed, the length of flame depends on many factors, such as fuel physical and chemical parameters and the environmental conditions. Considering that green roofs vegetation can vary greatly from simple grass cover to roof gardens, in case of fire the flames produced will also vary and will determine q''_{rad} to adjacent surfaces. For this reason, it is important to determine the flame lengths produced by different types of vegetation for the accurate calculation of q''_{rad}. The expression for calculating *F* is presented further.

Geometrical parameters of flames in wildfires can be found in previous experimental studies. Several field tests were conducted for different types of wildland in different climates, such as for grasslands in Australia and Brazil (Cheney *et al.*, 1993; Fidelis *et al.*, 2010), and shrublands in Europe (Silvani and Morandini, 2009; Santoni *et al.*, 2006; Morandini *et al.*, 2006) and Australia (Bradstock and Gill, 1993). Data from small-scale laboratory measurements is also available for litter fuel (Mutch, 1970; Simard *et al.*, 1989; Nelson Jr and Adkins, 1986). However, since fires were performed on natural landscapes, the results obtained in each study are for specific environmental conditions and fuel parameters.

6.4.2. Fire behavior models

It is also possible to obtain fire front parameters from mathematical fire behavior models, such as Catchpole *et al.* (1998) and Cruz *et al.* (2010) for shrublands in Australia, Noble *et al.* (1980) and Cheney *et al.* (1998) for grasslands, and the model of Rothermel (1972), developed generally for uniform wildlands. Based on theoretical predictions and on observation data such models were elaborated for prediction of fire spread during wildfires that allow to roughly estimate other flame characteristics. The rate of spread of fire (*RoS*) determines fire intensity (*I*) and the length of flame, L_f, which is the distance between the midpoint of the base of the flaming zone and the flame tip, which is equal to H_f for non-inclined flames on a flat surface. Models require different vegetation physical and chemical characteristics, and environmental conditions, such as wind speed and slope.

Australian standard AS3959 Method 2 (SAI Global, 2009) estimates the fire risk level for construction in bushfire-prone areas in Australia. In its Bushfire behavior model *RoS*, *I* and L_f can be calculated using existing formulas and coefficients. Required input parameters include fire danger index according to the region or wind speed; fuel characteristics (vegetation classification, fuel load and fuel height); measured parameters of the site (slope, distance to vegetation). The rate of spread is determined with the model of Catchpole *et al.* (1998) for shrublands (Eq. 6.3) and the model of Noble *et al.* (1980) for grasslands (Eq. 6.4).

$$RoS(shrub) = 0.023V^{1.21} \cdot VH^{0.54} \tag{6.3}$$

where *RoS* is the rate of spread (km/h), *V* is the wind speed (km/h), *VH* is the vegetation height (*m*) from the vegetation classification tables.

$$RoS(grass) = 0.13 \cdot GFDI \tag{6.4}$$

where *GFDI* is the Grass Fire Danger Index for grasslands taken from tables, according to environmental and fuel conditions in a specific Australian region.

Then the fireline intensity can be determined with Byram (1959b) equation (Eq. 6.5):

$$I = HW\frac{RoS}{36} \tag{6.5}$$

where I is the fireline intensity (kW/m), H is the heat of combustion assumed as 18600 kJ/kg, W is the overall fuel load (t/ha) from tables, RoS is the rate of spread (km/h).

The Lf (m) then can be determined using following expressions:

- Byram's equation for shrubland (Wilson, 1980):

$$L_{f\ (shrubs)} = 0.0775 \cdot I^{0.46} \tag{6.6}$$

- for grassland:

$$L_{f\ (grasses)} = 1.192 \left(\frac{I}{1000}\right)^{0.5} \tag{6.7}$$

This Australian standard was developed specifically for wildfires, assuming that the fire is developed, and its spread reached a quasi-steady-state condition. The vegetation cover is assumed continuous and homogenous. Wind speed is constant. Also, the assessment fire area is equal to 1 ha (100×100 m), which means that Wf is equal to 100 m. This is the main limitation for using this standard for fires that are smaller and not fully developed.

To analyze smaller fire areas Penney (2017) described a method that introduces the modifications to available fuel load and area. Thus, the geometry of the vegetation fuel bed prevents the fire attaining its maximum potential rate of spread. Reductions of fuel load density is made by multiplying by a vegetation factor (V_f), which is a ratio of fuel area (available for contribution to the fire spread and intensity) to the assessment area from the standard (1 ha, 100×100 m). Additionally, reductions of head fire width W_f can be used. This model, however, can underestimate fire parameters and the emitted heat flux. Proposed improvement by estimation of RoS as that of accelerating fire from a point source (McAlpine, 1988) rather than developed steady-state fire spread is not suitable for grasslands and shrublands. It is considered that the fire can reach steady state in a shorter period than in treed vegetation.

Another method to assess fire risk from vegetation covering small areas, where fire is not fully developed, is the Short fire run (SFR) model. This method follows the standard AS3959, introducing the determination of the W_f. Example of Delany *et al.* (2017) shows that due to a smaller W_f the resultant heat flux was 56% smaller than that obtained by the standard

method of AS3959. It is considered that the fire develops from a point forming elliptical shape of a fire zone, which is determined by a distance at which the fire propagates (*L*, fire run) and the wind speed. It is suggested to take the width of formed ellipse (*B*, breadth) for W_f. Thus, it can be obtained from the length-to breadth (*L*/*B*) ratio equation, relationship of the length to the maximum width of the fire (breath) (Eq. 6.8) (Alexander, 1985).

$$\frac{L}{B} = 1 + 0.0012 \cdot V^{2.154} \tag{6.8}$$

where *L* is length (m); *B* is breadth (m); *V* is the wind speed (km/h) that can be taken as 30 km/h as a default value or measured from the site at 10 m height above the ground. However, it is noted by Penney (2017) that the model's assumption that the *RoS* of fire is the same as that of a fully developed fire can lead to the overestimation of the emitted radiant heat flux.

Another mathematical surface fire behavior model was described by Rothermel (1972), which is used in National Fire Danger Rating System (NFDRS, USA). The advantage of this model is its applicability to various types of wildlands found in North America. Required inputs parameters include topography data (slope), environmental conditions (fuel moisture and wind speed) and a set of fuel characteristics. These are factors that have greatest impact on fire behavior and thus careful selection of these parameters is critical for the reliability of results. As with the Australian model, the limitation of this model is its applicability to steadily propagating fire in uniform homogenous fuelbeds and stable environment independent of time and space. Rate of spread can be determined with Eq. 6.9.

$$RoS = \frac{I_r \xi (1 + \phi_W + \phi_S)}{\rho_b \varepsilon Q_{ig}} \tag{6.9}$$

where *RoS* is the rate of spread (m/min), I_r is the reaction intensity (kJ/(min·m²)), ξ is the propagating flux ratio, ϕ_W is the wind coefficient, ϕ_S is the slope factor, ρ_b is the ovendry bulk density (kg/m³), ε is the effective heating number, Q_{ig} is the heat of pre-ignition (kJ/kg).

Rate of spread is then used to determine fire intensity using Byram's equation modified by Wilson (1980) for SI units:

$$I = \frac{1}{60} I_r RoS \left(\frac{12.6}{\sigma}\right) \quad (6.10)$$

where σ is surface area to volume ratio of the fuel bed (m^{-1}).

L_f can then be calculated using Byram's expression (Eq. 6.6). Application of this model is simplified by categorizing fuels into separate groups (fuel models) with a set of specific parameters as inputs that represent typical field conditions. Quick estimation of fire parameters according to Rothermel's model can be made numerically using modelling tools, such as BehavePlus Fire Modeling System (Andrews, 2014). It includes original 13 fuel models by Albini (1976), and 40 refined fuel models by Scott and Burgan (2005) that allow for more flexibility in characterizing the fuelbed and more precise predictions.

Possible fires on green roofs are expected to be less intense than wildfires due to smaller areas necessary to develop steady-state fire. However, due to the lack of information on fire behavior modelling specifically for urban environment and to a number of factors affecting small fires it is difficult to make exact predictions or rely on existing experimental data on combustion characteristics of several plants or vegetation. Thus, for this research the prediction of flame length was performed with the existing fire behavior model. Even though the results can be very conservative, it can help to analyze most hazardous situations. The surface fire spread model of Rothermel (1972) was chosen due to its applicability for all types of wildland and the possibility to choose more precisely the fuel type models that were developed for vegetation in North American climate. The determination of flame length was performed using BehavePlus 6.0.0 Beta 3 (USA, 2018). The parameters for modelling are described in the next section.

6.4.3. Parameters

Main parameters to set for fire behavior models for this study are fuel models, which is to associate green roof vegetation with certain types of wildlands, and weather conditions, such as fuel moisture content and wind speed. It is assumed that the surface is flat, thus for the topography parameter, the site slope θ is equal to 0.

6.4.3.1. Vegetation Types (Fuel Models)

It is possible to install a great variety of plants on roofs, from grasses to trees. However, it is generally considered that short vegetation of less than 10 cm, as well as maintained gardens and parklands do not present a fire risk due to insufficient fuel to support fire propagation (SAI Global, 2009). Therefore, in this study only 3 categories (types) of fuel models are taken for calculations: grasslands (GR), shrublands (SH) and grass-shrub mixed wildlands (GS). Three models in each category were chosen according to three main parameters, such as fuel load, vegetation height (fuelbed depth) and density of vegetation cover (by description). Other parameters, such as moisture of extinction, packing ratio and surface-area-to-volume ratio were not considered. However, these characteristics can affect the results. Table 6.1 lists fuel models chosen and their parameters. It must be noted that, typically, vegetation cover on green roofs does not present dense stands. Thus, GR-2, GS-1 and SH-2 are more representative for green roofs. Other models were taken to cover a greater variety of green roof vegetation.

Grasses are thin fuels that easily support fire spread at favorable moisture conditions, producing large flames, increasing in length with increasing fuel load and height.

Table 6.1. Fuel models.

Fuel model	Fine dead fuel load (kg/m^2)	Live herbaceous load (kg/m^2)	Live woody load (kg/m^2)	Mean Fuel height (m)
		Grass		
GR-2	0.02	0.25	-	0.3
GR-3	0.02	0.37	-	0.6
GR-4	0.06	0.47	-	0.6
		Grass-Shrub		
GS-1	0.05	0.12	0.16	0.3
GS-2	0.12	0.15	0.25	0.5
GS-3	0.07	0.36	0.31	< 0.6
		Shrub		
SH-2	0.33	-	0.95	0.3
SH-4	0.21	-	0.63	0.9
SH-8	0.51	-	1.07	0.9

GR-2 is a low grass with a small fuel load. Other two grass models are twice as high and with larger fuel loads. GR-2 and GR-4 models are dry climate grasses, while GR-3 is from a humid climate. This determines the moisture of extinction percentage, being 15% and 30-40% for given dry climate and humid climate fuel models respectively (Scott and Burgan, 2005). This parameter shows a state at which fire does not spread. GS models present a wildland where both grasses and small shrubs can be found. GS-1 contains very low shrubs and small grass fuel load, while GS-2 and GS-3 contain twice higher shrubs and moderate grass loads. GS-1 and GS-2 are dry climate models and GS-3 is a humid climate model. Finally, shrubs are models with no or very small grass load and shrubs occupy at least 50% of area. SH-2 is a dry-climate vegetation with very low shrubs, while other shrubs models vegetation height is 3 times greater. For Grass-shrub and Shrub types flame lengths are expected to be from low (GS-1, SH-2) to high (GS-4, SH-8) with increasing fuel load, vegetation height and density. It must be noted that GR live fuel is only herbaceous, SH live fuel is only woody, while GS is a mix of herbaceous and woody parts. The composition greatly determines the fire behavior, due to different moisture content of each part, which is explained in the next section.

6.4.3.2. Moisture Content (MC)

Green roofs with intensive greening must be provided with sufficient irrigation to support plant life and are not supposed to dry out. It is expected that MC of vegetation will not drop to the lowest point. However, considering seasonal changes in weather and related naturally occurring drying process, which takes place in the end of summer and in autumn (Pyne, 1984), it would be necessary to investigate the fire risk during this most fire hazardous period.

Fuel moisture content is an important parameter that greatly affects the availability of fuel in fire and determines the possibility and the rate of fire spread. For Rothermel (1972) fire behavior model the fuel load is presented as a sum of separate fuel loads, such as dead and live, due to different moisture uptake and fluctuation processes for each of the group. Dead plant material MC is regulated mostly by the environment, while for the live part it changes with the season. Both fuels consist of categories according to plant material and size. Dead fuel consists of categories according to size of the particles: 1-, 10-, 100- and 1000-hour time lag, which means the amount of time needed for a particle to reach equilibrium MC. Live

fuel consists of herbaceous (foliage, grass) and woody part (brush).Thus, for all categories MC is specified separately.

When MC of herbaceous part decreases from 120 to 30%, the transition from live to dead material occurs. Once it drops to 30% the fuel is considered cured, or dead, which occurs in the end of summer, from the end of July (Burgan, 1979). In late spring and early summer plants produce new herbaceous material that contains more than 120% of MC and is considered green (Pyne, 1984). Such material acts as a heat sink, where spread of flame does not occur. Live woody material similarly undergoes seasonal changes in MC, however, with different percentages. Live woody fuel becomes dormant, or dead, when MC drops to 50% (Burgan, 1979), and is considered fully green at 150% (Scott and Burgan, 2005).

For grasses, that mostly consist of herbaceous fuel, moisture condition is usually characterized by a degree of curing, converted MC of live herbaceous into two parts, green fuel and dead (live fuel that became dead). Fig. 6.2 shows the level of curing according to herbaceous MC.

In BehavePlus, models that contain herbaceous fuel are considered dynamic. This means that according to MC of herbaceous fuel one part is transferred to a dead load and its moisture is set equal to a specified 1-h dead fuel load (Fig. 6.2). Scott and Burgan (2005) suggest standard MC of fuels in 16 combinations of moisture scenarios: very low (D1, L1), low (D2, L2), moderate (D3, L3) and high (D4, L4) for dead and live parts. In BehavePlus, these combinations are presented as default input options. For live woody fuels the values are of 60% (two thirds are cured), 90% (one third is cured), 120% (green) and 150% (green) MC respectively. MCs of herbaceous fuel are 30, 60, 90 and 120% for each of the scenarios respectively. Fuel MC scenarios are shown in Table 6.2.

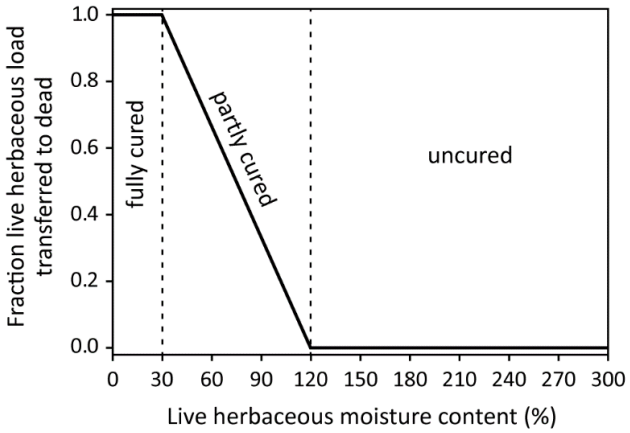

Figure 6.2. Dynamic fuel model process from Scott and Burgan (2005).

Table 6.2. Moisture scenarios according to Scott and Burgan (2005).

Fuel	MC, %			
	Very low	Low	Moderate	High
Dead	*D1*	*D2*	*D3*	*D4*
1-h	3	6	9	12
10-h	4	7	10	13
100-h	5	8	11	14
Live	*L1*	*L2*	*L3*	*L4*
Herbaceous	30	60	90	120
Woody	60	90	120	150

In the present work only default combinations of dead and live fuels were used for each type of vegetation in order to compare the most and least hazardous cases. Moisture scenarios used in this study are given in Table 6.3.

Table 6.3. Moisture scenarios used.

		Dead fuel moisture			
		D1	*D2*	*D3*	*D4*
Live fuel moisture	*L1*	GR, GS, SH			
	L2		GR, GS, SH	GR, GS, SH	GR, GS, SH
	L3		GR, GS, SH	GR, GS, SH	GR, GS, SH
	L4		SH	SH	SH

6.4.3.3. Wind Speed

Wind greatly affects fire behavior and is an important component in fire spread models. It is known that windy conditions lead to increase in forward rate of spread and therefore to greater fire intensity and larger flames (Pyne, 1984). For this study mean daily values of wind speed in the city of Montreal (Canada) are taken for the period of May-October 2019 (Environment Canada, 2019). Fig. 6.3 shows daily average values for the whole period with a mean value of 14.5 km/h and mean 25^{th} and 75^{th} percentiles of 9.7 and 18.1 km/h. Weekly average wind speed is shown as well. For this study, wind speed is considered constant in time. Wind speeds of 0, 5, 10, 20 km/h and the mean value of 15 km/h were taken for the analysis.

At Beaufort Wind Force Scale the wind of up to 5 km/h is characterized as light air, 10 km/h is considered a light breeze, causing leaves rustling, 12-19 km/h is a gentle breeze, at which leaves and twigs are constantly moving, and 20 km/h is a moderate breeze, at which movement of small branches is observed (Environment and natural resources, 2017).

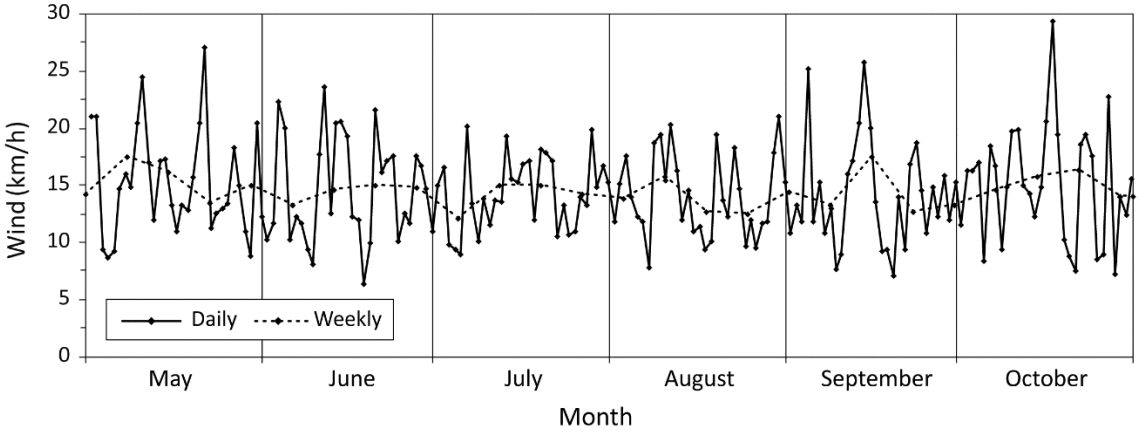

Figure 6.3. Daily and weekly average wind speed in Montreal 2019.

6.4.3.4. Radiation Model Parameters

Eq. 6.1 and 6.2 are used following several assumptions from the AS3959 standard. The emissivity (ε) is taken equal to 0.95 and the flame temperature is equal to 1090 K. Flame width (W_f) is set to 10 m assuming a medium-sized roof area covered by vegetation. The shape factor is obtained with the following equations from AS3959 (SAI Global, 2009):

$$F = \frac{1}{\pi}\left[\frac{X_1}{\sqrt{1+X_1^2}}tan^{-1}\left(\frac{Y_1}{\sqrt{1+X_1^2}}\right) + \frac{Y_1}{\sqrt{1+Y_1^2}}tan^{-1}\left(\frac{X_1}{\sqrt{1+Y_1^2}}\right) + \frac{X_2}{\sqrt{1+X_2^2}}tan^{-1}\left(\frac{Y_2}{\sqrt{1+X_2^2}}\right) + \frac{Y_2}{\sqrt{1+Y_2^2}}tan^{-1}\left(\frac{X_2}{\sqrt{1+Y_2^2}}\right)\right] \quad (6.11)$$

where

$$X_1 = \frac{L_f \sin(\alpha) - 0.5L_f \cos(\alpha)\tan(\theta) - d\tan(\theta) - h}{d - 0.5L_f cos\alpha} \quad (6.12)$$

$$X_2 = \frac{h + (d - 0.5L_f \cos(\alpha))\tan(\theta)}{d - 0.5L_f cos\alpha} \quad (6.13)$$

$$Y_1 = Y_2 = \frac{0.5W_f}{d - 0.5L_f \cos(\alpha)} \quad (6.14)$$

where L_f is the flame length (m); h is the elevation of the target (m) (equal to $L_f/2$); d is the distance to the target (m); W_f is the fire front width (m); α (°) is the flame inclination (flame angle or tilt); θ is the site slope (°). The geometrical representation is shown in Fig. 6.4. The flame angle α is equal to 90° and H_f is equal to L_f in no wind condition, where vertical flames are produced. In windy condition flames incline. The determination of the angle as a function of wind speed is very complex and produces great uncertainty in the results. Thus, α is determined with the algorithm proposed in the standard AS3959 according to the worst case scenario to obtain maximum view factor. In other words, the goal is to obtain the maximum value of $\ddot{q}_{rad}$, particularly, the greatest distance d at which 12.5 kW/m² is reached ($d_{12.5}$).

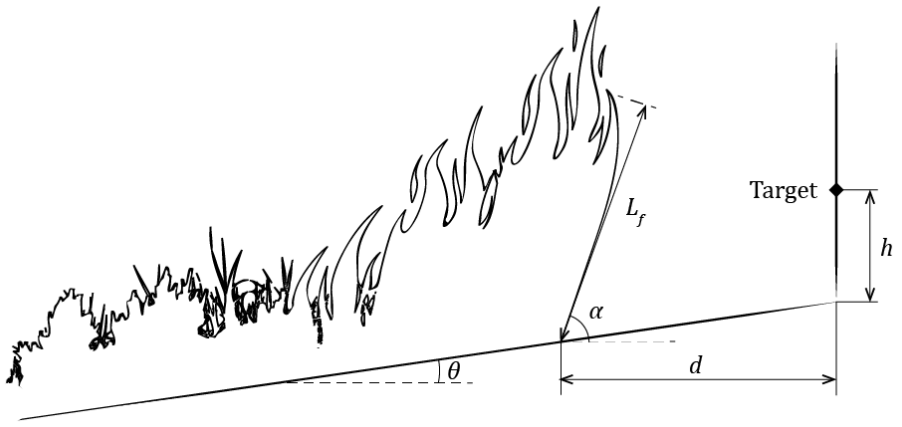

Figure 6.4. Configuration of fire front and the target, as presented in AS3959 (SAI Global, 2009).

According to AS3959, the flame angle algorithm consists of the following steps:

1.) Setting the initial value for the angle (α_0) and determination of the view factor (F_0) with the Equations 6.11-14. The target height h is taken in the middle of L_f.
2.) Setting the increment for the angle ($\Delta\alpha$) and maximum error allowed (°).
3.) Calculate view factor (F_1) for α_1 which is equal to $\alpha_0 + \Delta\alpha$
4.) Calculate view factor (F_2) for α_2 which is equal to $\alpha_1 + \Delta\alpha$
5.) Comparison of obtained view factors. In case F_1 is greater than F_0 and F_2, then checking the error. If it is greater than the set value, then decreasing $\Delta\alpha$ and repetition of the steps 3 and 4. In case F_2 is greater than F_0 and F_1 then setting new values: α_0 is equal to α_1, α_1 is equal to α_2 , thus F_0 becomes equal to F_1, and F_1 equal to F_2. Then repetition of steps 4 and 5.

6.5. Results

The heat flux emitted by burning vegetation was 75 kW/m² based on the assumed parameters. From the results of flame lengths determined with BehavePlus (Table 6.4, Annexe A) for different fuel models and specified wind and moisture conditions the q''_{rad} were calculated. Cases where the flame lengths were less than 0.5 m were not considered. The results of q''_{rad} as a function of separation distance are presented for the average wind speed. The results of

the analysis of the effect of wind speed and MC on $d_{12.5}$ are presented for each moisture scenario and are grouped by the fuel type.

6.5.1. Radiative Heat Flux

The q''_{rad} for daily average wind condition of 15 km/h is presented in Fig. 6.5 for each fuel category at most hazardous moisture condition (D1L1). Results at moisture scenarios at which flames of the smallest length are produced (but not less than 0.5 m) are presented as well for the comparison of the most and the least hazardous cases.

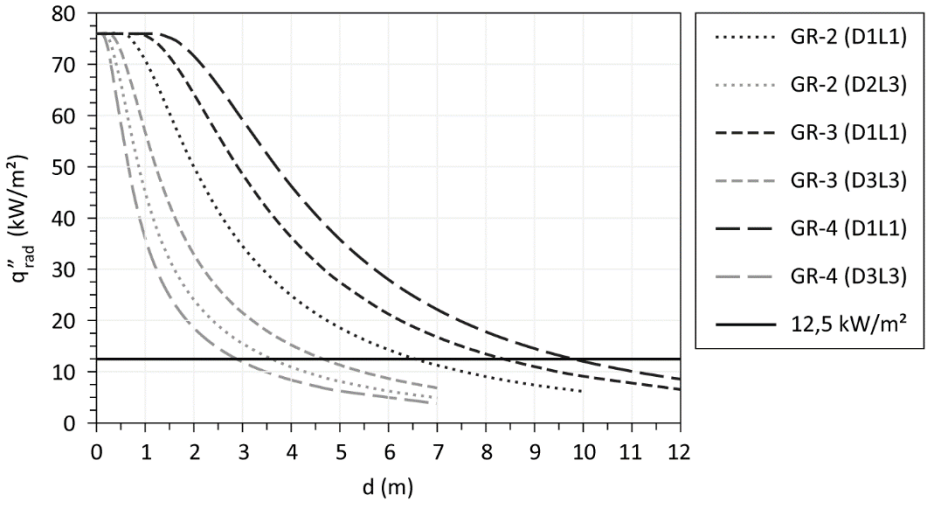

a

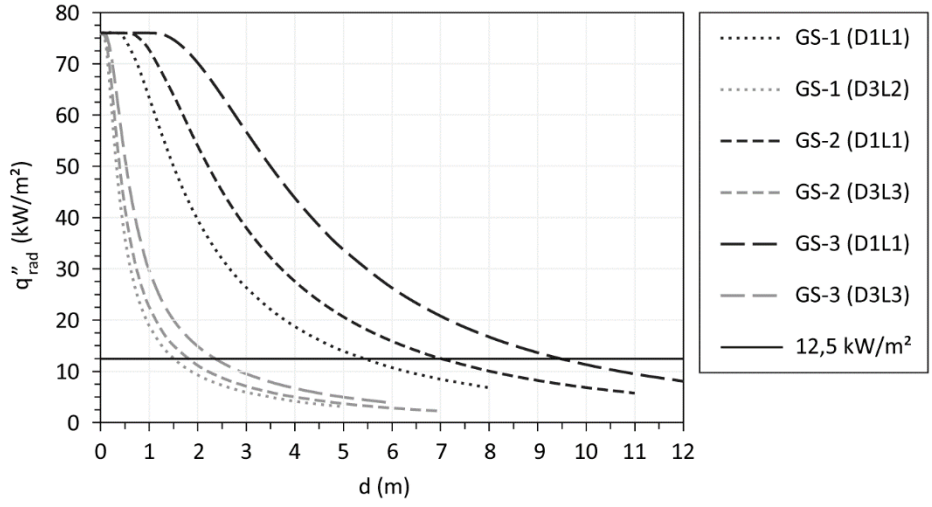

b

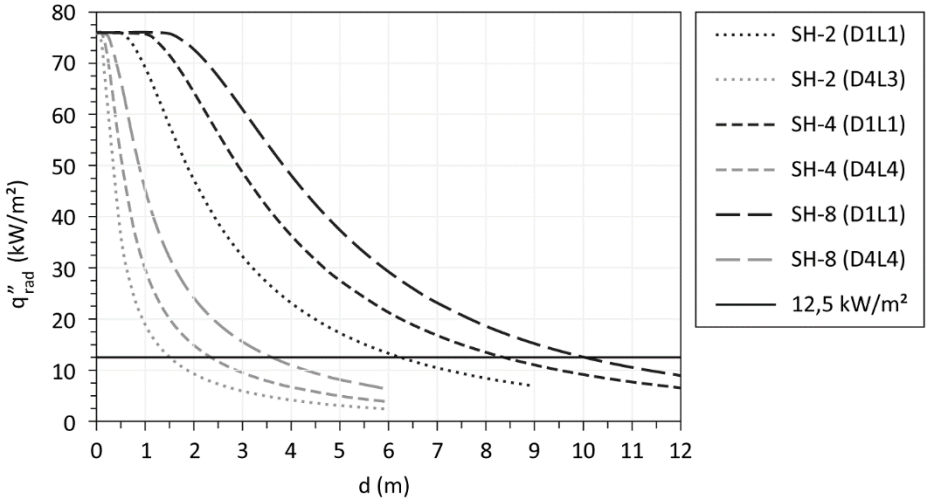

c

Figure 6.5. Radiation heat flux as a function of distance to the façade (d) for different fuel categories: (a) for Grasses; (b) for Grass-Shrubs; (c) for Shrubs.

Considering that a critical level of heat flux is equal to 12.5 kW/m² (horizontal line on the graph), the graph presents the separation distance ranges for each fuel model. For GR category models GR-3 and GR-4 smallest flames were produced at moderate moisture condition for dead and live loads, while for GR-2 flames were not presented at this moisture scenario due to a small load and height of the vegetation. Smallest flames of 1.3 m were obtained where dead load was at low MC and live load at moderate MC (D2L3). $d_{12.5}$ at most hazardous condition was 6.6 m for GR-2, 8.4 m for GR-3 and 9.8 m for GR-4. At moderate moisture contents $d_{12.5}$ is reduced to more than three times for GR-4 (2.9 m) and almost twice for GR-2 and GR-3 (3.6 and 4.7 m).

Grass-Shrub models show almost the same results for $d_{12.5}$ at very low MC, which are 6.5, 7.0 and 9.5 m for GS-1, GS-2 and GS-3 models. At moderate moisture conditions, a 2.4 m separation zone is sufficient for all fuel models.

Results of $d_{12.5}$ for the SH models are the same as for the GR models at very low MC, which are 6.3, 8.4 and 10 m for SH-2, SH-4 and SH-8 respectively. However, smallest flame lengths were obtained when both dead and live loads were at high MC for SH-4 and SH-8. For SH-2 flame length of 0.5 m were obtained at dead load at high MC and live load at moderate MC (D4L3). Smallest $d_{12.5}$ are thus between 1.8 and 3.6 m.

6.5.2. Wind and Moisture Effect

Wind has a strong effect on the flame spread since it provides greater oxygen supply to a burning fuel which increases burning rate. It also causes flames to incline to the unburned vegetation–which thus becomes exposed to greater radiation and convection heat fluxes (Byram, 1959a). Consequently, fire intensity and flame length increase. Fig. 6.6a,b,c presents the effect of wind speed on $d_{12.5}$ for D1L1 scenario.

This scenario represents very dry atmospheric conditions, when lack of precipitations for a long period and/or increased solar radiation leads to reduced MC of dead fuel. The live fuel in its turn becomes dead or entering dormancy, which usually happens during drought or late-summer-early-autumn period. In Fig. 6.6 the curves present condition at which the q''_{rad} is 12.5 kW/m². In the absence of wind $d_{12.5}$ for all vegetation categories does not exceed 3 m, particularly 2 m for grasses, 2.5 m for grass-shrub vegetation and 3 m for shrubs. At windy condition flame lengths substantially increase even at low winds, that requires much greater separation zones from the vegetation. For example, at only 5 km/h flames of GR fuel models become longer more than 3 times, from 0.4 to 1.4 m for GR-2, from 0.6 to 2.3 m for GR-3 and from 0.8 to 2.7 m for GR-4. This leads to an increase of $d_{12.5}$ to more than 2.5 times, from 1.5 to 3.8 m for GR-2, from 1.8 to 5.6 for GR-3 and from 2.3 to 6.2 m for GR-4.

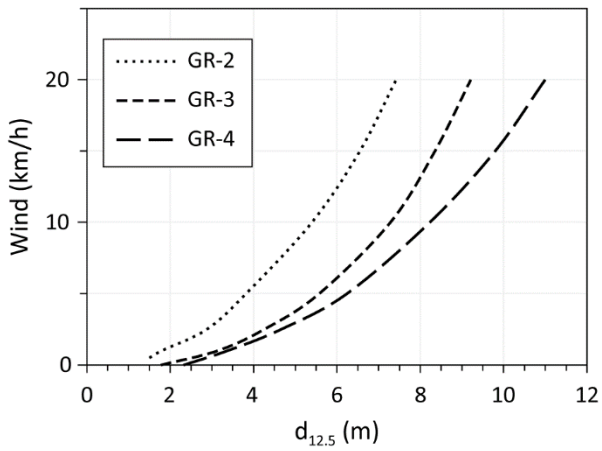

a

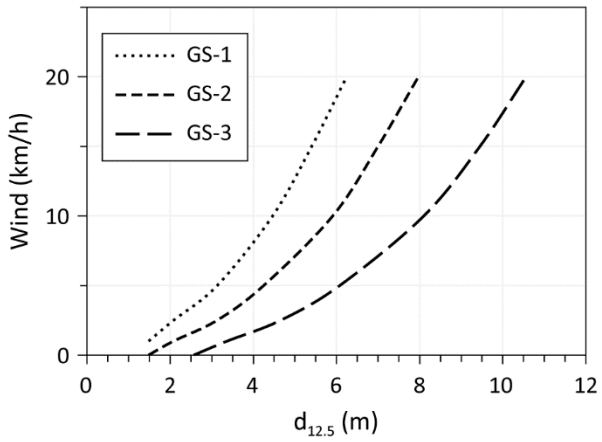

b

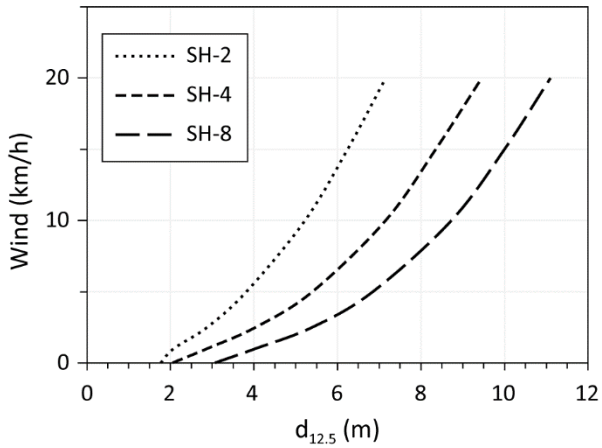

c

Figure 6.6. Safe separation distances as a function of wind speed at Very low MC (D1L1) for each fuel model: (a) Grasses; (b) Grass-Shrubs; (c) Shrubs.

At strong winds larger flames are produced. Winds speed of 20 km/h results in flames of 3.5, 4.9 and 6.5 m for GR-2, GR-3 and GR-4 models respectively, and therefore $d_{12.5}$ increase to 7.4, 9.2 and 11 m for the same fuel models. With increasing wind speed, however, its effect is slightly reduced, while the effect of fuel load and height becomes much more pronounced compared to no-wind condition. For GS and SH categories the same behavior is observed, with smaller results for GS-1 compared to other low-load fuel models, which is explained by the difference in proportions of dead and live fuel loads as well as the presence of both herbaceous and woody parts in live fuel. GS-1 is composed of small amount of dead fuel compared to SH-2, and smaller amount of herbaceous fuel compared to GR-2 which are the

main contributors to fire for these models (Table 6.1). Also, GR curves are slightly more inclined. Increased wind effect is explained by the structure of the fuel. Grass particles are of small diameters, have high surface area-to-volume ratio and low bulk density of the fuel bed, which allows it to burn at high rates and which is more noticeable at high winds.

Less fire hazardous conditions when plants have higher MC were analyzed and presented in Fig. 6.7-16 for each moisture scenario. The effect of environmental condition, expressed through the variation of MC of dead fuel, is presented as well.

Fig. 6.7-12 present $d_{12.5}$ as functions of wind speed for D2L2 scenario. Such condition can be expected in the middle or end of summer season. Two times higher MC of herbaceous and fine dead fuels (Table 6.2) leads to smaller flame lengths, being about two thirds the size of flames for D1L1 condition, at all wind speeds. The exception is for the SH-2 model, for which flame lengths are almost one third of the size of flames at extremely dry condition. This is because SH-2 represents low-growing shrubs with average fuel bed depth of only 0.3 m, and thus plant height does not contribute to the development of flame size. The size of separation zones for all models are smaller accordingly to the flame lengths.

For GR category flame lengths vary between 0 and 2.4 for low grasses (GR-2) and between 0.6 and 4.8 m for taller grass cover with greater fuel load (GR-4) for a taken range of wind speeds. Calculated $d_{12.5}$ for this fuel category is shown in Fig. 6.7. The curves presenting results for each model are less steep compared to those obtained for extremely dry state (Fig. 6.6a). $d_{12.5}$ for all models decreased by at least 1 m in the presence of wind. For example, low grasses will require a separation zone of 2.9 m, while at very low MC it must be 3.8 m at a wind speed of 5 km/h, and 5.8 m compared to 7.4 m at a wind speed of 20 km/h.

To assess the effect of weather conditions, which is reflected in changes of MC of fine dead fuel, the results of D2L2 scenario were compared to results obtained for conditions with more elevated humidity of dead part. Since primary contributor to fire for grasses is live herbaceous fuel and the dead fuel load is very low, variable MC of dead fuel does not remarkably affect the results of fire behavior and radiation models. This can be observed in Fig. 6.8a,b,c

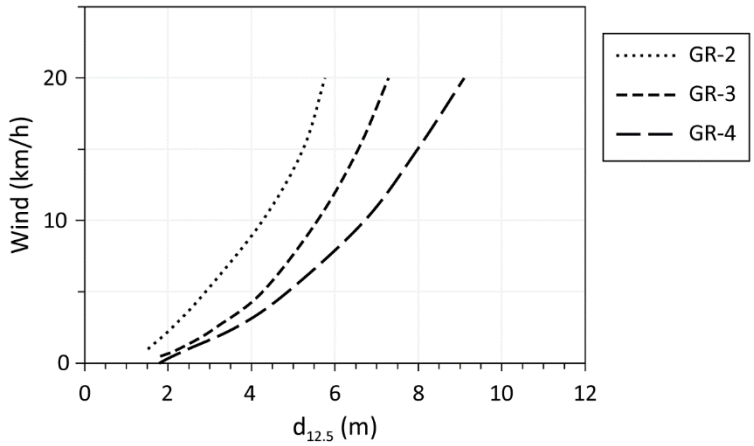

Figure 6.7. Safe separation distances as a function of wind speed at Low MC (D2L2) for GR fuel models.

showing $d_{12.5}$ as functions of the wind speed for each of GR model at three moisture scenarios (D2L2, D3L2, D4L2). Results of models with dead fuel moisture at low (D2) and moderate (D3) states are nearly similar at wind speeds of up to 15 km/h. Higher MC (D4) allows to reduce separation zone for about 1 m at a wind speed of 10 km/h and 2 m at 20 km/h.

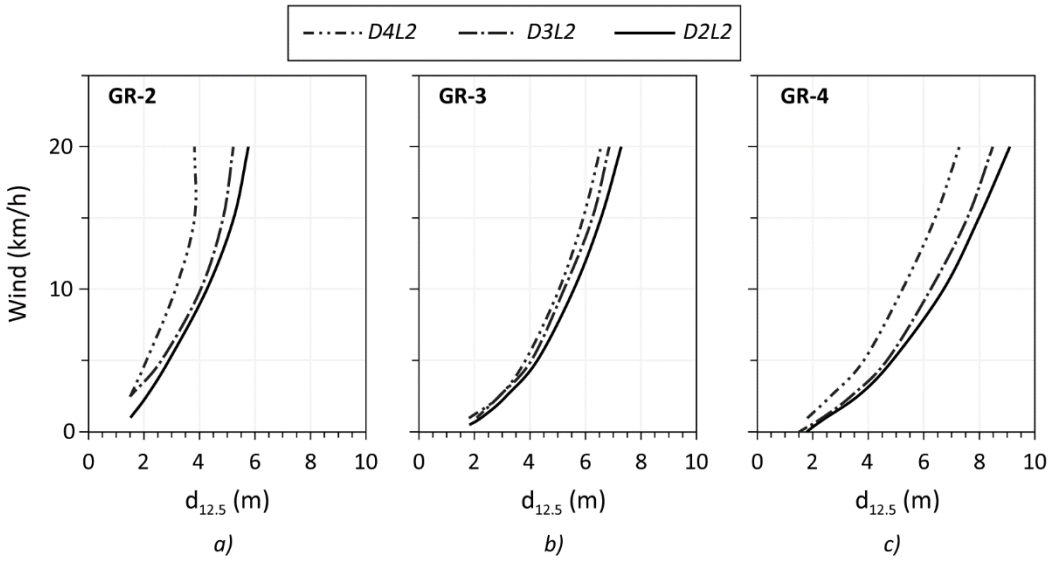

Figure 6.8. Safe separation distances as a function of wind speed at Low MC of live fuel (L2) and variable MC of dead fuel (D2, D3, D4) for each fuel model of GR category: (a) GR-2; (b) GR-3; (c) GR-4.

For GS and SH categories same analyzes were performed. Fig. 6.9 shows the dependence of the $d_{12.5}$ on the wind speed for GS models for D2L2 scenario. Flames reached 1.8 m for low

fuel load model GS-1, and 4.1 m for GS-3. Compared to the results of D1L1 scenario, the possible reduction of separation zones was by 1.3 m at 10 km/h and by 1.6 at 20 km/h for GS-1 and GS-2 models. For GS-4 model the separation zone was at least 2 m smaller at 10 km/h, and 2.3 m smaller at 20 km/h.

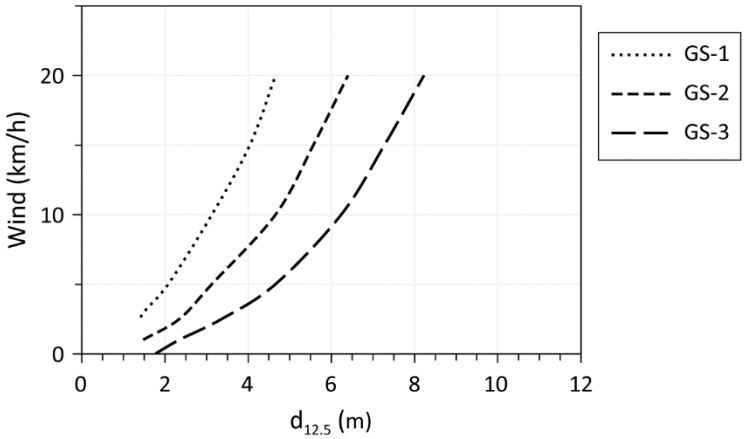

Figure 6.9. Safe separation distances as a function of wind speed at Low MC (D2L2) for GS fuel models.

The weather effect for GS category is presented in Fig. 6.10. GS models have different proportions of dead, live herbaceous and live woody fuel, and therefore, the variation of dead fuel MC had a different effect on the results. For GS-1 at D4L2 flames were not observed. It can be explained by its fuel proportions, and the modelling method. Both herbaceous and dead fuel loads are very low, and because this is a dynamic fuel model, a big portion of herbaceous fuel is transferred to dead and its MC is set to 12%, the same as for 1-h dead fuel. This MC is close to the moisture of extinction presumed in this model. Therefore, such vegetation does not effectively support fire. On the contrary GS-3 model has a fuel bed twice as deep as GS-1, its herbaceous fuel load is 3 times greater and the dead fuel moisture of extinction is 40%. These parameters allow such vegetation to support fire independently of weather conditions at the given range of dead MC, provided that the live fuel is at 60% of moisture (Fig. 6.10c).

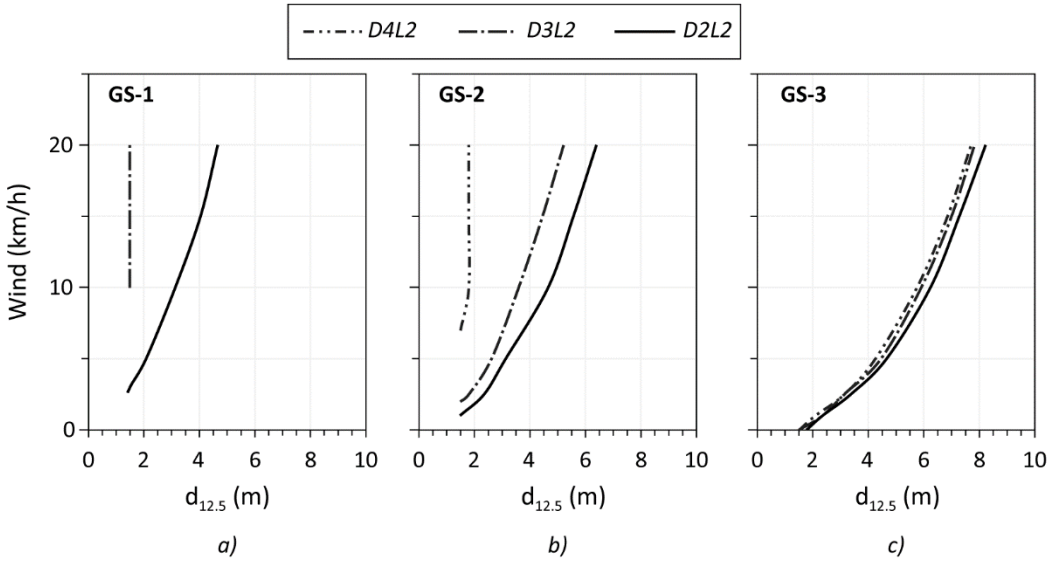

Figure 6.10. Safe separation distances as a function of wind speed at Low MC of live fuel (L2) and variable MC of dead fuel (D2, D3, D4) for each fuel model of GS category: (a) GS-1; (b) GS-2; (c) GS-3.

Results for $d_{12.5}$ for the SH category at D2L2 scenario are shown in Fig. 6.11. The SH-2 model, as mentioned above, consists of low-growing shrubs which make this model be quite sensitive to moisture changes. This is reflected in a relatively small $d_{12.5}$, which is 3.1 m at 20 km/h. For the other SH models, similarly to GR and GS categories required separation zones can be reduced by at least 1 m. Specifically, for SH-4 $d_{12.5}$ is 5.6 m at 10 km/h and 7.6 m at 20 km/h, and for SH-8 it is 7.6 and 9.6 for the same wind speeds respectively.

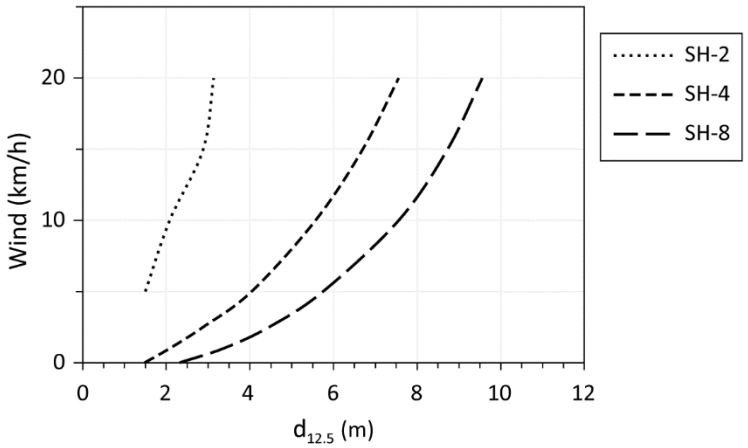

Figure 6.11. Safe separation distances as a function of wind speed at Low MC (D2L2) for SH fuel models.

All SH models are not dynamic, since no herbaceous fuel is present. Therefore, the atmospheric condition effect depends directly on the amount of dead fuel and fuel bed depth. However, not all models show such behavior (Fig. 6.12a,b,c). SH-8 model presents dense shrub cover with fuel bed depth similar to that of SH-4, but with higher fuel load. The graph shows very small effect of variation of dead MC on fire behavior and thus on $d_{12.5}$ at any wind speed. This can be explained by the difference in packing ratio of these fuels, 0.00227 for SH-4 and 0.00509 for SH-8 (Scott and Burgan, 2005). This parameter for SH-8 model is probably closer to its optimum value that allows the fire to propagate more effectively and being less dependent on MC. The SH-4 model is quite responsive to the variations of dead fuel moisture. Flames become greatly smaller with increasing dead moisture, which allows for shorter distance of separation zones. For D4L2 scenario $d_{12.5}$ can be reduced by 3.5 m at 10 km/h and by 5 m at 20 km/h compared to D2L2.

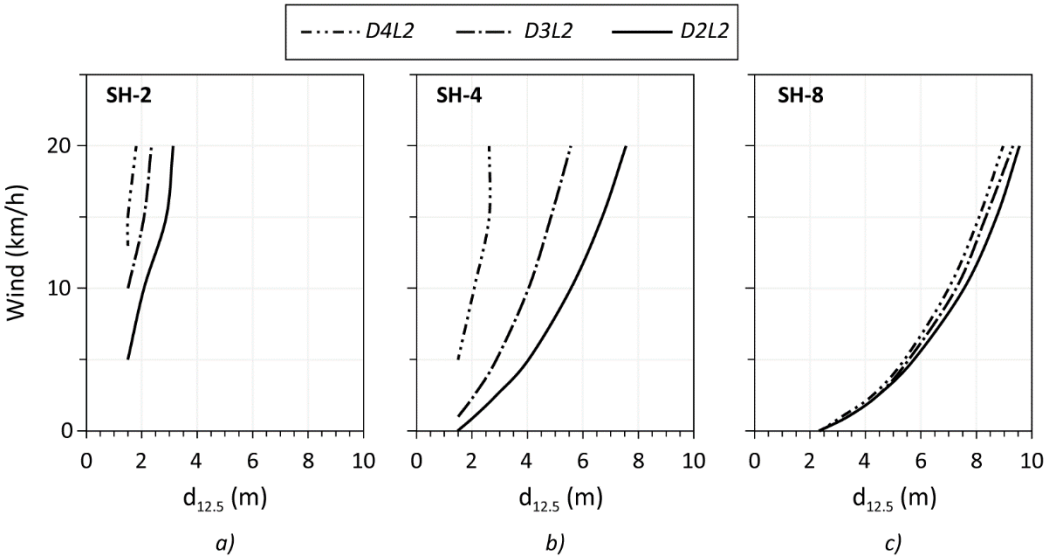

Figure 6.12. Safe separation distances as a function of wind speed at Low MC of live fuel (L2) and variable MC of dead fuel (D2, D3, D4) for each fuel model of SH category: (a) SH-2; (b) SH-4; (c) SH-8.

The results for higher moisture scenario (D3L3) are presented in Fig. 6.13-15. Moderate moisture condition is observed at maturity of live fuels. Grasses at this stage are 1/3 cured, have a green color with noticeable yellow inclusions, which is considered end of green phase. At this stage vegetation presents low fire hazard. Fig. 6.13 shows that GR-2 does not support fire, due to the low fuel load. In GR-3 and GR-4, taller and heavier grasses, some short flames

can be observed, of maximum 2 m for GR-3 and 1 m for GR-4. $d_{12.5}$ at highest winds for GR-3 is 5 m and for GR-4 is 2.9 m. Under calm conditions $d_{12.5}$ of 1.5 m is sufficient to prevent the fire attack by thermal radiation. Variations of MC of dead fuel show that GR-3 is not sensitive to such changes, while GR-4 on the contrary is sensitive, especially when MC is low. Greater quantity of dead fuel leads to increased $d_{12.5}$ in case when ambient conditions are dry leading to drying out of dead fuels.

Smaller amount of herbaceous fuel in GS category makes the vegetation less capable to support the fire at moderate moisture condition. Fig. 6.14 presents the results of $d_{12.5}$ for GS-2 and GS-3 categories only. Flame reached maximum of 0.8 m in the presence of wind. Therefore, separation zone of 2.4 m is enough to provide safety. In case dead fuel MC drops to low values, only small changes occur. Flames size increase to 1 m requiring $d_{12.5}$ to be increased to 2.9 m (results not shown).

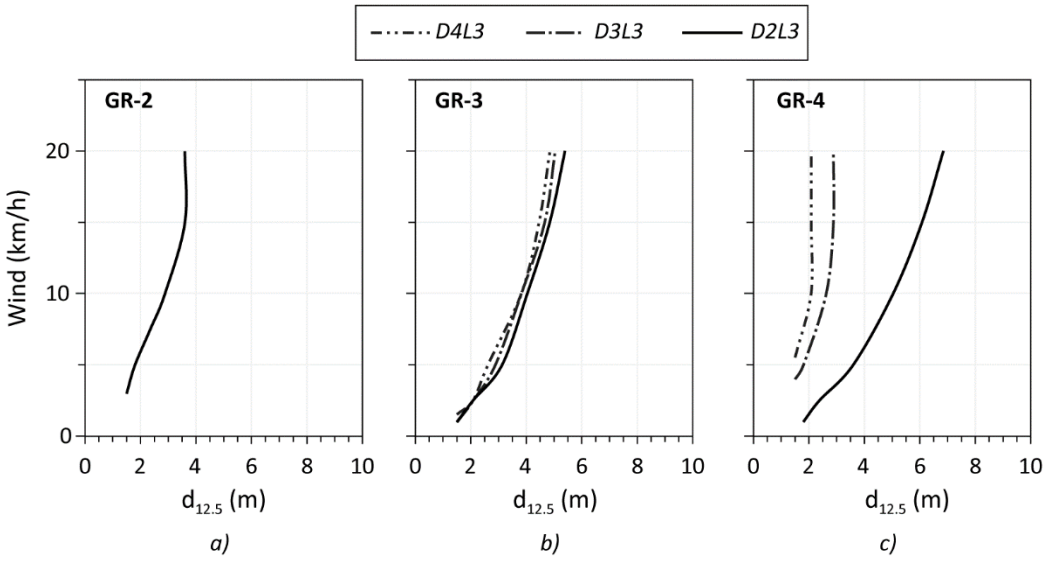

Figure 6.13. Safe separation distances as a function of wind speed at Moderate MC of live fuel (L3) and variable MC of dead fuel (D2, D3, D4) for each fuel model of GR category: (a) GR-2; (b) GR-3; (c) GR-4.

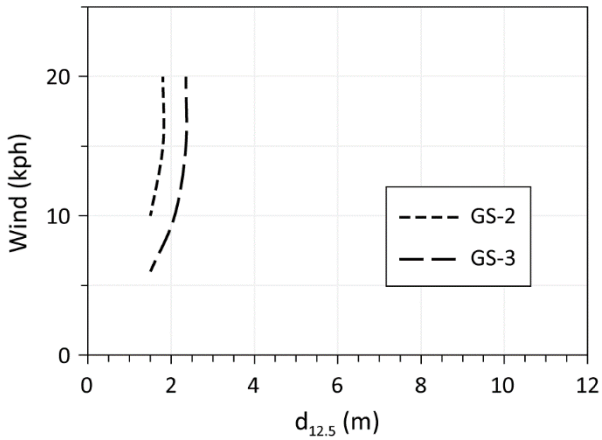

Figure 6.14. Safe separation distances as a function of wind speed at Moderate MC (D3L3) for GS fuel models.

Results on SH behavior are shown in Fig. 6.15 comparing three moisture scenarios with live fuel at moderate MC. Generally, this vegetation category produced flames of almost same size as other categories. Specifically, the lengths of flames were slightly smaller than those of GR and slightly larger than flames of GS. The exception is for the SH-8, which flames reached 4.1 m at 20 km/h. The variation of dead fuel MC has relatively small effect on fire behavior of all shrub models. SH-2 and SH-4 models present low fire risk at such moisture scenario, requiring $d_{12.5}$ of 3 m at high wind. The SH-8 model, however, presents higher fire risk, which is explained by its higher fuel load. $d_{12.5}$ is 8.7 m for D2L3 scenario and 7.4 for D4L3 at 20 km/h.

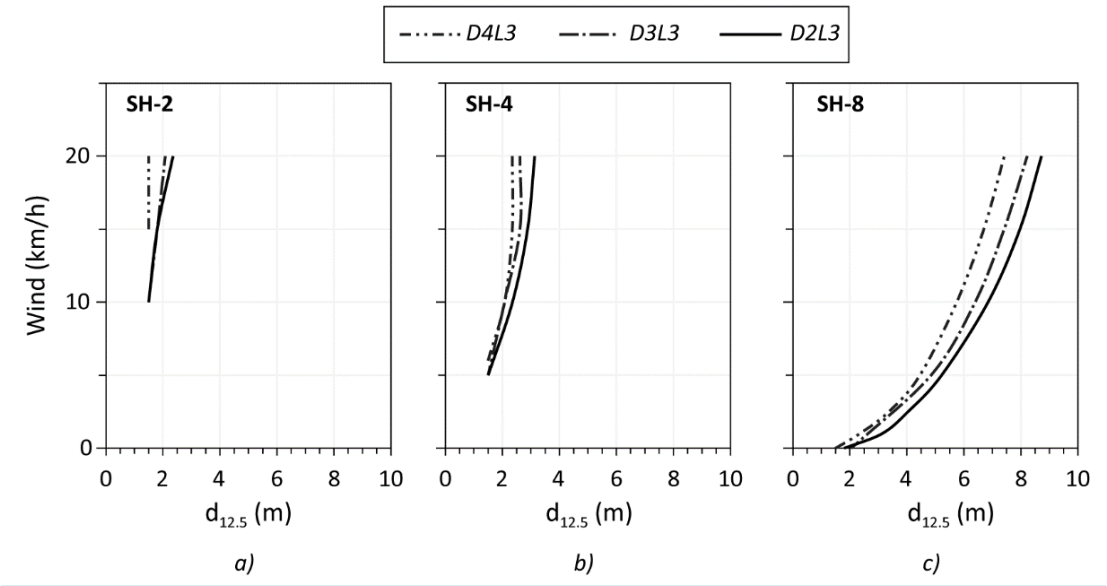

Figure 6.15. Safe separation distances as a function of wind speed at Moderate MC of live fuel (L3) and variable MC of dead fuel (D2, D3, D4) for each fuel model of SH category: (a) SH-2; (b) SH-4; (c) SH-8.

Finally, least hazardous scenario D4L4 was analyzed. This scenario occurs in spring-early-summer period with the apparition of new foliage and grass and the growth of new woody parts. Since in such conditions live fuel is considered green, the vegetation acts as a heat sink, and therefore no sustaining flaming can occur in models consisting mostly of herbaceous fuels, GR and GS. Fig. 6.16 shows results of $d_{12.5}$ for the SH category for D4L4 scenario, as well as D2L4 and D3L4 scenarios to assess the risk when dead fuel MC decreases.

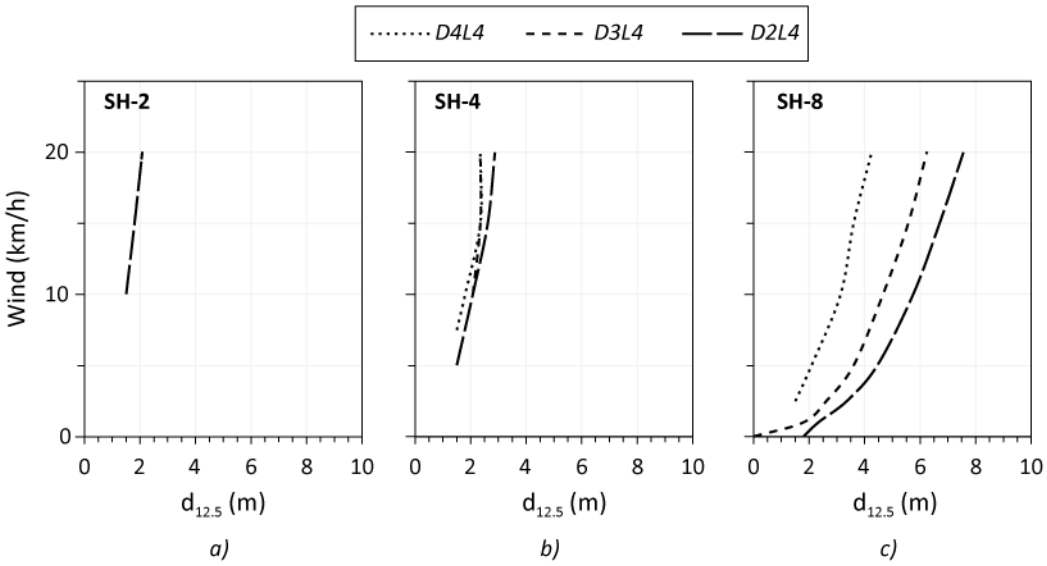

Figure 6.16. Safe separation distances as a function of wind speed at High MC (D4L4) for SH fuel models.

It is seen that at low winds up to 5 km/h no flames were supported at D4L4. For SH-2 small flames of 0.5 m appeared only at 20 km/h, and for SH-4 at about 10 km/h. Maximum flame height reached by this fuel category was 0.8 m by SH-4 and 1.6 m by SH-8, requiring $d_{12.5}$ of 2.4 m and 4 m respectively. In case dead fuel dries out, scenario D2L4, the effect is visible for SH-2 and SH-8 models. Low shrubs (SH-2) support small flames of up to 0.7 m length at high winds. For dense shrub cover (SH-8) fire intensity greatly increases leading to flames of up to 3.6 m at 20 km/h and $d_{12.5}$ of 7.6 m. Negligible effect is observed for SH-4 model.

6.6. Discussions

According to the results q''_{rad} rapidly decreases with the distance for all types of vegetation (grasses, shrubs), especially for low-growing plants with low fuel load even at very low level of moisture content. This shows that the separation zone can greatly reduce the fire risk to adjacent buildings with combustible facades and can be considered when planning a green roof. However, it is important to consider factors that determine the minimum separation distance to facades, such as the vegetation characteristics, moisture content and wind speed. The analysis of $d_{12.5}$ as a function of wind speed and moisture conditions for different vegetation types produced different results showing the importance of each of these parameters and their effect. Each of the fuel category and chosen fuel models (GR, GS, SH),

despite presenting a relatively narrow range of parameters of fuel load and fuelbed depth, with maximum values of 1.6 kg/m² and 0.9 m, have different capacities to support fire. Therefore, it is necessary to take into account the type of vegetation on the roof, due to a different fire risk it can present. Low grasses and shrubs, that typically can be found on green roofs, are not expected to support fire unless at low and very low moisture conditions and in the presence of wind. Considering that at least some moisture is usually present in vegetation, such as D2L2 scenario, $d_{12.5}$ for short grass (GR-2) is 5.2 m, 4.0 m for grass-shrub mix (GS-1) and 2.9 for low shrubs (SH-2) at average wind speed of 15 km/h. Dense tall grasses and dense and heavy shrubs can produce much higher flames that require greater separation zones. For the same conditions $d_{12.5}$ is 8.0 m for tall grasses (GR-4), 7.3 m for grass-shrub mix (GS-3) and 8.8 m for dense tall shrubs (SH-8).

Large vegetation for green roofs is usually provided with permanent irrigation systems, not allowing them to die. Therefore, D3L3 scenario, when live and dead fuels are at moderate MC, is more realistic. $d_{12.5}$ decrease to 2.9 m for tall grasses (GR-4), 2.4 m for grass-shrub mix (GS-3) and 7.4 m for dense shrubs (SH-8) at 15 km/h when compared to D2L2 moisture scenario. For all other fuel models with smaller fuel loads the effect is visible as well. These results show that the presence of moisture has a great effect on safety zones necessary to protect adjoining structures from exposure to thermal radiation produced by burning vegetation. Providing enough moisture level in plants can help to successfully control the fire hazard.

The presence of wind has a great influence on fire spread rate and size and therefore on $d_{12.5}$. Compared to 15 km/h and D2L2 scenario, at 5 km/h, flame length greatly decreases and leads to much smaller $d_{12.5}$ for all fuel models. For example, for tall and dense vegetation $d_{12.5}$ decreases from 8 to 4.9 m for GR-4, from 7.3 to 4.7 for GS-3 and from 8.8 to 5.8 m for SH-8. For short and low fuel load vegetation its effect is even greater. Comparing the same scenarios and wind speeds, $d_{12.5}$ decrease from 5.2 to 2.9 m for GR-2, from 4 to 2.1 m for GS-1 and from 2.9 to 1.5 m for SH-2. In the absence of wind, only small flames of 0.5-0.6 m with $d_{12.5}$ of less than 2 m are observed and only for fuel models with high fuel loads in each category, such as GR-4, GS-3, SH-4. For the SH-8 model a slightly greater $d_{12.5}$ of 2.4 m is required. The effect of wind is greatly reduced at high moisture content of the vegetation.

This analysis shows the importance of considering the wind speed that a roof is exposed to when assessing the fire risk and proposing safety measures.

It may seem that results in this study are quite severe. However, this is explained by the assumptions made. The values obtained are to be expected for steady-state fires. The limitations of roof area and time availability can prevent fire to reach fully developed state. It is also known that for fires with small combustion rates, such as at the developing stage, the wind effect is not proportional to its speed and can be much lower (Pyne, 1984). Therefore, results of the analysis in this study can serve as an example of extremely hazardous cases and a confirmation of the importance of the presence of moisture in green roofs especially with intensive greening for the reduction of fire risk for adjacent building.

6.7. Conclusion

This study assesses the risk of possible fire hazard from green roofs to adjoining structures when exposed to radiant heat. The separation distances to radiation heat exposure were obtained for different moisture and wind conditions and compared. A range of types of vegetation that can be found on green roofs was considered.

Low MC of dead load, that is present in moderate and high amount in shrubs, greatly increases fire risk. This can be regulated by creating more humid environment, by irrigation, and, if possible, less exposure to solar radiation by providing some shading, as well as less wind exposure. This is especially important for dry climates with low precipitations and drought periods. Irrigation also can retard the curing process, which is particularly important for grasses, that mostly consist of live fuel. Therefore, presence of moisture is a primary essential parameter in protection from fire spread and thus the risk of radiation attack of the adjoining structures. Providing irrigation system for tall plants and the vegetation presenting moderate or high fuel load is a simple solution.

Removal of dead plant material, when possible, also helps to reduce fire risk by reduction of fuel load. This is specifically important during most fire hazardous periods, like autumn, when live load becomes dead or plants become dormant.

Due to the method chosen, the results of the study are conservative and most likely overpredicted the calculated separation distances. However, they can be regarded as results

of extreme conditions and point out the parameters that are necessary to consider when planning and maintaining green roof, such as vegetation type and height, wind exposure and moisture conditions.

To investigate fire effect on adjacent buildings in less idealized conditions, fire behavior models for limited vegetation areas need to be developed. Series of large-scale test for different vegetation simulating roof conditions could confirm modeling effort.

6.8. Acknowledgments

The authors are grateful to Natural Sciences and Engineering Research Council of Canada for the financial support through its ICP and CRD programs (IRCPJ 461745-12 and RDCPJ 445200-12) as well as the industrial partners of the NSERC industrial chair on eco-responsible wood construction (CIRCERB). Authors also acknowledge the Green Roof Working Group of the Green Building Council of Canada, Quebec's section for technical data and mobility funding.

Conclusion générale

L’objectif général de ce projet de caractériser les problèmes de la sécurité incendie des TV a permis d’analyser les risques de différents côtés. La recherche a permis d’obtenir de nouvelles connaissances sur les risques incendie et sur les facteurs les plus importants affectant la gravité d’un feu.

Le premier objectif spécifique était de déterminer la conductivité thermique du substrat de croissance de TV à l’état sec en fonction de la température. Les propriétés à des températures allant jusqu’à 800 °C étaient requises pour les utiliser dans une modélisation de transfert thermique à travers un assemblage de TV. La méthode comportait deux étapes. La première partie était la détermination de la conductivité thermique du substrat à partir de chaque composant du mélange en utilisant un modèle existant de calcul de conductivité thermique des matériaux à deux phases. La méthode a été adaptée pour les substrats de TV, c’est-à-dire un mélange de matériaux inorganiques et organiques. Pour cela, des essais en laboratoire sur les composants de mélange du substrat ont été faits et la conductivité du substrat à la température ambiante a été calculée. La deuxième partie consiste en la prédiction de la conductivité thermique à l’aide des bases de données de la littérature sur les propriétés thermiques du sol à haute température. De plus, la contribution du rayonnement thermique entre les particules du substrat fut ajoutée pour obtenir une conductivité thermique effective. Ensuite, des tests de validation ont été effectués. La courbe obtenue montre que la conductivité thermique effective augmente considérablement avec la température. Les résultats des tests de validation ont été comparés avec les modèles numériques. Les résultats pour les substrats de deux porosités étaient concluants, ce qui démontre la possibilité d'utiliser les valeurs obtenues dans l’analyse de transfert thermique. Cette étude confirme également que le modèle de calcul de la conductivité thermique à deux phases est approprié pour les substrats de TV. Lors de la simulation numérique de transfert thermique à des température élevées des sols contenant de la MO, il est recommandé de prendre en compte l’effet de production de la chaleur quant à la décomposition de la MO pour avoir des résultats plus précis.

Le deuxième objectif spécifique était d’analyser le transfert de chaleur à travers un assemblage de TV exposée à des températures élevées, notamment d’évaluer le risque pour

le platelage d'un toit et les conditions dans lesquelles il peut être endommagé par ces hautes températures. Les variables choisies étaient l'épaisseur d'une couche de substrat de croissance dans un assemblage, la porosité d'un substrat et l'intensité d'une charge (flux) thermique appliquée. Deux types de platelage étaient utilisés : 1 en bois et 1 en acier. Il a été supposé que l'assemblage soit complètement sec, pour simuler le pire scénario. La principale conclusion est qu'une couche de substrat agit comme un isolant. Avec l'augmentation d'une épaisseur, le temps de défaillance de la structure augmente presque proportionnellement lorsque soumis aux diverses charges thermiques. La structure de toit en bois couverte par la TV avec une couche du substrat de seulement 3 cm d'épaisseur atteint sa température critique de 300°C après 30 min lorsqu'elle est exposée à une charge thermique de 200 kW/m². L'effet de porosité d'un substrat est relativement faible. Le résultat démontre que la TV avec un substrat de croissance plus compacté et une porosité de 0.5, retarde la propagation de la chaleur un peu mieux qu'avec celui ayant une porosité de 0.7. Cet effet fut observé seulement sous une charge thermique très intense de 200 kW/m². Le temps de défaillance d'une toiture avec le platelage en acier était plus long qu'avec le platelage en bois, principalement à cause de sa température critique plus élevée de 538 °C. Également, il a été démontré qu'un panneau de gypse sur le platelage en bois augmente considérablement le temps de défaillance. L'étude a permis d'analyser des situations extrêmes et de déterminer les conditions dans lesquelles la défaillance de la structure peut se produire. Pour les travaux futurs, la recherche sur le transfert thermique dans des conditions naturelles, dont lorsque le substrat contient une certaine quantité d'humidité et une charge thermique adéquate, aidera à comprendre davantage et en toute plénitude les performances de TV en situation d'incendie. Une autre chose à considérer est l'importance d'un test de validation pour les résultats de simulations numériques. En l'absence d'un tel test, cette étude était basée sur les résultats de validation sur une couche du substrat dans la première partie et l'utilisation des propriétés standards des autres matériaux de l'assemblage. Dans les travaux futurs, il serait nécessaire de développer un essai ou d'effectuer des simulations tridimensionnelles plus complexes en 3D.

Dans la troisième partie de la recherche, les contributions au feu d'un substrat de croissance et de la végétation ont été déterminées. Les paramètres d'inflammabilité telle que la charge combustible et le débit calorifique ont été mesurés pour le substrat contenant 15% de MO. Les échantillons à l'état sec et avec 30% d'humidité ont été choisis pour comparer ces

conditions extrêmes avec une condition plus réelle. Les résultats montrent que pendant la combustion, le substrat humide dégage très peu de chaleur en atteignant une valeur maximale de débit calorifique de seulement 33 kW/m². Le substrat sec a la valeur maximale plus élevée de 95 kW/m². Cependant, cette valeur n'a été maintenue que pendant la première minute du test. Par la suite, le débit calorifique n'a pas excédé 40 kW/m² tout au long du test. De plus, en les comparant avec une couverture typique, spécifiquement une membrane en bitume modifiée avec des retardateurs des flammes, le substrat dégage beaucoup moins de chaleur. Le débit calorifique d'une membrane n'a jamais été inférieur à 50 kW/m². Les résultats d'autres recherches réalisées à partir d'essais similaires sur des plants ont également montré la meilleure performance au feu du substrat par rapport à celle de la membrane en bitume typiquement modifiée. La densité d'une charge combustible pour les trois types de TV a été calculée. Les toitures ont varié selon le type de plants, de graminées basses ou de grands arbustes. Il a été montré que la TV extensive présente seulement 22% d'une charge combustible additionnelle. La TV intensive ajoute jusqu'à 95% d'une charge combustible.

Le quatrième objectif spécifique était d'analyser le risque d'incendie des TV pour les bâtiments adjacents. Sachant que le flux de chaleur rayonnante maximale tolérable aux façades exposées est de 12.5 kW/m², les distances sécuritaires entre la TV et un bâtiment voisins ont été déterminées. La méthode utilisée dans la prédiction de comportement d'un feu naturel a été choisie pour estimer la hauteur des flammes produites par ce feu de végétation, ce qui était nécessaire pour le calcul du flux thermique émis aux façades avoisinantes. Différents types de végétation, teneur en humidité des plantes et vitesses du vent ont conduits à plusieurs scénarios d'analyse. Il a été démontré que la présence d'humidité est essentielle pour diminuer le risque d'incendie. En l'absence du vent, la végétation de tous les types (graminées, arbustes) avec une teneur d'humidité très basse, nécessite une séparation d'au moins 1.5 m, tandis qu'avec une teneur en humidité modérée, seulement les arbustes hauts et densément plantés présentent un risque et nécessitent une séparation d'au moins 2.1 m. La force du vent a également eu un grand effet sur la distance sécuritaire. En comparant avec la condition calme (sans vent), une vitesse de 5 km/h conduit à une augmentation substantielle de la longueur des flammes et par conséquent la distance sécuritaire. Ainsi, les résultats démontrent la nécessité de considérer la vitesse du vent et la présence d'une source d'eau dans la conception d'une TV. Dans cette étude, les résultats

peuvent être surestimés à cause d'une méthode utilisée qui convient aux plus grandes surfaces végétalisées. Toutefois, les résultats de cette recherche peuvent être considérés comme une analyse de situations extrêmes permettant d'évaluer les facteurs les plus importants influençant le risque d'incendie.

En général, cette recherche a aidé à mieux comprendre les possibilités de feu dans les TV et le risque qu'elles présentent pour le bâtiment et les structures adjacentes. Le comportement au feu dans les conditions les plus sévères a été caractérisé. Il a été démontré que même dans les situations extrêmes, c'est-à-dire en l'absence d'humidité dans le substrat, la contribution au feu n'est pas plus élevée qu'une couverture typique en bitume. De plus, lorsqu'exposé à une charge thermique extrême, l'assemblage de TV peut retarder efficacement la propagation de la chaleur au-travers cet assemblage. Finalement, il a été confirmé que la présence d'une source d'eau et l'entretien, spécifiquement dans les climats chauds, sont essentiels pour assurer la sécurité incendie. Cependant, il sera important d'étudier la performance des TV dans des conditions réelles avec une présence d'humidité dans l'assemblage et la végétation. L'adaptation d'une méthode de prédiction de propagation du feu à travers les TV considérant ses particularités, comme la surface limitée et le type de végétation, donnera une image plus crédible de son comportement au feu. Enfin, pour compléter la caractérisation des risques incendie dans les TV, une analyse de situation quand le feu est à l'intérieur peut être faite. La présence d'une TV dans le bâtiment, spécifiquement installée sur les bâtiments existants en bois, peut poser un risque incendie à cause d'une charge additionnelle qu'elle compose. Cela peut mener au temps d'effondrement d'une structure plus court dans le feu.

Bibliographie

Àgueda, A., Pastor, E., Pérez, Y. and Planas, E. (2010) Experimental study of the emissivity of flames resulting from the combustion of forest fuels. *International Journal of Thermal Sciences* 49: 543-554.

Albini, F. A. (1976) Estimating wildfire behavior and effects. *Gen. Tech. Rep. INT-GTR-30. Ogden, UT: US Department of Agriculture, Forest Service, Intermountain Forest and Range Experiment Station. 92 p.*

Alexander, M. E. (1985) Estimating the length-to-breadth ratio of elliptical forest fire patterns. In: L.R. Donoghue and R.E. Martin (ed) *Proceedings of the Eighth Conference on Fire and Forest Meteorology.* Detroit, Michigan, USA: Society of American Foresters, Bethesda, Maryland. SAF Publication 85-04., 287-304.

Anderson, W. R., Cruz, M. G., Fernandes, P. M., McCaw, L., Vega, J. A., Bradstock, R. A., Fogarty, L., Gould, J., McCarthy, G. and Marsden-Smedley, J. B. (2015) A generic, empirical-based model for predicting rate of fire spread in shrublands. *International Journal of Wildland Fire* 24: 443-460.

Andreucci, F. and Arbolino, M. V. (1993) A study on forest fire automatic detection systems. *Il Nuovo Cimento C* 16: 35-50.

Andrews, P. L. (2014) Current status and future needs of the BehavePlus Fire Modeling System. *International Journal of Wildland Fire* 23: 21-33.

Ang, C. N. and Wang, Y. C. (2009) Effect of moisture transfer on specific heat of gypsum plasterboard at high temperatures. *Construction and Building Materials* 23: 675-686.

ANSI/SPRI VF-1. (2010) External Fire Design Standard for Vegetative Roofs. Waltham, MA: American National Standards Institute/SPRI.

ANSI/SPRI VF-1. (2017) External Fire Design Standard for Vegetative Roofs. Waltham, MA: American National Standards Institute/SPRI.

Antilén, M., Fudym, O., Vidal, A., Foerster, J. E., Moraga, N. and Escudey, M. (2006) Mathematical modelling of temperature profile of volcanic soils affected by an external thermal impact. *Australian Journal of Soil Research* 44: 57-61.

Appl, R. (2011) New fire protection tests on green roofs.

Argo, W. B. and Smith, J. M. (1953) Heat transfer in packed beds-prediction of radial rates in gas-solid beds. *Chemical Engineering Progress* 49: 443-451.

ASHRAE. (2017) Heat, Air, and Moisture Control in Building Assemblies — Material Properties. In: Owen, M. S. (ed) *2017 ASHRAE® Handbook - Fundamentals (SI*

Edition). Atlanta, GA, usa: American Society of Heating, Refrigerating and Air-Conditioning Engineers, Inc. (ASHRAE), 26.21-26.23.

ASTM D854-14. (2014) Standard Test Methods for Specific Gravity of Soil Solids by Water Pycnometer. ASTM International, West Conshohocken, PA, USA.

ASTM D2974. (2014) Standard Test Methods for Moisture, Ash, and Organic Matter of Peat and Other Organic Soils. ASTM International, West Conshohocken, PA, USA.

ASTM D5334-14. (2014) Standard Test Method for Determination of Thermal Conductivity of Soil and Soft Rock by Thermal Needle Probe Procedure. ASTM International, West Conshohocken, PA, USA.

ASTM E108. (2017) Standard Test Methods for Fire Tests of Roof Coverings. ASTM International, West Conshohocken, PA, USA.

ASTM E119. (2012) Standard Test Methods for Fire Tests of Building Construction and Materials. ASTM International, West Conshohocken, PA, USA.

Aston, A. R. and Gill, A. M. (1976) Coupled soil moisture, heat and water vapour transfers under simulated fire conditions. *Soil Research* 14: 55-66.

Babrauskas, V. (1995) Specimen heat fluxes for bench-scale heat release rate testing. *Fire and materials* 19: 243-252.

Babrauskas, V. (2016a) The cone calorimeter. In: Hurley, M. J. (ed) *SFPE Handbook of Fire Protection Engineering.* New York, NY, USA: Springer, 956-960.

Babrauskas, V. (2016b) Heat Release Rates. In: Hurley, M. J. (ed) *SFPE Handbook of Fire Protection Engineering.* New York, NY, USA: Springer, 799-905.

Babrauskas, V. and Peacock, R. D. (1992) Heat release rate: the single most important variable in fire hazard. *Fire Safety Journal* 18: 255-272.

Beadle, N. (1940) Soil Temperatures During Forest Fires and Their Effect on the Survival of Vegetation. *Journal of Ecology* 28: 180-192.

Becker, D. and Wang, D. (2011) Green roof heat transfer and thermal performance analysis. *Civil and Environmental Engineering*.

Benichou, N., Sultan, M. A., MacCallum, C. and Hum, J. K. (2001) Thermal properties of wood, gypsum and insulation at elevated temperatures (IR-710). National Research Council of Canada, Ottawa, ON, Canada.

Bergman, T. L. and Incropera, F. P. (2011) *Fundamentals of heat and mass transfer*: John Wiley & Sons.

Beyler, C. L. (2016) Fire hazard calculations for large, open hydrocarbon fires. *SFPE handbook of fire protection engineering.* Springer, 2591-2663.

Bond, W. J. and Van Wilgen, B. W. (2012) *Fire and plants,* London, UK: Chapman & Hall.

Bosworth, S. and Kelly, T. (2013) Evaluation of Warm Season Grasses for Biomass Potential in Vermont 2009 - 2012. Burlington, Vermont: University of Vermont Extension.

Bourbigot, S., Cerin, O., Duquesne, S. and Clavel, N. (2013) Flame retardancy of bitumen: A calorimetry study. *Journal of fire sciences* 31: 112-130.

Bradshaw, L. S., Deeming, J. E., Burgan, R. E. and Cohen, J. D. (1983) The 1978 national fire-danger rating system: technical documentation. *General Technical Report INT-169. Ogden, UT: US Department of Agriculture, Forest Service, Intermountain Forest and Range Experiment Station. 44 p.*

Bradstock, R. A. and Gill, A. M. (1993) Fire in semiarid, mallee shrublands-size of flames from discrete fuel arrays and their role in the spread of fire. *International Journal of Wildland Fire* 3: 3-12.

Brenneisen, S. (2003) The Benefits of Biodiversity from Green Roofs: Key Design Consequences. *The 1st North American Green Roof Conference: Greening Rooftops for Sustainable Communities.* Chicago, IL, USA: Green Roofs for Healthy Cities (GRHC), 500.

Breuning, J. (2008) Fire & wind on extensive green roofs. *Greening Rooftops for Sustainable Communities Conference.* Baltimore, MD, USA.

Buchanan, A. H. and Abu, A. K. (2017) Fires and Heat. *Structural Design for Fire Safety.* John Wiley & Sons, Ltd, UK, 35-83.

Burgan, R. E. (1979) Estimating live fuel moisture for the 1978 national fire danger rating system. *Research Paper INT-226.* Ogden, UT, USA: Intermountain Forest and Range Experiment Station, Forest Service, U.S. Department of Agriculture, 17.

Busse, M. D., Hubbert, K. R., Fiddler, G. O., Shestak, C. J. and Powers, R. F. (2005) Lethal soil temperatures during burning of masticated forest residues. *International Journal of Wildland Fire* 14: 267-276.

Butler, B. W., Cohen, J., Latham, D. J., Schuette, R. D., Sopko, P., Shannon, K. S., Jimenez, D. and Bradshaw, L. S. (2004) Measurements of radiant emissive power and temperatures in crown fires. *Canadian Journal of Forest Research* 34: 1577-1587.

Butler, B. W. and Cohen, J. D. (1998) Firefighter safety zones: a theoretical model based on radiative heating. *International Journal of Wildland Fire* 8: 73-77.

Byram, G. M. (1959a) Combustion of Forest Fuels. In: Davis, K. P. (ed) *Forest Fire: Control and Use.* New York: McGraw-Hill, 61-90.

Byram, G. M. (1959b) Forest fire behavior. In: Davis, K. P. (ed) *Forest Fire: Control and Use.* New York: McGraw-Hill, 90-123.

Campbell, G. S., Jungbauer, J., J. D., Bristow, K. L. and Hungerford, R. D. (1995) Soil temperature and water content beneath a surface fire. *Soil Science* 159: 363-374.

Campbell, G. S., Jungbauer, J., J. D.,, Bidlake, W. R. and Hungerford, R. D. (1994) Predicting the effect of temperature on soil thermal conductivity. *Soil Science* 158: 307-313.

CAN/ULC-S101. (2014) Standard Methods of Fire Endurance Tests of Building Construction and Materials. Underwriters Laboratories of Canada, Ottawa, ON, Canada.

CAN/ULC-S107. (2010) Standard Methods of Fire Tests of Roof Coverings. Underwriters Laboratories of Canada, Ottawa, ON, Canada.

Carlsson, E. (1999) External fire spread to adjoining buildings. Lund, Sweden: Department of Fire Safety Engineering, Lund University, Sweden.

Carson, T. B., Hakimdavar, R., Sjoblom, K. J. and Culligan, P. J. (2012) Viability of recycled and waste materials as green roof substrates. *GeoCongress 2012: State of the Art and Practice in Geotechnical Engineering.* Oakland, CA, USA, 3644-3653.

Catchpole, W. R., Bradstock, R. A., Choate, J., Fogarty, L. G., Gellie, N., McCarthy, G., McCaw, W. L., Marsden-Smedley, J. B. and Pearce, G. (1998) Cooperative development of equations for heathland fire behaviour. *Proceedings of 3rd International Conference on Forest Fire Research and 14th Conference on Fire and Forest Meteorology.* 16-20.

Cermak, V. and Rybach, L. (1982) Thermal Conductivity and Specific Heat of Minerals and Rocks. In: G. Angenheister (ed) *Numerical Data and Functional Relationships in Science and Technology, New Series, Group V (Geophysics and Space Research), Volume Ia,(Physical Properties of Rocks),.* Springer, Berlin-Heidelberg, 305–343.

Chen, P.-Y., Li, Y.-H., Lo, W.-H. and Tung, C. (2015) Toward the practicability of a heat transfer model for green roofs. *Ecological Engineering* 74: 266-273.

Cheney, N. P., Gould, J. S. and Catchpole, W. R. (1993) The influence of fuel, weather and fire shape variables on fire-spread in grasslands. *International Journal of Wildland Fire* 3: 31-44.

Cheney, N. P., Gould, J. S. and Catchpole, W. R. (1998) Prediction of fire spread in grasslands. *International Journal of Wildland Fire* 8: 1-13.

Clark, S. P. (1966) *Handbook of physical constants*: Geological Society of America.

Clarke, R. E., Pianella, A., Shabani, B. and Rosengarten, G. (2016) Steady-state thermal measurement of moist granular earthen materials. *Journal of Building Physics* 41: 101-119.

Clauser, C. and Huenges, E. (1995) Thermal conductivity of rocks and minerals. *Rock physics & phase relations: a handbook of physical constants*: 105-126.

Cohen, J. D. and Butler, B. W. (1998) Modeling potential structure ignitions from flame radiation exposure with implications for wildland/urban interface fire management. *In: Proceedings of the 13th Fire and Forest Meteorology Conference, International Association of Wildland Fire. p. 81-86.*

Coma, J., Pérez, G., Solé, C., Castell, A. and Cabeza, L. F. (2016) Thermal assessment of extensive green roofs as passive tool for energy savings in buildings. *Renewable Energy* 85: 1106-1115.

Côté, J. and Konrad, J.-M. (2005) Thermal conductivity of base-course materials. *Canadian Geotechnical Journal* 42: 61-78.

Côté, J. and Konrad, J.-M. (2009) Assessment of structure effects on the thermal conductivity of two-phase porous geomaterials. *International Journal of Heat and Mass Transfer* 52: 796-804.

CRCA. (2006) Roof gardens Tech bulletin V56B.

Cruz, M. G., Matthews, S., Gould, J., Ellis, P., Henderson, M., Knight, I. and Watters, J. (2010) Fire dynamics in mallee-heath: fuel, weather and fire behaviour prediction in south Australian semi-arid shrublands. *Bushfire Cooperative Research Centre, Report A.10.01*. CSIRO Sustainable Ecosystems, Canberra, ACT, Australia.

Dalgleish, S. A., Van Etten, E. J. B., Stock, W. D. and Knuckey, C. (2015) Fuel dynamics and vegetation recovery after fire in a semiarid Australian shrubland. *International Journal of Wildland Fire* 24: 613-623.

Damant, G. H. and Nurbakhsh, S. (1994) Christmas trees—what happens when they ignite? *Fire and materials* 18: 9-16.

DD CEN/TS 1187. (2012) "Test methods for external fire exposure to roofs". London, UK: BSI, 62.

De Vries, D. and de Wit, C. T. (1954) Die Thermischen eigenschaften der Moorboden und die beeinflussing der nachtfrostgefahr durch eine Sanddecke,. *Meteorologische Rundschau* 7: 5-28.

De Vries, D. A. and Van Wijk, W. R. (1963) Physics of plant environment. In: Evans, L. T. (ed) *Environmental control of plant growth.* Academic Press, New York, NY, USA, 5-22.

DeBano, L. F., Neary, D. G. and Ffolliott, P. F. (1998) Combustion processes and heat transfer. *Fire effects on ecosystems.* USA: John Wiley & Sons, 19-45.

DeBano, L. F., Rice, R. M. and Eugene, C. C. (1979) Soil heating in chaparral fires: effects on soil properties, plant nutrients, erosion, and runoff. *Pacific Southwest Forest and Range Experiment Station.* Res. Paper PSW-RP-145. Berkeley, CA: U.S. Department of Agriculture, Forest Service. 21 p.

Delany, J., Boverman, D. and Matthews, S. (2017) Short fire runs: Assessing bush fire risk from small areas of vegetation. *Fire Safety Engineering Stream Conference: Quantification of Fire Safety: Fire Australia 2017.* Engineers Australia, 260.

Department for Communities and Local Government. (2013) Fire Performance of Green Roofs and Walls. London, UK: Department for Communities and Local Government.

Department for Communities and Local Government UK. (2013) Fire Performance of Green Roofs and Walls. London, UK, 31-36.

Diablo Firesafe Council. *List of References for Plant Fire Performance Ratings*. Available at: http://www.diablofiresafe.org/tolerance.html.

Dibble, A. C., White, R. H. and Lebow, P. K. (2007) Combustion characteristics of north-eastern USA vegetation tested in the cone calorimeter: invasive versus non-invasive plants. *International Journal of Wildland Fire* 16: 426-443.

Dimitrakopoulos, A. P. and Papaioannou, K. K. (2001) Flammability assessment of Mediterranean forest fuels. *Fire Technology* 37: 143-152.

Drysdale, D. (2011) Diffusion Flames and Fire Plumes. *An Introduction to Fire Dynamics.* 3 ed. Chichester, West Sussex, United Kingdom: John Wiley & Sons, 121-179.

Dunnett, N. and Kingsbury, N. (2008) *Planting green roofs and living walls*: Timber press Portland, OR.

EN 1991-1-2. (2003) "Eurocode 1: Actions on structures - Part 1-2: General actions - Actions on structures exposed to fire". European Committee for Standardization.

EN 1993-1-2. (2005) "Eurocode 3: Design of Steel Structures - Part 1-2: General - Structural Fire Design". European Committee for Standardization.

EN 1995-1-2. (2003) "Eurocode 5: Design of timber structures - Part 1-2 : General - Structural fire design". European Committee for Standardization.

Energie Cités. (2014) Zielone dachy i żyjące ściany – systemowe rozwiązania i przegląd inwestycji w polskich gminach.: Stowarzyszenie Gmin Polska Sieć „Energie Cités".

Enninful, E. K. (2006) Predicting temperature profiles during simulated forest fires. University of Saskatchewan, Saskatchewan, Canada.

Environment and natural resources. (2017) *Beaufort wind scale table*. Available at: www.canada.ca/en/environment-climate-change/services/general-marine-weather-information/understanding-forecasts/beaufort-wind-scale-table.html.

Environment Canada. (2019) Historical Climate Data. Hourly Data Report. .

Eppelbaum, L., Kutasov, I. and Pilchin, A. (2014) *Thermal Properties of Rocks and Density of Fluids*.

Erik van Lennep, S. F. (2008) A green roof policy guidance paper for dublin.

Farouki, O. T. (1981) Thermal properties of soils. HANOVER, NH, USA: U.S. Army Cold Regions Research and Engineering Laboratory pp. 12-29.

Fidelis, A. T., Delgado Cartay, M. D., Blanco, C. C., Muller, S. C., Pillar, V. P. and Pfadenhauer, J. S. (2010) Fire intensity and severity in Brazilian campos grasslands. *Interciencia: revista de ciencia y tecnologia de america. Caracas.* 35: 739-745.

Fillion, M.-H., Côté, J. and Konrad, J.-M. (2011) Thermal radiation and conduction properties of materials ranging from sand to rock-fill. *Canadian Geotechnical Journal* 48: 532-542.

FireSmart Canada. (2019) *FireSmart Guide to Landscaping*. Available at: https://firesmartcanada.ca/wp-content/uploads/2019/10/FireSmart-Guide-to-Lanscaping.pdf.

Fleury, R. (2010) Evaluation of thermal radiation models for fire spread between objects. *Department of Civil and Natural Resources Engineering.* Christchurch, New Zealand: University of Canterbury, 130.

FLL. (2008a) Guidelines for the Planning, Construction and Maintenance of Green Roofing – Green Roofing Guideline. *Fire characteristics.* Bonn, Germany: FLL (Forschungsgesellschaft Landschaftsentwicklung Landschaftsbau), Research Society for Landscape Development and Landscape Construction, p. 36.

FLL. (2008b) Guidelines for the Planning, Construction and Maintenance of Green Roofing – Green Roofing Guideline. *Preface.* Bonn, Germany: Research Society for Landscape Development and Landscape Construction, p. 8.

FM Global. (2011) Property Loss Prevention Data Sheet (1-35) Green roof systems. Factory Mutual Insurance Company, 1-27.

FM Global. (2012) Property Loss Prevention Data Sheet (1-28R, 1-29R) Roof systems. Factory Mutual Insurance Company.

Fontana, M., Kohler, J., Fischer, K. and De Sanctis, G. (2016) Fire load density. In: Hurley, M. J. (ed) *SFPE handbook of fire protection engineering.* New York, NY, USA: Springer, 1131-1142.

Frandsen, W. H. and Ryan, K. C. (1986) Soil moisture reduces belowground heat flux and soil temperatures under a burning fuel pile. *Canadian Journal of Forest Research* 16: 244-248.

Fuss, S. P. and Hamins, A. (2002) An estimate of the correction applied to radiant flame measurements due to attenuation by atmospheric CO2 and H2O. *Fire Safety Journal* 37: 181-190.

Gerzhova, N., Côté, J., Blanchet, P., Dagenais, C. and Ménard, S. (2019) A conceptual framework for modelling the thermal conductivity of dry green roof substrates. *BioResources Journal* 14: 8573-8599.

Gil, A., Nicolas, C., Ortega, I., Risueño, E., Faik, A., Blanco, P. and Rodrıguez-Aseguinolaza, J. (2014) Characterization of a by-product from steel industry applied to thermal energy storage in Concentrated Solar Power. *Proceedings of the 99th Eurotherm Seminar, Lleida, Spain, Paper No. EUROTHERM99-01-066.*

GNPC. *Green Roof Species*. Available at: www.nycgovparks.org/greening/greenbelt-native-plant-center/garden-species-lists/garden-green-roof.

González-González, B. D., Sixto, H., Alberdi, I., Esteban, L., Guerrero, S., Pasalodos, M., Vázquez, A. and Cañellas, I. (2017) Estimation of shrub biomass availability along two geographical transects in the Iberian Peninsula for energy purposes. *Biomass and bioenergy* 105: 211-218.

Green Roofs for Healthy Cities. (2013) *Green Roof Design and Installation, Resource Manual*, Toronto, Canada.

GRO. (2011) The GRO Green Roof Code. Green Roof Code of Best Practice for the UK.: Groundwork Sheffield.

GRÖNATAKHANDBOKEN. (2017).

Guide. Toronto Green Roof Construction Standard. Supplementary Guidelines.

Hadjisophocleous, G. V. and Mehaffey, J. R. (2016) Fire scenarios. In: Hurley, M. J. (ed) *SFPE Handbook of Fire Protection Engineering.* New York, NY, USA: Springer, 1262-1288.

Hashin, Z. and Shtrikman, S. (1962) A variational approach to the theory of the effective magnetic permeability of multiphase materials. *Journal of applied Physics* 33: 3125-3131.

Heaton, E., Voigt, T. and Long, S. P. (2004) A quantitative review comparing the yields of two candidate C4 perennial biomass crops in relation to nitrogen, temperature and water. *Biomass and bioenergy* 27: 21-30.

Hirsch, K. G. (1996) Canadian forest fire behavior prediction (FBP) system: user's guide. Ottawa, ON, Canada, 122.

Howell, J. R. and Siegel, R. (2010) Optically Thin and Thick Limits for Radiative Transfer in Participating Media. In: Press, C. (ed) *Thermal Radiation Heat Transfer.* Boca Raton, FL, USA, 581-614.

IFC. (2012) Section 317 - Rooftop Gardens and Landscaped Roofs.

Incropera, F. P. and Dewitt, D. P. (2007) Fundamentals of Heat and Mass Transfer, 2007, pp. A-5. Wiley: Asia.

ISO 5660-1. (2015) Reaction-to-fire tests -- Heat release, smoke production and mass loss rate -- Part 1: Heat release rate (cone calorimeter method) and smoke production rate (dynamic measurement). International Organization for Standardization, Geneva, Switzerland.

Jaffal, I., Ouldboukhitine, S.-E. and Belarbi, R. (2012) A comprehensive study of the impact of green roofs on building energy performance. *Renewable Energy* 43: 157-164.

Jefferson, P. G., McCaughey, W. P., May, K., Woosaree, J., MacFarlane, L. and Wright, S. M. (2002) Performance of American native grass cultivars in the Canadian prairie provinces. *Native Plants Journal* 3: 24-33.

Jervis, F. X. and Rein, G. (2016) Experimental study on the burning behaviour of Pinus halepensis needles using small-scale fire calorimetry of live, aged and dead samples. *Fire and materials* 40: 385-395.

Jungels, J., Rakow, D. A., Allred, S. B. and Skelly, S. M. (2013) Attitudes and aesthetic reactions toward green roofs in the Northeastern United States. *Landscape and Urban Planning* 117: 13-21.

Kaviany, M. (1995) Conduction Heat Transfer In: Ling, F. F. (ed) *Principles of heat transfer in porous media.* . Springerverlag, New York, NY, USA.

Kidnie, S. M. (2009) Fuel load and fire behaviour in the southern Ontario tallgrass prairie. *Graduate Department of Forestry.* University of Toronto, Toronto, ON, Canada.

Köhler, M., Schmidt, M., Wilhelm, G. F., Laar, M., Lúcia de Assunção Paiva V. and Tavares, S. (2002) Green roofs in temperate climates and in the hot-humid tropics–far beyond the aesthetics. *Environmental management and health* 13: 382-391.

LFB (London Fire Brigade). (2018) *Roof garden alight - Ealing.* Available at: www.london-fire.gov.uk/incidents/2018/august/roof-garden-alight-ealing/.

Li, A., Dhakal, S., Glenn, N., Spaete, L., Shinneman, D., Pilliod, D., Arkle, R. and McIlroy, S. (2017) Lidar aboveground vegetation biomass estimates in shrublands: Prediction, uncertainties and application to coarser scales. *Remote Sensing* 9: 903.

Lin, S., Sun, P. and Huang, X. (2019) Can peat soil support a flaming wildfire? *International Journal of Wildland Fire* 28: 601-613.

Madrigal, J., Guijarro, M., Hernando, C., Diez, C. and Marino, E. (2011) Effective heat of combustion for flaming combustion of Mediterranean forest fuels. *Fire Technology* 47: 461-474.

Madrigal, J., Marino, E., Guijarro, M., Hernando, C. and Díez, C. (2012) Evaluation of the flammability of gorse (Ulex europaeus L.) managed by prescribed burning. *Annals of Forest Science* 69: 387-397.

Marsden-Smedley, J. B. and Catchpole, W. R. (1995) Fire modelling in Tasmanian buttongrass moorlands. I. Fuel characteristics. *International Journal of Wildland Fire* 5: 203-214.

Marsden-Smedley, J. B. and Catchpole, W. R. (2001) Fire modelling in Tasmanian buttongrass moorlands. III. Dead fuel moisture. *International Journal of Wildland Fire* 10: 241-253.

McAlpine, R. S. (1988) Acceleration of point source fire to equilibrium spread.

McGuire, J. H. (1965) Fire and the spatial separation of buildings. *Fire Technology* 1: 278-287.

Meacham, B., Poole, B., Echeverria, J. and Cheng, R. (2013) Fire safety challenges of green buildings. In: Milke, J. A. (ed) *Springer Briefs in Fire.* New York, NY, USA: Springer Science & Business Media, 22-24.

meinbezirk.at. (2016) *Brand im Internat der Berufsschule Altmünster: 15 Millionen Euro Schaden*. Available at: www.meinbezirk.at/salzkammergut/c-lokales/brand-im-internat-der-berufsschule-altmuenster-15-millionen-euro-schaden_a1742228.

Modak, A. T. and Croce, P. A. (1977) Plastic pool fires. *Combustion and Flame* 30: 251-265.

Molineux, C. J., Fentiman, C. H. and Gange, A. C. (2009) Characterising alternative recycled waste materials for use as green roof growing media in the UK. *Ecological Engineering* 35: 1507-1513.

Morandini, F., Silvani, X., Rossi, L., Santoni, P.-A., Simeoni, A., Balbi, J.-H., Rossi, J. L. and Marcelli, T. (2006) Fire spread experiment across Mediterranean shrub: influence of wind on flame front properties. *Fire Safety Journal* 41: 229-235.

Mudan, K. S. (1984) Thermal radiation hazards from hydrocarbon pool fires. *Progress in energy and combustion science* 10: 59-80.

Mutch, R. W. (1970) Wildland Fires and Ecosystems--A Hypothesis. *Ecology* 51: 1046-1051.

Nelson Jr, R. M. and Adkins, C. W. (1986) Flame characteristics of wind-driven surface fires. *Canadian Journal of Forest Research* 16: 1293-1300.

NFPA. (2012) NFPA 550: Guide to the Fire Safety Concepts Tree. Quincy, MA, USA: National Fire Protection Association.

Noble, I. R., Gill, A. M. and Bary, G. A. V. (1980) McArthur's fire-danger meters expressed as equations. *Australian Journal of Ecology* 5: 201-203.

NRCC. (2015) National Building Code of Canada 2015. Ottawa, ON, Canada: National Research Council of Canada.

ÖNORM L 1131. (2010) Gartengestaltung und Landschaftsbau - Begrünung von Dächern und Decken auf Bauwerken (Garden design and landscaping - Greening of roofs and ceilings on buildings).

Ouldboukhitine, S.-E., Belarbi, R., Jaffal, I. and Trabelsi, A. (2011) Assessment of green roof thermal behavior: A coupled heat and mass transfer model. *Building and Environment* 46: 2624-2631.

Overholt, K. J., Kurzawski, A. J., Cabrera, J., Koopersmith, M. and Ezekoye, O. A. (2014) Fire behavior and heat fluxes for lab-scale burning of little bluestem grass. *Fire Safety Journal* 67: 70-81.

Pacific Northwest Extension publication. (2006) Fire-resistant plants for home landscapes. In: University, O. S. (ed). 48.

Parmar, K. (2017) Biomass- An Overview on Composition Characteristics and Properties. *IRA-International Journal of Applied Sciences* 7: 42-51.

Pastor, E., Rigueiro, A., Zárate L., Gimenez, A., Arnaldos, J. and Planas, E. (2002) Experimental methodology for characterizing flame emissivity of small scale forest fires using infrared thermography techniques. *IV International Conference on Forest Fire Research 2002 Wildland Fire Safety Summit.* 1-11.

Penney, G. (2017) Bushfire fuels–representation in empirical and physics based bushfire models. *Department of Fire and Emergency Services Western Australia.*

Pompeii II, W. C. and Hawkins, T. W. (2011) Assessing the Impact of Green Roofs on Urban Heat Island Mitigation: A Hardware Scale Modeling Approach. *Geographical Bulletin* 52.

Portland Fire Bureau. (2018) Incident report RP180057217. City of Portland, OR, USA, 1-2.

Pourhashemi, S. A., Hao, O. J. and Chawla, R. C. (1999) An experimental and theoretical study of the nonlinear heat conduction in dry porous media. *International Journal of Energy Research* 23: 389-401.

Pyne, S. J. (1984) *Introduction to wildland fire. Fire management in the United States,* USA: John Wiley & Sons.

Quezada-García, S., Espinosa-Paredes, G., Escobedo-Izquierdo, M., Vázquez-Rodríguez, A., Vázquez-Rodríguez, R. and Ambriz-García, J. (2017) Heterogeneous Model for Heat Transfer in Green Roof Systems. *Energy and Buildings* 139: 205-213.

Raison, R. J., Woods, P. V., Jakobsen, B. F. and Bary, G. A. V. (1986) Soil temperatures during and following low-intensity prescribed burning in a Eucalyptus pauciflora forest. *Australian Journal of Soil Research* 24: 33-47.

RBQ. (2015) *Critères techniques visant la construction de toits végétalisés Quebec,* Montréal, Canada: RBQ.

Rein, G. (2016) Smoldering combustion. In: Hurley, M. J. (ed) *SFPE Handbook of Fire Protection Engineering.* New York, NY, USA: Springer, 581-603.

Robertson, E. C. (1988) Thermal properties of rocks. US Geological Survey.

Rossiter, N. A., Setterfield, S. A., Douglas, M. M. and Hutley, L. B. (2003) Testing the grass-fire cycle: alien grass invasion in the tropical savannas of northern Australia. *Diversity and distributions* 9: 169-176.

Rothermel, R. C. (1972) A mathematical model for predicting fire spread in wildland fuels. *Res. Pap. INT-115.* Ogden, UT: US Department of Agriculture, Intermountain Forest and Range Experiment Station: USDA Forest Service, 40.

Saadatian, O., Sopian, K., Salleh, E., Lim, C. H., Riffat, S., Saadatian, E., Toudeshki, A. and Sulaiman, M. Y. (2013) A review of energy aspects of green roofs. *Renewable and Sustainable Energy Reviews* 23: 155-168.

SAI Global. (2009) AS3959: 2009 Construction of Buildings in Bushfire-Prone Areas. Standards Australia: Sydney, Australia.

Sailor, D., Hutchinson, D. and Bokovoy, L. (2008) Thermal property measurements for ecoroof soils common in the western US. *Energy and Buildings* 40: 1246-1251.

Sailor, D. J. and Hagos, M. (2011) An updated and expanded set of thermal property data for green roof growing media. *Energy and Buildings* 43: 2298-2303.

Sampson, C. (2012) Logistics of Agricultural-Based Biomass Feedstock for Saskatchewan, Project No. E7810. Humboldt, SK, Canada: ABC Steering Committee, SaskPower, NRCan, 100-101.

Sandoval, V., Bonilla, C. A., Gironás, J., Vera, S., Victorero, F., Bustamante, W., Rojas, V., Leiva, E., Pastén, P. and Suárez, F. (2017) Porous Media Characterization to Simulate Water and Heat Transport through Green Roof Substrates. *Vadose Zone Journal* 16.

Santoni, P. A., Simeoni, A., Rossi, J. L., Bosseur, F., Morandini, F., Silvani, X., Balbi, J.-H., Cancellieri, D. and Rossi, L. (2006) Instrumentation of wildland fire: characterisation of a fire spreading through a Mediterranean shrub. *Fire Safety Journal* 41: 171-184.

Scarff, F. R. and Westoby, M. (2006) Leaf Litter Flammability in Some Semi-Arid Australian Woodlands. *Functional Ecology* 20: 745-752.

Scott, J. H. and Burgan, R. E. (2005) Standard fire behavior fuel models: a comprehensive set for use with Rothermel's surface fire spread model. *Gen. Tech. Rep. RMRS-GTR-153. Fort Collins, CO: US Department of Agriculture, Forest Service, Rocky Mountain Research Station. 72 p.*, 72.

Shokri, M. and Beyler, C. L. (1989) Radiation from large pool fires. *Journal of Fire Protection Engineering* 1 (4): 141-150.

Silvani, X. and Morandini, F. (2009) Fire spread experiments in the field: temperature and heat fluxes measurements. *Fire Safety Journal* 44: 279-285.

Simard, A. J., Blank, R. W. and Hobrla, S. L. (1989) Measuring and interpreting flame height in wildland fires. *Fire Technology* 25: 114-133.

Snodgrass, E. C. and McIntyre, L. (2010) *The green roof manual: a professional guide to design, installation, and maintenance,* China: Timber Press.

Stovin, V., Vesuviano, G. and Kasmin, H. (2012) The hydrological performance of a green roof test bed under UK climatic conditions. *Journal of hydrology* 414: 148-161.

Sudheer, S. and Prabhu, S. V. (2012) Measurement of flame emissivity of hydrocarbon pool fires. *Fire Technology* 48: 183-217.

Sullivan, A., Ellis, P. and Knight, I. (2003) A review of radiant heat flux models used in bushfire applications. *International Journal of Wildland Fire* 12: 101-110.

Sultan, M. A. (2006) Incident heat flux measurements in floor and wall furnaces of different sizes. *Fire and Materials: An International Journal* 30: 383-396.

Sutton, R. K. (2015) *Green Roof Ecosystems,* Switzerland: Springer International Publishing.

Sutton, R. K., Harrington, J. A., Skabelund, L., MacDonagh, P., Coffman, R. R. and Koch, G. (2012) Prairie-based green roofs: literature, templates, and analogs. *Journal of Green Building* 7: 143-172.

Tabares-Velasco, P. C. and Srebric, J. (2012) A heat transfer model for assessment of plant based roofing systems in summer conditions. *Building and Environment* 49: 310-323.

The council of the city of Vancouver. Building By-law no. 10908.

Thureson, P. and Nilsson, M. (1994) Degradation of fire properties of approved products as a result of ageing, SP Repot 1994:61. Borås, Sweden, 44.

Tien, C.-L. and Drolen, B. L. (1987) Thermal radiation in particulate media with dependent and independent scattering. *Annual Review of Heat Transfer* 1.

Todor, D. N. (1976) Classification of thermal analysis methods. In: Morgan, D. J. (ed) *Thermal Analysis of Minerals.* Abacus Press, London, UK, 9-33.

Toitures Végétalisées. (2012) Cahier technique, Paris.

Toronto Municipal Code. (2017) Chapter 492 "Green roofs". City of Toronto 9-14.

Torrance, S. (2013) City of Toronto Guidelines for Biodiverse Green Roofs. In: Toronto City Planning (ed).

Torvi, D. A., Kashef, A. and Benichou, N. (2005) FIERAsystem Radiation to Adjacent Buildings Model (RABM) Theory Report. Institute for Research in Construction, National Research Council Canada.

Tramoni, J.-B., Santoni, P.-A. and Morandini, F. (2018) Experimental and numerical investigation of shrub combustion. *Journal of Physics: Conference Series.* Nancy, France: IOP Publishing, 052002.

Valette, J.-C., Gomendy, V., Maréchal, J., Houssard, C. and Gillon, D. (1994) Heat-transfer in the soil during very low-intensity experimental fires-the role of duff and soil-moisture content. *International Journal of Wildland Fire* 4: 225-237.

Van Genuchten, M. T. (1980) A closed-form equation for predicting the hydraulic conductivity of unsaturated soils *Soil Science Society of America Journal* 44: 892-898.

Viana, H., Vega-Nieva, D. J., Torres, L. O., Lousada, J. and Aranha, J. (2012) Fuel characterization and biomass combustion properties of selected native woody shrub species from central Portugal and NW Spain. *Fuel* 102: 737-745.

Ville de Lausanne. (2014) Toitures végétalisées. Guide de recommandations. Pourquoi et comment accueillir la nature sur son toit. Lausanne, Switzerland.

Ville de Montréal. (2014) La construction de toits végétalisés. Guide technique pour préparer une solution de rechange. Cahier explicatif.

Vosteen, H.-D. and Schellschmidt, R. (2003) Influence of temperature on thermal conductivity, thermal capacity and thermal diffusivity for different types of rock. *Physics and Chemistry of the Earth, Parts A/B/C* 28: 499-509.

Waples, D. W. and Waples, J. S. (2004) A review and evaluation of specific heat capacities of rocks, minerals, and subsurface fluids. Part 1: Minerals and nonporous rocks. *Natural resources research* 13: 97-122.

Weiler, S. K. and Scholz-Barth, K. (2009) Component Parts: Inert and Dynamic. *Green roof system. A guide to the planning, design and construction of landscape over structure.* Hoboken, New Jersey, USA: John Wiley & Sons, Inc., 120-175.

Weise, D. R., White, R. H., Beall, F. C. and Etlinger, M. (2005) Use of the cone calorimeter to detect seasonal differences in selected combustion characteristics of ornamental vegetation. *International Journal of Wildland Fire* 14: 321-338.

White, R. H. and Zipperer, W. C. (2010) Testing and classification of individual plants for fire behaviour: plant selection for the wildland–urban interface. *International Journal of Wildland Fire* 19: 213-227.

Wilson, R. (1980) Reformulation of forest fire spread equations in SI units. Research Note INT-292. Ogden, UT: U.S.: Department of Agriculture, Forest Service, Intermountain Range and Forest Experiment Station. 5 p.

Wotton, B. M., Alexander, M. E. and Taylor, S. W. (2009) Updates and revisions to the 1992 Canadian forest fire behavior prediction system. Sault Ste. Marie, ON, Canada: Information Report GLC-X-10, Great Lakes Forestry Centre 45.

Yang, J., Yu, Q. and Gong, P. (2008) Quantifying air pollution removal by green roofs in Chicago. *Atmospheric environment* 42: 7266-7273.

Yio, M. H. N., Stovin, V., Werdin, J. and Vesuviano, G. (2013) Experimental analysis of green roof substrate detention characteristics. *Water Science and Technology* 68: 1477-1486.

Zárate, L., Arnaldos, J. and Casal, J. (2008) Establishing safety distances for wildland fires. *Fire Safety Journal* 43: 565-575.

Zelené střechy. (2016) Vegetační souvrství zelených střech. Standardy pro navrhování, provádění a údržbu. In: zeleně, S. z. a. ú. (ed).

Zilverberg, C. J., Teoh, K., Boe, A., Johnson, W. C. and Owens, V. (2016) Strategic use of native species on environmental gradients increases diversity and biomass relative to switchgrass monocultures. *Agriculture, Ecosystems & Environment* 215: 110-121.

Zoth, G. and Haenel, R. (1988) Appendix. In: Haenel, R., Rybach, L. and Stegena, L. (eds) *Handbook of Terrestrial Heat-Flow Density Determination: with Guidelines and Recommendations of the International Heat-Flow Commission.* Dordrecht: Springer Netherlands, 449-468.

Annexe A

Table 6.4. Flame length (m).

	Moisture scenario									
	D1L1	D2L2	D3L3	D4L4	D2L3	D3L2	D4L2	D4L3	D2L4	D3L4
Fuel model	Wind 0 kph									
Grass										
GR-2	-	-	-	-	-	-	-	-	-	-
GR-3	0.6	-	-	-	-	-	-	-	-	-
GR-4	0.8	0.6	-	-	-	0.5	-	-	-	-
Grass-Shrub										
GS-1	-	-	-	-	-	-	-	-	-	-
GS-2	0.5	-	-	-	-	-	-	-	-	-
GS-3	0.9	0.6	-	-	-	0.5	0.5	-	-	-
Shrub										
SH-2	0.6	-	-	-	-	-	-	-	-	-
SH-4	0.7	0.5	-	-	-	-	-	-	-	-
SH-8	1.1	0.8	0.7	-	0.7	0.8	0.8	0.6	0.6	-
Fuel model	Wind 5 kph									
Grass										
GR-2	1.4	1.0	-	-	0.6	0.9	0.7	-	-	-
GR-3	2.3	1.6	1.0	-	1.1	1.5	1.4	0.9	-	-
GR-4	2.7	1.9	0.6	-	1.3	1.8	1.4	-	-	-
Grass-Shrub										
GS-1	1.1	0.7	-	-	-	-	-	-	-	-
GS-2	1.6	1.1	-	-	-	0.9	-	-	-	-
GS-3	2.6	1.8	-	-	0.5	1.7	1.6	-	-	-
Shrub										
SH-2	1.4	0.5	-	-	-	-	-	-	-	-
SH-4	2.2	1.5	0.5	-	0.5	1.0	0.5	-	0.5	-
SH-8	3.1	2.4	1.9	0.7	2.1	2.3	2.2	1.7	1.7	1.3
Fuel model	Wind 10 kph									
Grass										
GR-2	2.2	1.6	-	-	1.0	1.5	1.1	-	-	-
GR-3	3.4	2.3	1.4	-	1.5	2.1	2.0	1.4	-	-
GR-4	4.1	3.0	0.9	-	2.0	2.7	2.1	0.7	-	-
Grass-Shrub				-						
GS-1	1.7	1.1	-	-	-	0.5	-	-	-	-
GS-2	2.5	1.8	0.5	-	0.6	1.3	0.6	-	-	-
GS-3	4.0	2.7	0.7	-	0.7	2.5	2.4	-	-	-
Shrub										

	Moisture scenario									
	D1L1	D2L2	D3L3	D4L4	D2L3	D3L2	D4L2	D4L3	D2L4	D3L4
SH-2	2.1	0.7	0.5	-	0.5	0.5	-	-	0.5	-
SH-4	3.3	2.3	0.7	0.6	0.8	1.5	0.7	0.7	0.7	0.7
SH-8	4.5	3.6	2.8	1.1	3.1	3.4	3.2	2.4	2.4	1.8
Fuel model	Wind 15 kph									
Grass										
GR-2	2.9	2.1	-	-	1.3	1.9	1.4	-	-	-
GR-3	4.2	2.9	1.8	-	1.9	2.7	2.5	1.7	-	-
GR-4	5.4	3.9	1.0	-	2.6	3.6	2.8	0.7	-	-
Grass-Shrub										
GS-1	2.2	1.5	-	-	-	0.5	-	-	-	-
GS-2	3.2	2.3	0.6	-	0.6	1.7	0.6	-	-	-
GS-3	5.1	3.4	0.8	-	1.0	3.2	3.1	0.7	-	-
Shrub										
SH-2	2.7	1.0	0.6	-	0.6	0.7	0.5	0.5	0.6	0.6
SH-4	4.2	3.0	0.9	0.8	1.0	1.9	0.9	0.8	0.9	0.8
SH-8	5.6	4.5	3.5	1.3	3.9	4.2	4.0	3.0	3.0	2.3
Fuel model	Wind 20 kph									
Grass										
GR-2	3.5	2.4	-	-	1.3	2.1	1.4	-	-	-
GR-3	4.9	3.4	2.0	-	2.2	3.1	2.9	1.9	-	-
GR-4	6.5	4.8	1.0	-	3.1	4.3	3.4	0.7	-	-
Grass-Shrub										
GS-1	2.7	1.8	-	-	-	0.5	-	-	-	-
GS-2	3.9	2.8	0.6	-	0.6	2.1	0.6	-	-	-
GS-3	6.1	4.1	0.8	-	1.0	3.8	3.7	0.7	-	-
Shrub										
SH-2	3.3	1.1	0.7	0.5	0.8	0.8	0.6	0.5	0.7	0.7
SH-4	5.1	3.6	0.9	0.8	1.1	2.3	0.9	0.8	1.0	0.8
SH-8	6.6	5.2	4.1	1.6	4.5	5.0	4.7	3.5	3.6	2.7

Annexe B

PhD 8 - Caractérisation et analyse des risques incendie dans les toitures végétalisées

Étudiant : Nataliia Gerzhova
Direction : Pierre Blanchet
Codirection : Sylvain Ménard, Christian Dagenais

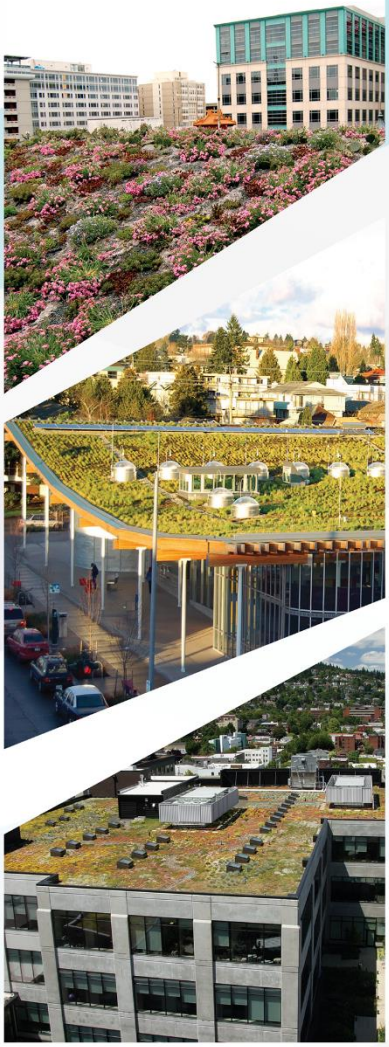

Problèmes

Présentement au Québec, la construction de toitures végétalisées est limitée. La préoccupation principale est un problème de sécurité incendie. Les plantes ainsi que les autres couches de ce système présentent une charge combustible et peuvent contribuer à la propagation du feu à travers le toit du bâtiment, qui pose un danger à la fois pour le bâtiment lui-même et pour les bâtiments adjacents. De plus, les exigences actuelles dans la construction pour les couvertures ne peuvent pas être remplies, parce qu'une grande variété de composants et configurations ne permet pas de classifier ces systèmes à l'exposition extérieure au feu.

Les règles élaborées spécifiquement pour ce type de toiture contiennent des options de lutte contre le feu assez strictes à cet égard, ce qui limite le choix de conception. Cela empêche le développement et l'utilisation généralisée de toits verts et donc d'obtenir tous les avantages de ces systèmes dans leur totalité.

Résultats attendus

L'étude permettra d'approfondir la connaissance sur le comportement du feu dans les toitures végétalisées et son impact sur les bâtiments. Plus précisément, de comprendre clairement les problèmes liés aux risques d'incendie et de propagation du feu et de la chaleur à travers le système.

La simulation de divers types de systèmes avec différents matériaux et différentes configurations aidera à réaliser une analyse précise sur la base de ce qui est proposé, soit un système sécuritaire de toit végétal.

Retombées pour l'industrie

L'adoption de solutions pour les toitures végétalisées sécures permettra de faciliter le processus d'installation et d'accroître les options de conception. Cela contribuera à une utilisation plus répandue de ces systèmes dans l'industrie de la construction.

CHAIRE INDUSTRIELLE DE RECHERCHE SUR LA CONSTRUCTION ÉCORESPONSABLE EN BOIS

CRSNG NSERC

Comportement au feu des toitures végétalisées

Nataliia Gerzhova[1] • Christian Dagenais[1,2] • Jean Côté[1] • Sylvain Ménard[3] • Pierre Blanchet[1]
[1]Université Laval, Québec, QC, Canada | [2]FPInnovations, Québec, QC, Canada | [3]Université du Québec à Chicoutimi (UQAC), Chicoutimi, QC Canada

INTRODUCTION

Considérant les toits végétalisés en termes de sécurité incendie, il peut sembler que ceux-ci puissent fournir une protection au bâtiment, en raison de la présence d'humidité dans les plantes et le sol. Cependant, dans certaines régions, il existe une préoccupation, même si aucun cas d'incendie dû à la présence de tels toits n'a encore été enregistré. Les plantes et la matière organique (MO) du substrat de croissance présentent une charge combustible additionnelle qui peut contribuer à la propagation du feu, surtout en période de sécheresse [1]. Le problème est que les toitures végétalisées sont considérées comme faisant partie du toit du bâtiment, mais actuellement, aucun test de résistance au feu n'existe spécifiquement pour ce type de toit. Les instructions techniques pour assurer un certain niveau de sécurité sont parfois trop strictes, comme au Québec, ce qui limite les possibilités de conception et empêche ainsi le développement de ces systèmes dans la région.

Cette étude vise à caractériser le substrat de toiture végétalisée en tant que charge combustible et à étudier la propagation du feu à travers le système typique d'un toit végétalisé.

MATÉRIEL ET MÉTHODES

Au départ, inspiré d'un rapport britannique [2], la contribution possible d'un substrat à un incendie a été évaluée. Les paramètres d'inflammabilité suivants ont été mesurés à l'aide d'un calorimètre à cône:

- Débit calorifique (HRR, kW/m²), paramètre le plus important dans l'évaluation d'un risque d'incendie
- Temps d'allumage

Deux paramètres principaux affectent la performance au feu d'un substrat:

- Quantité de matière organique (MO)
- Teneur en humidité

Pour les essais, deux types communs (de composition différente) de substrat de croissance contenant 20% de MO et un type contenant 35% de MO (maximum autorisé au Québec) ont été utilisés. Puisqu'un substrat sec constitue un enjeu, les échantillons ont été conditionnés à 0% et 30% de la teneur en humidité pour la comparaison.

Pour analyser la propagation du feu à travers un assemblage d'un toit vert vers le bas, une analyse de transfert thermique a été réalisée par simulation numérique, en utilisant la méthode des éléments finis. Cela donne des prévisions réalistes de l'évolution de la température avec le temps d'un assemblage en feu. Une charge thermique de 50 kW/m² pendant 1 heure a été appliquée sur la surface d'un assemblage présentant une couche de substrat de 10 cm d'épaisseur, sous laquelle se trouvaient le drainage, l'isolant et la structure de toit. Le substrat de croissance typique avec 20% de MO à l'état sec a été choisi pour la simulation.

RESULTATS

INFLAMMABILITÉ

Le débit calorifique des substrats dans des conditions sèches et humides est comparé à la membrane d'étanchéité en bitume modifié [3]. On peut voir que la membrane libère plus d'énergie que les substrats. Les courbes des substrats secs montent rapidement jusqu'à 100 et 230 kW/m² dans les premières secondes, mais une diminution rapide jusqu'à 22-24 kW/m² est observée dans les 50 secondes suivantes. La courbe pour la membrane montre une augmentation beaucoup plus longue, pendant les 300 premières secondes. Le débit calorifique maximal est plus de trois fois supérieur à celui des substrats secs contenant 20% de MO.

Débit calorifique

production d'energie lors de la combustion du substrat de croissance et de membrane d'etancheité

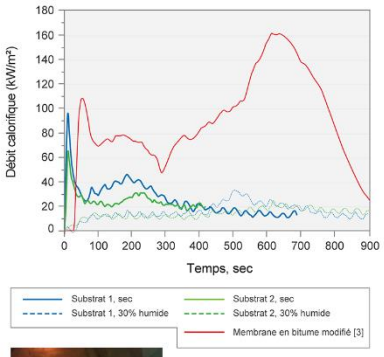

Temps d'ignition, secondes

	sec	30 % humide
Substrat 1	5	462
Substrat 2	7	-

Temps d'extinction, secondes

	sec	30 % humide
Substrat 1	560	686
Substrat 2	294	636

ANALYSE DU TRANSFERT THERMIQUE

L'analyse du transfert de chaleur montre qu'après une exposition de 1 heure, la température à laquelle la décomposition de MO commence (160-190°C) ne dépasse pas une profondeur de 6,5 cm (165°C). Au fond de la couche de substrat de croissance, la température est 40°C. La structure du toit reste à la temperature ambiante.

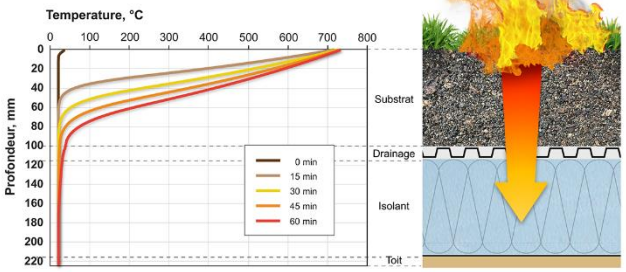

CONCLUSION

La caractérisation de l'inflammabilité montre que le sol d'un toit vert contenant 20% de MO, même à l'état sec, présente un risque d'incendie relativement faible par rapport à une membrane en bitume modifié. L'humidité, qui est normalement présente dans le sol, réduit considérablement le dégagement de la chaleur pendant la combustion et augmente le temps d'inflammation. La simulation de transfert de chaleur a permis de constater qu'un substrat sec d'épaisseur suffisante transmettait mal la chaleur, agissant comme isolant.

RÉFÉRENCES

[1] RBQ. Critères techniques visant la construction de toits végétalisés Quebec. 2015. p. 15-16.
[2] Report of Department for Communities and Local Government UK, Fire Performance of Green Roofs and Walls. 2013.
[3] Bourbigot S, Cerin O, Duquesne S, et al. (2013) Flame retardancy of bitumen: A calorimetry study. Journal of fire sciences 31: 112-130.

Fire behavior of green roof substrate

Nataliia Gerzhova[1] • **Pierre Blanchet**[1] • **Christian Dagenais**[1,2] • **Sylvain Ménard**[3] • **Jean Côté**[1]
[1]Université Laval, Québec, QC, Canada | [2]FPInnovations, Québec, QC, Canada | [3]Université du Québec à Chicoutimi (UQAC), Chicoutimi, QC Canada

BACKGROUND

Considering green roofs in terms of fire safety, it may seem that they can provide protection for the building, due to the presence of moisture in plants and soil. However still in some regions it is a matter of concern even though no fire cases due to a presence of such roofs have been registered yet. Plants and organic part of soil media present additional fire load that may contribute to the spread of fire in drought periods. The problem is that as a part of a covering, green roofs cannot be fire rated since there is a large variety of composition and configurations of assembly. Technical instructions for providing some level of security are sometimes too strict, like in Quebec, which limits design possibilities and thus prevent from widespread use of these systems.

This study aims to characterize green roof substrate as a combustible load and to investigate fire propagation through this layer.

METHODOLOGY AND MATERIALS

At first, inspired by a UK report [1] a possible contribution of a substrate to a fire was evaluated. The following flammability parameters were measured using a cone calorimeter:

- Rate of heat release (HRR, kW/m²), the most important parameter in evaluating a fire hazard
- Time to ignition

Two main parameters affect fire performance of a substrate:

- Amount of organic matter (OM)
- Moisture content

For the experiment two common types (with different composition) of soil with 20% of OM and one type containing 35% of OM (maximum allowed in Quebec) were used. As particularly dry state is a concern, samples were conditioned to 0% and 30% of moisture content for comparison.

To analyze the spread of fire through a substrate layer downwards, heat transfer analysis was performed by numerical calculation, using a finite element method. This gives realistic predictions of temperature development with time in the substrate as fire progresses. Heating load of 50 kW/m² for 45 min was applied to the surface of a soil layer of 10 cm thickness. Typical soil mix with 20% OM in a dry state was chosen for the simulation.

RESULTS

HRR of substrates in dry and moist conditions are compared with typical roof membranes – modified bitumen [2], PVC [3] and EPDM [4]. It may be seen that typical membranes generally release more energy compared to substrates containing 20% of organic content. Dry substrates curves show a rapid increase and a rapid decrease to 22-24 kW/m² at first minute, while the same process for membranes takes a much longer time, going down to only 65-70 kW/m². Moist substrates show very low values, not exceeding 35 kW/m². Peak heat release for all materials except moist substrates with 20% OM is reached at first 100 seconds. However modified bitumen exhibits the peak value that is more than three times higher than for Soil 1 (95 kW/m²) and Soil 2 (64 kW/m²).

FLAMMABILITY

Heat released

during burning of green roof substrates and roof membranes

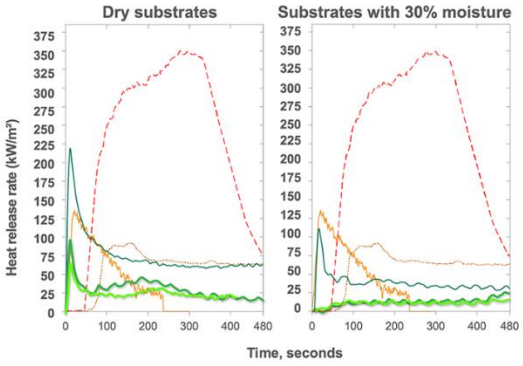

Green roof substrates
- Substrate 1, 20% OM
- Substrate 2, 20% OM
- Substrate 3, 35% OM

Typical roof membranes
- Polymer modified bitumen [2]
- PVC [3]
- EPDM [4]

Ignition

	Time to ignition	Time to flameout
	seconds	
Dry		
Soil 1	5	560
Soil 2	7	294
Soil 3	4	863
30 % moisture		
Soil 1	462	686
Soil 2	599	636
Soil 3	10	-

Soil 1 and 2 - 20% OM
Soil 3 - 35% OM

HEAT TRANSFER ANALYSIS

Heat transfer analysis show that after exposure to 45 min temperature at which thermal decomposition of organic matter generally starts (160-190°C) is reached at depth of 4 cm (179°C). At the bottom of a layer at 10 cm depth, the temperature remains at an ambient level.

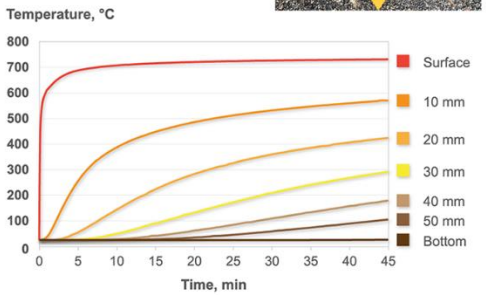

CONCLUSION

Flammability characterization shows that green roof soil with 20% of OM even in dry state represents relatively low fire hazard compared to typical roofing membranes. Moisture, which is normally present in soil, greatly reduces heat release during heat exposure and augment the time to ignition. Though increasing OM content negatively affects fire performance, the amount of 20% is safe, which is enough high for green roof substrates.

From heat transfer simulation, it is seen that dry substrate of enough thickness poorly propagates heat, acting more as an insulation.

REFERENCES

[1] Report of Department for Communities and Local Government UK, Fire Performance of Green Roofs and Walls. 2013.
[2] Bourbigot S, Cerin O, Duquesne S, et al. (2013) Flame retardancy of bitumen: A calorimetry study. Journal of fire sciences 31: 112-130.
[3] Xia, Y., et al., Effect of DPK flame retardant on combustion characteristics and fire safety of PVC membrane. Case Studies in Thermal Engineering, 2017. 10: p. 656-663.
[4] Chen R, Lu S, Li C, et al. (2016) Correlation analysis of heat flux and cone calorimeter test data of commercial flame-retardant ethylene-propylene-diene monomer (EPDM) rubber. Journal of Thermal Analysis and Calorimetry 123: 545-556.